

AD-A243 434



✓ ✓ (2)

NAVAL POSTGRADUATE SCHOOL

Monterey, California

DTIC
ELECTE
DEC 11 1991
S D D



THESIS

EFFECTS OF POWER PULSATIONS
ON HEAT TRANSFER FROM
DISCRETE HEAT SOURCES

by

Erhan M. Akdeniz

March, 1991

Thesis Advisor:

Yogendra Joshi

Approved for public release; distribution is unlimited

91 1210 078

91-17527



Unclassified

security classification of this page

REPORT DOCUMENTATION PAGE

1a Report Security Classification Unclassified			1b Restrictive Markings		
2a Security Classification Authority			3 Distribution Availability of Report		
2b Declassification Downgrading Schedule			Approved for public release; distribution is unlimited.		
4 Performing Organization Report Number(s)			5 Monitoring Organization Report Number(s)		
6a Name of Performing Organization Naval Postgraduate School		6b Office Symbol (if applicable) ME	7a Name of Monitoring Organization Naval Postgraduate School		
6c Address (city, state, and ZIP code) Monterey, CA 93943-5000			7b Address (city, state, and ZIP code) Monterey, CA 93943-5000		
8a Name of Funding Sponsoring Organization		8b Office Symbol (if applicable)	9 Procurement Instrument Identification Number		
8c Address (city, state, and ZIP code)			10 Source of Funding Numbers		
			Program Element No	Project No	Task No
			Work Unit Accession No		
11 Title (Include security classification) EFFECTS OF POWER PULSATIONS ON NATURAL CONVECTION FROM DISCRETE HEAT SOURCES					
12 Personal Author(s) Erhan Murat Akdeniz					
13a Type of Report Master's Thesis		13b Time Covered From To		14 Date of Report (year, month, day) March 1991	
15 Page Count 112					
16 Supplementary Notation The views expressed in this thesis are those of the author and do not reflect the official policy or position of the Department of Defense or the U.S. Government.					
17 Cosati Codes			18 Subject Terms (continue on reverse if necessary and identify by block number)		
Field	Group	Subgroup	LIQUID IMMERSION COOLING, POWER PULSATION, TEMPERATURE VARIATION, NUMERICAL HEAT TRANSFER		
19 Abstract (continue on reverse if necessary and identify by block number)					
<p>The natural convection heat transfer from an array of heaters flush mounted on a vertical test surface in response to both step and periodic input power has been investigated. Baseline surface temperature measurements in water were obtained for several steady power inputs, ranging from 0.2 W to 1.0 W for the vertical test surface. Also, the effects of the presence of a parallel shroud near the test surface on measured temperature values were studied. The effects of periodic variations in input power on the heater element temperatures were then examined at selected locations. The resulting transient heater temperatures were measured for various amplitudes, frequencies and average levels of the periodic input power. These transient measurements are compared with a two-dimensional numerical simulation of the relevant fluid flow and heat transfer processes. The computed heater surface temperatures supported the trends of the measurements and were within the expected range.</p>					
20 Distribution Availability of Abstract			21 Abstract Security Classification		
<input checked="" type="checkbox"/> unclassified unlimited <input type="checkbox"/> same as report <input type="checkbox"/> DTIC users			Unclassified		
22a Name of Responsible Individual Yogendra Joshi			22b Telephone (include Area code) (408) 646-3400		22c Office Symbol ME/Ji

DD FORM 1473,84 MAR

83 APR edition may be used until exhausted
All other editions are obsolete

security classification of this page

Unclassified

Approved for public release; distribution is unlimited.

Effects of Power Pulsations On Natural Convection From Discrete Heat Sources

by

Erhan Murat Akdeniz
LTJG., TURKISH NAVY
B.S., Turkish Naval Academy, Istanbul, 1984

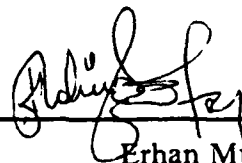
Submitted in partial fulfillment of the
requirements for the degree of

MASTER OF SCIENCE IN MECHANICAL ENGINEERING

from the

NAVAL POSTGRADUATE SCHOOL
March 1991

Author:




Erhan Murat Akdeniz

Approved by:



Yogendra Joshi, Thesis Advisor



Anthony J. Healey, Chairman,
Department of Mechanical Engineering

ABSTRACT

The natural convection heat transfer from an array of heaters flush mounted on a vertical test surface in response to both step and periodic input power has been investigated. Baseline surface temperature measurements in water were obtained for several steady power inputs, ranging from 0.2 W to 1.0 W for the vertical test surface. Also, the effects of the presence of a parallel shroud near the test surface on measured temperature values were studied. The effects of periodic variations in input power on the heater element temperatures were then examined at selected locations. The resulting transient heater temperatures were measured for various amplitudes, frequencies and average levels of the periodic input power. These transient measurements are compared with a two-dimensional numerical simulation of the relevant fluid flow and heat transfer processes. The computed heater surface temperatures supported the trends of the measurements and were within the expected range.

Accession For	
NTIS CRA&I	✓
DTIC TAB	<input type="checkbox"/>
Unannounced	<input type="checkbox"/>
Justification	
By	
Distribution/	
Availability Codes	
Dist	Accession For Special
A-1	

TABLE OF CONTENTS

I. INTRODUCTION	1
II. EXPERIMENTAL SETUP AND PROCEDURE	5
A. MODIFICATIONS IN APPARATUS	5
B. EXPERIMENTAL PROCEDURE	10
III. EXPERIMENTAL RESULTS	14
A. SINGLE HEATER ELEMENT DATA	14
1. Measurements in The Absence of Shroud	14
2. Measurements With Shroud	15
B. SINGLE COLUMN DATA	30
1. Measurements In The Absence of Shroud	30
2. Measurements With Shroud	31
C. DATA WITH ALL THREE COLUMNS POWERED	38
1. Measurements In The Absence of Shroud	38
2. Measurements With Shroud	39
IV. NUMERICAL MODEL AND COMPARISON WITH MEASUREMENTS	48
A. MATHEMATICAL FORMULATION	48
B. COMPUTATIONAL PROCEDURE	51
C. COMPARISON OF COMPUTATIONS WITH EXPERIMENTAL MEASUREMENTS	53
V. CONCLUSIONS	75
VI. RECOMMENDATIONS	77
APPENDIX A. SUBROUTINE USER	78
APPENDIX B. STEADY STATE AND TRANSIENT POWER PROGRAMS FOR HP_85	83

APPENDIX C. TEMPERATURE AND POWER ACQUISITION PROGRAM FOR THE HEATER AT THE BOTTOM OF THE CENTRAL COLUMN . . .	84
APPENDIX D. TEMPERATURE ACQUISITION PROGRAM	85
APPENDIX E. POWER INPUT PROGRAM	86
APPENDIX F. TEMPERATURE ACQUISITION AND REDUCTION PRO- GRAM (STEADY STATE)	88
LIST OF REFERENCES	91
INITIAL DISTRIBUTION LIST	94

LIST OF TABLES

Table 1. EXPERIMENTAL PROCEDURE FOR DIFFERENT CASES	12
Table 2. EXPERIMENTAL PROCEDURE FOR SPECIAL RUNS	13
Table 3. EFFECT OF SELECTING DIFFERENT TIME STEPS ON COMPUTED QUANTITIES	54
Table 4. THERMOPHYSICAL PROPERTIES OF MATERIALS IN HEATER ELEMENT	54

LIST OF FIGURES

Figure 1. Test Assembly (After Gaiser [Ref. 10])	6
Figure 2. Experimental Apparatus	8
Figure 3. Power Distribution to The Heater at The Bottom of The Central Column	9
Figure 4. Oscillations in Surface Temperature of Bottom Heater Due To Input Power Pulsations at 0.2 W. Pulsation Amplitude and Period are 0.06 W and 20 sec	16
Figure 5. Oscillations in Surface Temperature of Bottom Heater Due To Input Power Pulsations at 0.4 W. Pulsation Amplitude and Period are 0.07 W and 20 sec	17
Figure 6. Oscillations in Surface Temperature of Bottom Heater Due To Input Power Pulsations at 0.6 W. Pulsation Amplitude and Period are 0.1 W and 20 sec.	18
Figure 7. Oscillations in Surface Temperature of Bottom Heater Due To Input Power Pulsations at 0.8 W. Pulsation Amplitude and Period are 0.12 W and 20 sec	19
Figure 8. Oscillations in Surface Temperature of Bottom Heater Due To Input Power Pulsations at 1.0 W. Pulsation Amplitude and Period are 0.13 W and 20 sec	20
Figure 9. Oscillations in Surface Temperature of Bottom Heater Due To Input Power Pulsations with a Period of 10 sec. at 0.2 W. Pulsation Amplitude is 0.06 W.	21

Figure 10. Oscillations in Surface Temperature of Bottom Heater Due To Input Power Pulsations with a Period of 40 sec. at 0.2 W. Pulsation Amplitude is 0.06W.	22
Figure 11. Oscillations in Surface Temperature of Bottom Heater Due To Input Power Pulsations with a Period of 10 sec. at 0.6 W. Pulsation Amplitude is 0.1 W.	23
Figure 12. Oscillations in Surface Temperature of Bottom Heater Due To Input Power Pulsations with a Period of 40 sec. at 0.6 W. Pulsation Amplitude is 0.1 W.	24
Figure 13. Oscillations in Surface Temperature of Bottom Heater Due To Input Power Pulsations with Mean Power of 0.4 W, Amplitude of 0.03 W and Period of 20 sec.	25
Figure 14. Oscillations in Surface Temperature of Bottom Heater Due To Input Power Pulsations with Mean Power of 0.4 W, Amplitude of 0.13 W and Period of 20 sec.	26
Figure 15. Oscillations in Surface Temperature of Bottom Heater Due To Input Power Pulsations with Mean Power of 0.8 W, Amplitude of 0.06 W and Period of 20 sec.	27
Figure 16. Oscillations in Surface Temperature of Bottom Heater Due To Input Power Pulsations with Mean Power of 0.8 W, Amplitude of 0.19 W and Period of 20 sec.	28
Figure 17. Oscillations in Surface Temperature of Bottom Heater Due To Input Power Pulsations with Mean Power of 0.2 W, Amplitude of 0.06 W and Period of 20 sec.	29

Figure 18. Oscillations in Surface Temperature of Bottom Heater Due To Input Power Pulsations with Mean Power of 1.0 W, Amplitude of 0.13 W and Period of 20 sec.	29
Figure 19. x/L versus ΔT at 0.2 W Input Power	32
Figure 20. x/L versus ΔT at 0.4 W Input Power	32
Figure 21. x/L versus ΔT at 0.6 W Input Power	33
Figure 22. x/L versus ΔT at 0.8 W Input Power	33
Figure 23. x/L versus ΔT at 1.0 W Input Power	34
Figure 24. Nu versus Ra at 0.2 W	35
Figure 25. Nu versus Ra at 0.8 W	35
Figure 26. Monitoring The Surface Temperatures of Selected Heaters at 0.4 W When Input Power To The Bottom Heater Oscillated. Oscillation Amplitude and Period are 0.07 W and 20 sec. respectively.	36
Figure 27. Monitoring The Surface Temperatures of Selected Heaters at 0.8 W When Input Power To The Bottom Heater Oscillated. Oscillation Amplitude and Period are 0.07 W and 20 sec. respectively.	36
Figure 28. x/L versus ΔT at 0.4 W With 3 mm Shroud Spacing	37
Figure 29. x/L versus ΔT at 0.8 W With 3 mm Shroud Spacing	37
Figure 30. x/L versus ΔT at 0.2 W Input Power	40
Figure 31. x/L versus ΔT at 0.8 W Input Power	40
Figure 32. Monitoring The Surface Temperatures of Selected Heaters at 0.2 W When Input Power To The Bottom Heater Oscillated. Oscillation Amplitude and Period are 0.06 W and 20 sec. respectively.	41
Figure 33. Monitoring The Surface Temperatures of Selected Heaters at 0.2 W When Input Power To The Bottom Heater Oscillated. Oscillation Amplitude and Period are 0.06 W and 20 sec. respectively.	41

Figure 34. Monitoring The Surface Temperatures of Selected Heaters at 0.2 W When Input Power To The Bottom Heater Oscillated. Oscillation Amplitude and Period are 0.06 W and 20 sec. respectively.	42
Figure 35. Monitoring The Surface Temperatures of Selected Heaters at 0.8 W When Input Power To The Bottom Heater Oscillated. Oscillation Amplitude and Period are 0.12 W and 20 sec. respectively.	43
Figure 36. Monitoring The Surface Temperatures of Selected Heaters at 0.8 W When Input Power To The Bottom Heater Oscillated. Oscillation Amplitude and Period are 0.12 W and 20 sec. respectively.	43
Figure 37. Monitoring The Surface Temperatures of Selected Heaters at 0.8 W When Input Power To The Bottom Heater Oscillated. Oscillation Amplitude and Period are 0.12 W and 20 sec. respectively.	44
Figure 38. x/L versus ΔT for Different Shroud Spacings At 0.2 W	44
Figure 39. x/L versus ΔT for Different Shroud Spacings At 0.6 W	45
Figure 40. x/L versus ΔT for Different Shroud Spacings At 1.0 W	45
Figure 41. x/L versus ΔT for 3 mm Shroud Spacing At Various Power Levels	46
Figure 42. Comparison of Surface Temperatures Measured Without And With A Shroud at 3 mm For 0.4 W and 0.8 W	46
Figure 43. Effect of Shroud on Surface Temperatures of Heaters on Different Columns of Test Surface with The Same x/L	47
Figure 44. Numerical Model (After Haukeness [Ref. 10])	50
Figure 45. Development of Flow During Initial Transient Due To 0.2 W Step Input Power. The Figures are at (i)10, (ii)44, (iii)80 and (iv)120 seconds.	55
Figure 46. Development of Temperature Contours Due To 0.2 W Step Input Power. The Figures are at (i)10, (ii)44, (iii)80 and (iv)120 seconds.	56
Figure 47. Surface Temperature Calculated with Time Step of 0.1 sec.	57

Figure 48. Surface Temperature Calculated with Time Step of 0.5 sec.	58
Figure 49. Surface Temperature Calculated with Time Step of 1.0 sec.	58
Figure 50. Surface Temperature Calculated with Time Step of 5.0 sec.	59
Figure 51. Surface Temperature Calculated with the Properties of Plastic at 0.2 W Average Input Power	59
Figure 52. Surface Temperature Calculated with the Properties of Plastic at 1.0 W Average Input Power	60
Figure 53. Surface Temperature Calculated with the Properties of Inconel at 1.0 W Average Input Power ...	60
Figure 54. Temperature Contours and Streamlines with An Inconel Heater for Mean Power of 0.2 W, Amplitude of 0.06 W, Period of 20 sec at 15th sec ...	63
Figure 55. Temperature Contours and Streamlines with An Inconel Heater for Mean Power of 1.0 W, Amplitude of 0.13 W, Period of 20 sec at 15th sec ...	64
Figure 56. Surface Temperature Due to Power Pulsation with a Period of 40 sec. for 0.2 W Average Power and Amplitude of 0.06 W.	65
Figure 57. Surface Temperature Due to Power Pulsation with a Period of 10 sec. for 0.2 W Average Power and Amplitude of 0.06 W	66
Figure 58. Surface Temperature Due to Power Pulsation with a Period of 40 sec. for 0.6 W Average Power and Amplitude of 0.1 W	67
Figure 59. Surface Temperature Due to Power Pulsation with a Period of 20 sec. for 0.6 W Average Power and Amplitude of 0.1 W	67
Figure 60. Surface Temperature Due to Power Pulsation with a Period of 10 sec. for 0.6 W Average Power and Amplitude of 0.1 W	68
Figure 61. Surface Temperature Due to Power Pulsation with Different Amplitudes for 0.4 W Average Power	69

Figure 62. Surface Temperature Due to Power Pulsation with Different Amplitudes for 0.8 W Average Power	70
Figure 63. Temperature Contours and Streamlines for 0.4 W Average Power, 0.07 W Amplitude and 20 sec. Period of Oscillation	71
Figure 64. Temperature Contours and Streamlines for 0.8 W Average Power, 0.12 W Amplitude and 20 sec. Period of Oscillation	72
Figure 65. Effects of Thermophysical Properties on Calculated Temperatures	73
Figure 66. Effects of Heater Dimensions on Calculated Temperatures	73
Figure 67. Surface Temperature vs Time	74

NOMENCLETURE

c_p	specific heat at constant pressure (J/kg-K)
ΔT	$T - T_{amb}$ ($^{\circ}\text{C}$)
ΔT	time step (sec)
d	dimension in Fig. 1 (m)
g	gravitational acceleration (m/s^2)
h	heater element height (m)
H	enclosure height (m)
k	thermal conductivity (W/m-K)
L_i	dimension in Fig. 1 (m)
Nu	Nusselt number
P	pressure (N/m^2)
q''	heat generation per volume (W/m^3)
Ra	Rayleigh number ($g\beta qh^3/\alpha k\nu$)
R_L	equivalent resistance of two parallel resistors (Ω)
R_p	precision resistance (Ω)
S_i	dimension in Fig. 1 (m)
u	vertical velocity component (m/s)
v	horizontal velocity component (m/s)
V_L	voltage across precision resistance (Volt)
V_1	voltage across parallel resistance and heater combination (Volt)
x	vertical coordinate (m)
y	horizontal coordinate (m)
α	fluid thermal diffusivity (m^2/s)
β	coefficient of thermal expansion ($1/\text{K}$)
μ	dynamic viscosity (kg/m-s)
ν	kinematic viscosity (m^2/s)
ρ	density (kg/m^3)

Subscripts

<i>amb</i>	ambient
<i>f</i>	fluid
<i>s</i>	substrate
<i>H</i>	heater

ACKNOWLEDGMENTS

I would like to express my thanks to Professor Joshi for his guidance and technical assistance in putting together this research project. I also wish to thank my wife Tulay whose understanding and encouragement helped me through the long hours required to produce this thesis.

I. INTRODUCTION

A considerable increase in the volumetric power generation rates in electronic components has resulted due to both continued growth in functional capability and rapid decrease in feature size. The future enhancements in speed and size reduction of electronic systems are constrained by available heat removal techniques.

The performance and reliability of microelectronic components are very sensitive to junction temperature. The average failure rates of chips increase exponentially as the junction temperature increases Bar-Cohen and Kraus [Ref. 1]. In recent years, due to the relatively high heat transfer rates and other potential advantages such as high reliability, low cost, reduced noise and simpler design, complete immersion of microelectronic circuits in dielectric liquids has been examined.

Relatively few studies on natural convection liquid immersion cooling are available in literature. The heat transfer characteristics of flush mounted heat sources on vertical surface in several liquids were studied by Baker et al [Ref. 2]. Due to the three dimensional effects, large increases in heat transfer were noticed. Both flush and protruding arrangements were investigated in water and R-113 by Park and Bergles [Ref. 3]. Correlations for natural convection in a vertical channel dissipating uniform heat flux from sides were presented by Bar-Cohen and Schweitzer [Ref. 4]. Flow visualization and heat transfer measurements for natural convection from a long heated protrusion on a vertical insulated wall of a rectangular chamber filled with water were carried out by Kelleher and Knock [Ref. 5]. These measurements were supported by a computational investigation by Lee et al [Ref. 6].

Flow visualizations and component surface temperature measurements for natural convection cooling of a 3 by 3 array of discrete heated protrusions on the vertical wall of a rectangular enclosure filled with a dielectric fluid were performed by Joshi et al [Ref. 7]. In other experimental studies, the heat transfer and flow characteristics of protruding heat sources on a vertical surface [Ref. 8] and vertical channel [Ref. 9] were studied by Joshi et al. Flow visualizations and component surface temperature measurements were carried out for several power dissipation levels and channel spacings. For the smallest channel spacing, a significant increase in the component surface temperature due to a reduction in fluid velocity was observed.

Natural convection adjacent to a three column array of fifteen per column uniformly heated components flush mounted on a vertical flat plate in water was examined by Gaiser [Ref. 10]. Component temperature measurements both without and with a shroud parallel to the heated surface were reported and experimental correlations were developed for different power levels and shroud spacings. A significant increase in temperature due to reduction in fluid velocity for the smallest channel spacing was observed.

A numerical investigation of natural convection flow and heat transfer arising from a protruding heat source on a vertical plate was reported by Sathe and Joshi [Ref. 11]. Numerical predictions were obtained for a wide range of appropriate Ra and Pr numbers and substrate to fluid thermal conductivity ratios. Computed protrusion surface temperatures compared favorably with available experimental results from [Ref. 8]. A numerical investigation of two dimensional natural convection flow and heat transfer from a substrate-mounted flush heat source immersed in a liquid-filled square enclosure was conducted by Haukenes [Ref. 12]. Numerical predictions were in favorable agreement with the experimental data.

While the transport characteristics during steady state have been investigated for both discrete flush and protruding heat sources, very little information is available during transient phases of operation. In many applications power cycling may take place. The present investigation examines both numerically as well as experimentally the transient response of discrete heat sources flush mounted on a substrate. The experiments were conducted with the same test surface as of Gaiser [Ref. 10], and comparison between numerical model and experiments were made for the heat source closest to the leading edge of the surface.

The experimental studies reported here examine changes in the natural convection flow and heat transfer characteristics of a three column array of 45 flush mounted heaters on a vertical test surface. The power to the bottom heater of the center column oscillated with time while power to all the other heaters was kept constant. Component surface temperatures were measured over a period of time for a range of average power inputs from 0.2 W - 1.0 W. Various amplitudes and frequencies of the periodic variation were examined. Also reported here are the effects of the presence of a shroud. Numerical computations were performed to study heat transfer from a single heat source.

Specific goals of this study were:

- To measure oscillations in heater surface temperatures in response to input power fluctuations for a range of average component power levels, amplitudes and frequencies of power pulsations.
- To examine the same effects in the presence of a parallel shroud placed next to the test surface.
- To examine the effects of power pulsations in the bottom component on the steadily powered downstream components.

- To numerically investigate the two-dimensional transient natural convection flow and heat transfer for a single flush heat source and compare the results with the experimental measurements of component temperatures.

This study advances the work reported by Gaiser [Ref. 10] and Haukenes [Ref. 12] and is part of the study of the natural convection liquid immersion cooling of electronic equipment.

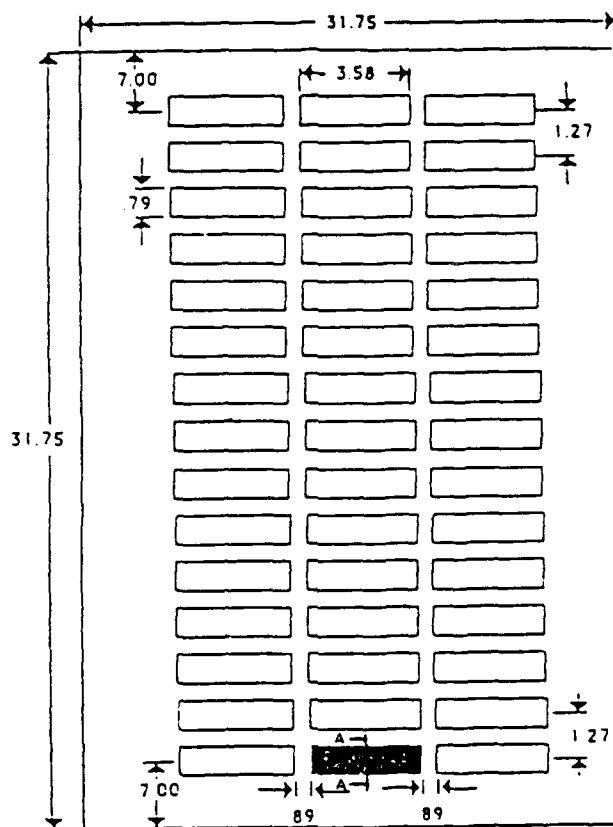
II. EXPERIMENTAL SETUP AND PROCEDURE

Detailed descriptions of the original experimental equipment design and construction can be found in Gaiser [Ref. 10] and further additions and changes done in the experimental setup in Haukenes [Ref. 12]. Only a brief review is presented and new noteworthy additions and changes are noted here.

As seen in Figure 1, the assembly consists of a vertical test surface with a total of 45 flush mounted rectangular heat sources in three columns of 15 elements per column. The test surface is immersed in a one cubic meter, plate glass tank filled with deionized water. A parallel shrouding plate, placed in front of the test surface to simulate a typical circuit board assembly, forms a channel with the test surface. Each heater has a copper-constantan thermocouple attached to its back. All the thermocouples are referenced individually to an ice bath as seen in Figure 2. Three thermocouples monitor the tank temperature at the top, middle and bottom. A Hewlett Packard Model 3852S data acquisition system measures the ice referenced voltage of each thermocouple to calculate temperatures and voltages delivered from the source and supplied to the heater to calculate power. The voltages are converted into temperatures and component input powers monitored by a Hewlett Packard Model 9153 computer interfaced to the data acquisition system. A filtration system consisting of four cartridges is used to ensure the purity and the resistivity of at least 0.7 megaohm.cm of the water inside the tank.

A. MODIFICATIONS IN APPARATUS

The most significant new feature was the design of a power assembly to provide pulsating input powers to the heating elements. Figure 2 shows a sketch of this assembly. All the heater strips in the left and right columns are powered by



SECTION AA

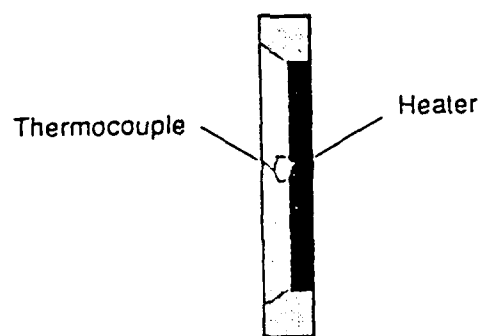


Figure 1. Test Assembly (After Gaiser [Ref. 10]). All Dimensions are in cm.

a 0-40 V, 0-50 A HP 6269B D.C. power supply unit through four distribution panels. In the central column all heater strips except the one at the bottom are powered by a 0-10 V, 0-10 A HP 6282A D.C. power supply unit through two distribution panels. There is a 2.01 ohm precision resistor in series with each heater resistor for current measurements. Details of the power distribution assembly are provided by Gaiser [Ref. 10].

A HP-85 computer, HP-59501B power supply programmer and 0-40 V, 0-1.5 A HP-6289A D.C. power supply units were added to the experimental setup to generate a periodic power input. The transient power input is provided only to the heater at the bottom of the central column. Appropriate programs were developed for the HP-85 computer to provide transient power to the bottom heater.

The following relation was used to determine the power:

(As seen from Figure 3)

$$POWER = \left(\frac{V_L - V_1}{R_p} \right) \times \left(V_1 - \left(\frac{V_L - V_1}{R_p} \right) \times R_L \right)$$

where the symbols are defined in the nomenclature. See Appendices B-F for program listings for power input and data reduction, developed for both steady and transient cases.

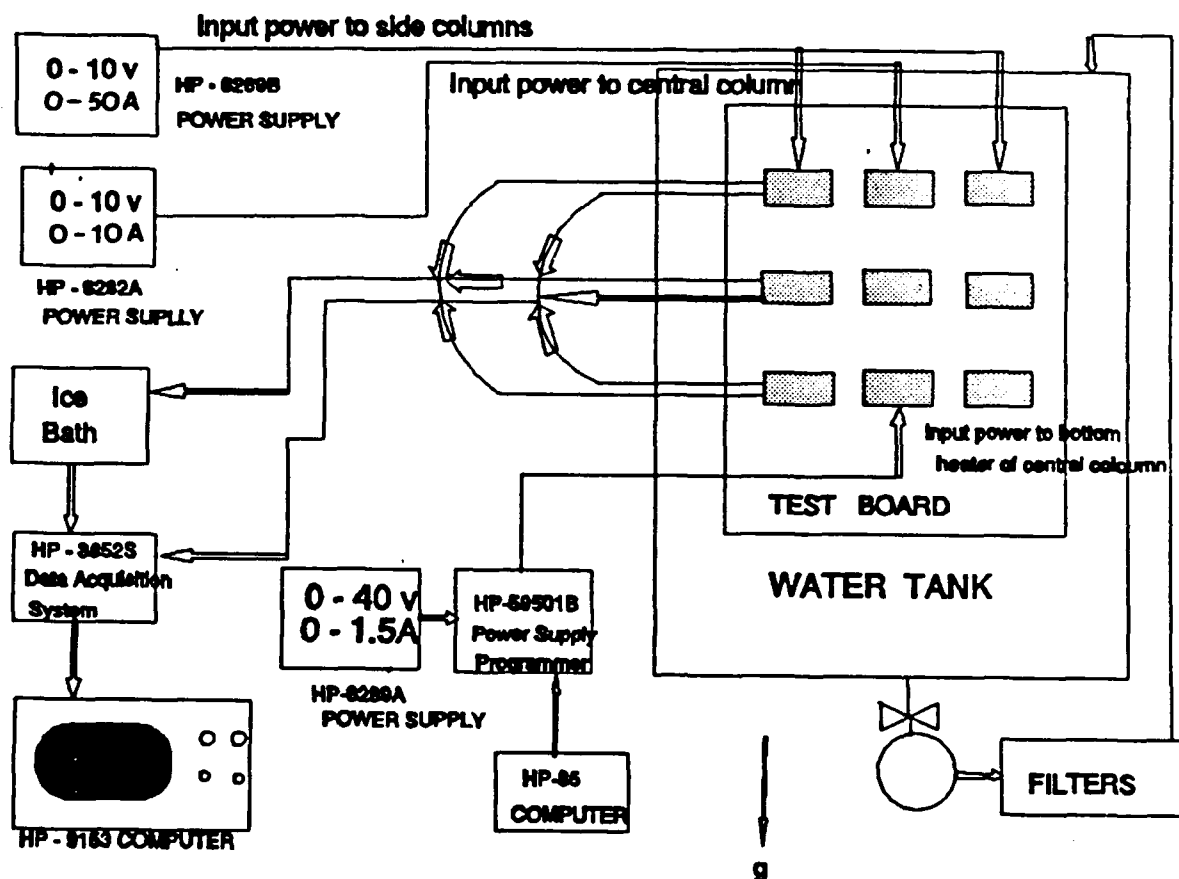


Figure 2. Experimental Apparatus

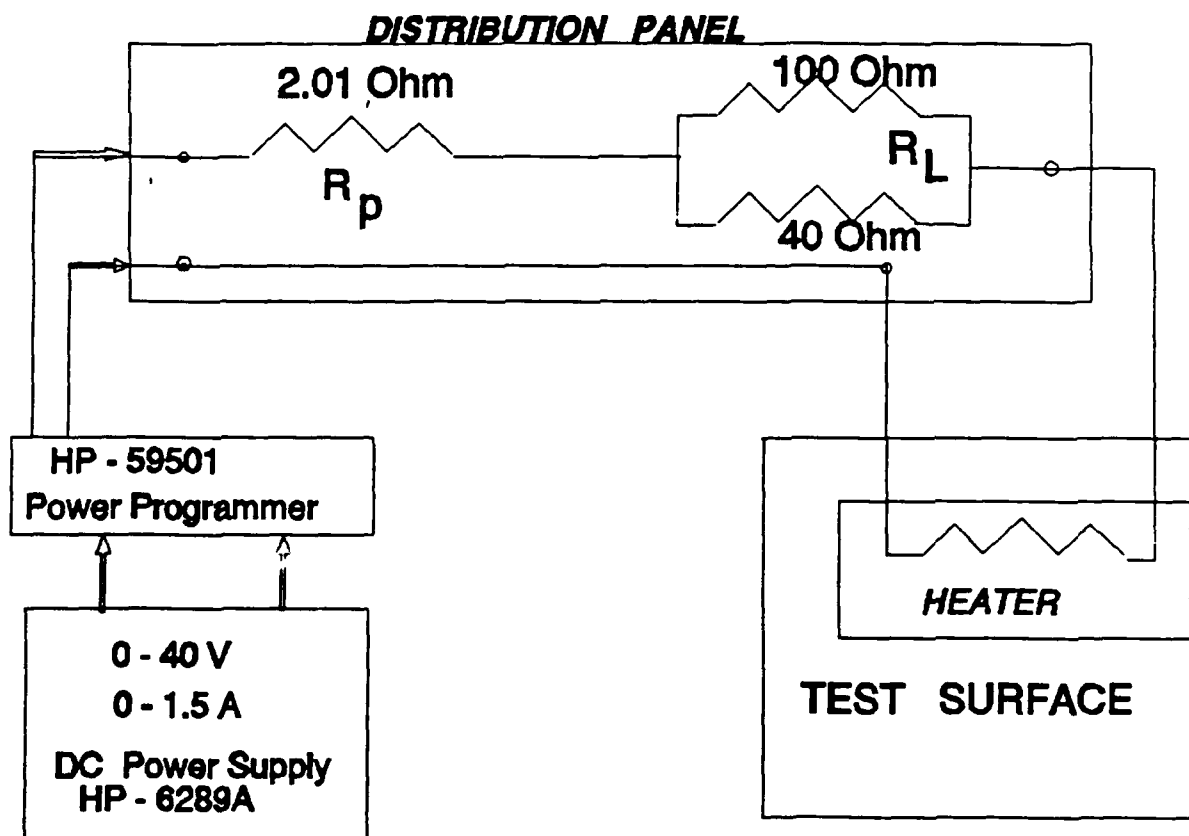


Figure 3. Power Distribution to The Heater at The Bottom of The Central Column

B. EXPERIMENTAL PROCEDURE

The preparation for each set of experiments started by stirring the water in the immersion tank with a propeller type stirrer for 5 to 10 minutes to achieve uniform temperature distribution. Crushed ice was placed into the thermocouple reference bath. A mercury thermometer was also inserted into the ice bath to make sure that the bath was at $0\text{ }^{\circ}\text{C} \pm 0.05\text{ }^{\circ}\text{C}$. The data acquisition system was turned on and warmed up. Typically in about one hour the data acquisition system warmed-up and also the immersion tank was quiescent. The temperature acquisition program (see Appendix D) was loaded and the temperatures of the heater surfaces and immersion tank were measured, before the power was supplied to the heaters. Typically all heaters and the tank were within $0.05\text{ }^{\circ}\text{C}$ of each other prior to power input.

The experimental study consisted of three major parts. The heater surface temperature measurements for three different cases were made as presented in Table 1. In the first case thermocouple measurements were taken every fifteen minutes until successive measurements remained unchanged. Once steady state was achieved, temperature measurements and heater voltage readings were recorded and saved for further processing. The computer program to generate a prescribed periodic power input, contained in Appendix B was then loaded and run. Once a steady periodic response was evident, temperature oscillations with time were sampled over a period of forty seconds with a sampling frequency of 180/40 Hz. The input power pattern was also recorded over a period of seventy seconds with a sampling frequency of 350/70 Hz.

As the amplitudes of the power variation increased, the accuracy in digitization of the input power by the data acquisition system decreased. While the power input to the heater was as programmed, the measurement of it by the HP-85 was sometimes slower than required. Another problem encountered was the monitoring of the voltage drops

across both the power supply and the resistor at the same time in order for the calculation of the power supplied to the heater.

In the second category of experiments in Table 1, the power to all heaters was increased incrementally. The output from the power calculation program was checked, until the desired power level was reached. The power and temperature measurements were recorded when steady state was attained. The periodic input power program was then loaded and run. Besides monitoring the temperature oscillations with time on the bottom heater, downstream elements with uniform power were also sampled to detect any temperature oscillations with time, over a period of five minutes.

In the third class of experiments in Table 1, the same procedure as for the second set was repeated. The temperatures of each heater element both for steady and transient cases were recorded. Additional runs for different average power levels and with different periods of applied power were also performed. For the first group of these runs, the effects of changing the pulsation frequency and for the second group, the effects of changing the amplitude of input power were examined. For the third group of runs, the effects of providing all the heaters with power different than supplied to the bottom one were studied.

Table 1. EXPERIMENTAL PROCEDURE FOR DIFFERENT CASES

CASE	PROCEDURE	POWER (Watts)	SHROUD SPA.(mm)
CASE 1: Single heater powered	<ul style="list-style-type: none"> • Constant power is applied to the heater at the bottom of central column, until steady state is achieved. • The power input is then modulated in time. 	.049, .082, .2, .235, .4, .6, .8, 1.	No shroud, 3
CASE 2: Central column powered	<ul style="list-style-type: none"> • Constant power is applied to all heaters until steady state is achieved. • The power to the heater at the bottom of central column is then timewise modulated while keeping the power to all other heaters steady. 	.2, .4, .6, .8, 1.0	Same as CASE 1
CASE 3: All heaters powered	Same as CASE 2	Same as CASE 2	No shroud (steady and transient), 3,6,9 (all steady)

Table 2. EXPERIMENTAL PROCEDURE FOR SPECIAL RUNS

CASE	PROCEDURE	POWER (Watts)
Change in period of input power	CASES 1 and 2 in Table 1 are repeated by changing the period from 20 sec. to 40 sec. and then 10 sec.	.2, .6
Change in amplitude of applied power	CASE 1 and 2 in Table 1 are repeated by changing the amplitude of applied power to selected values.	.4, .8
Different power to bottom heater than the others in central column	Same as CASE 2 in Table 1	.024 (bot)- .275 (others), .049 (bot)- .45 (others), .082 (bot)- 1.27 (others), .235 (bot)- 2.06 (others)

III. EXPERIMENTAL RESULTS

A. SINGLE HEATER ELEMENT DATA

The presentation and discussion of the single heater element data during this study is divided into two major parts. The first part refers to the case where the heater element is powered with uniform power, until steady state condition is reached. Within this part, heater temperature data from the thermocouple at the center of the heater surface are recorded for 40 sec. with a sampling frequency of 180/40 Hz. In the second set of experiments after an initial steady state condition is reached within the heater element, its input power is switched to a sawtooth form. In this form, input power is increased linearly then decreased in the same fashion between maximum and minimum amplitudes. Applied transient power has a period of 20 sec. The surface temperature of the heater element is recorded using the the same sampling frequency.

These two sets of measurements are repeated for five average power levels, ranging from 0.2 W to 1.0 W. Measurements are made without shroud and also with a shroud at 3 mm spacing from the test surface, in order to determine the effects of power level and channel spacing on the heat transfer performance. In order to compare measured surface temperatures with the numerical computations, the heater center temperatures are presented as differences between the heater surface and the ambient.

1. Measurements in The Absence of Shroud

In Figures 4-8 the temperature variations with time are displayed for various average power inputs with a fixed period of 20 sec. In Figures 9-12 the effects of changing the period of applied power, for 0.2 W and 0.6 W average power levels are examined. In Figures 13-16 the effects of changing the amplitude of the applied power to 0.4 W and 0.8 W are presented. From Figures 4-12, the trend of increasing average

surface temperature with increasing average power is as expected. The period of surface temperature variation, noted almost as 23 sec. from these figures, stays approximately constant for all power levels. It is also seen that the oscillations in surface temperature increase with an increase in both amplitude and the period of the applied power variation. For example in Figures 13 and 14 for an average input power of 0.4 W when the power variation is within 0.55 W and 0.29 W, the maximum difference in ΔT is 0.8 °C. This difference decreases to 0.25 °C, if the power variation is kept within 0.43 W and 0.36 W. For 0.6 W average power level in Figures 15-16 when the period of applied power is increased to 40 sec., the difference in ΔT increases to 1.0 °C. The difference in ΔT decreases to 0.3 °C when period is reduced to 10 sec. For higher power levels, the effect of amplitude and period of applied power is more evident.

2. Measurements With Shroud

Figures 17 and 18 show ΔT versus time at mean power levels of 0.2 W and 1.0 W for shroud spacing of 3 mm. When compared to the unshrouded measurements at the same power levels [Figures 4 and 8], it is seen that the ΔT values for a single element remain almost unchanged.

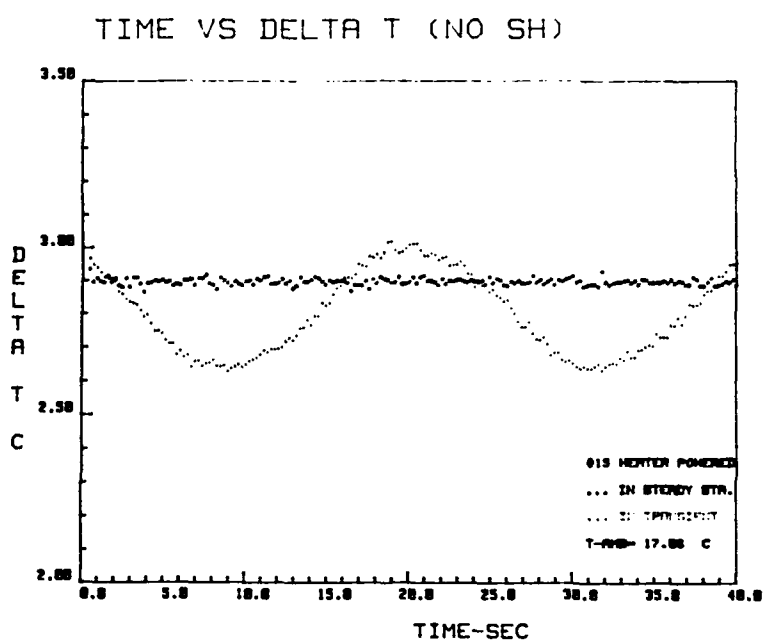
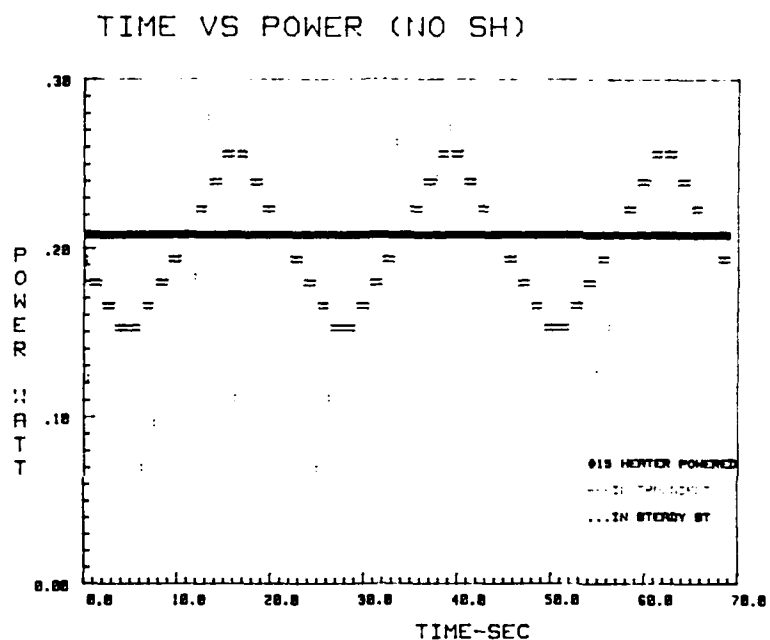


Figure 4. Oscillations in Surface Temperature of Bottom Heater Due To Input Power Pulsations at 0.2 W. Pulsation Amplitude and Period are 0.06 W and 20 sec

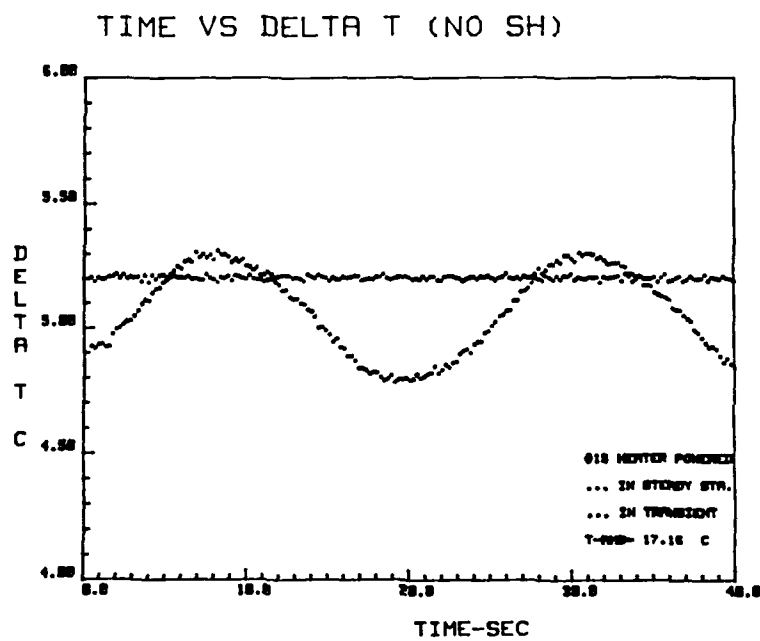
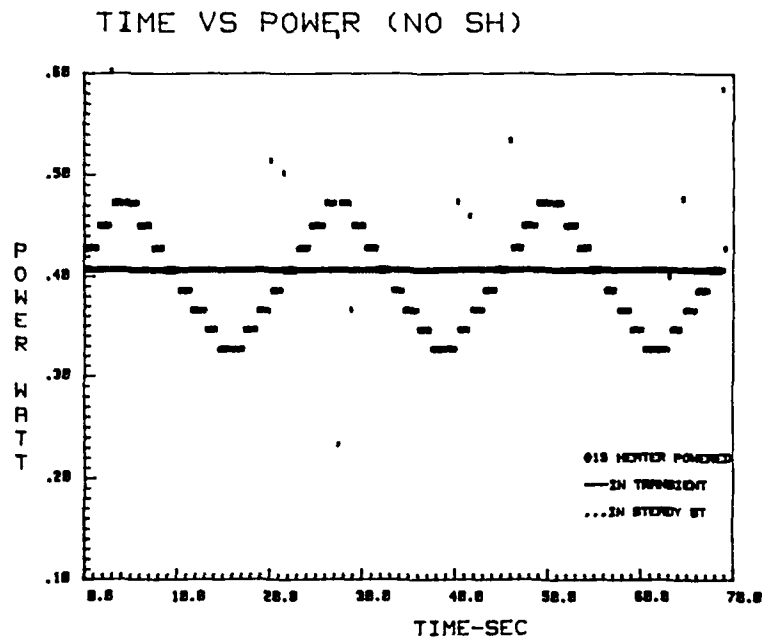


Figure 5. Oscillations in Surface Temperature of Bottom Heater Due To Input Power Pulsations at 0.4 W. Pulsation Amplitude and Period are 0.07 W and 20 sec

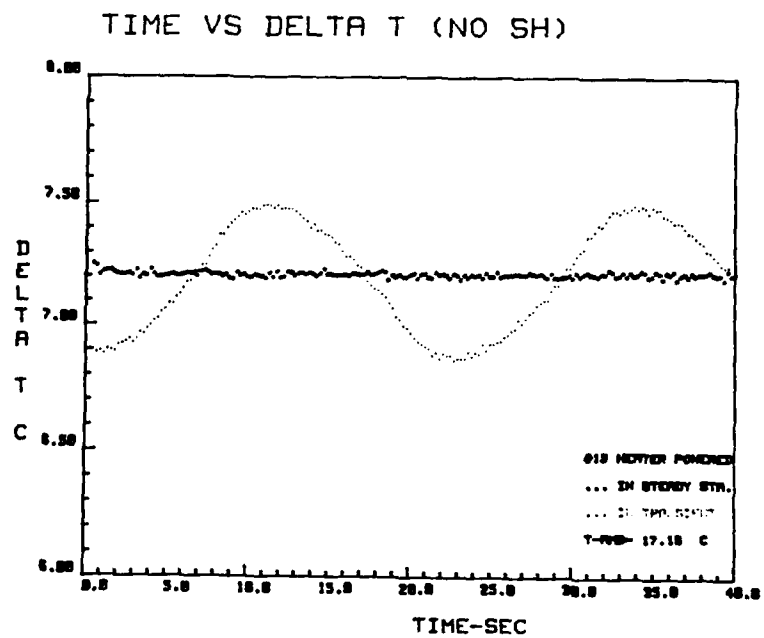
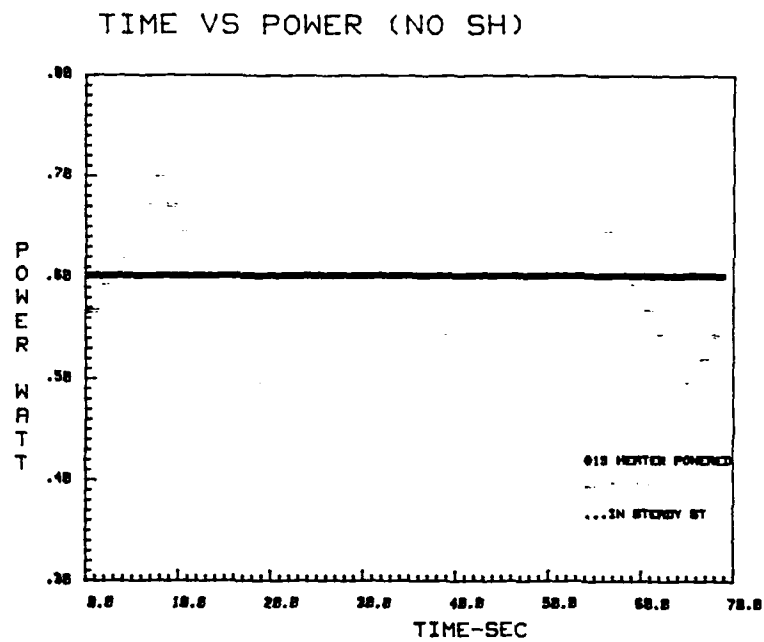


Figure 6. Oscillations in Surface Temperature of Bottom Heater Due To Input Power Pulsations at 0.6 W. Pulsation Amplitude and Period are 0.1 W and 20 sec.

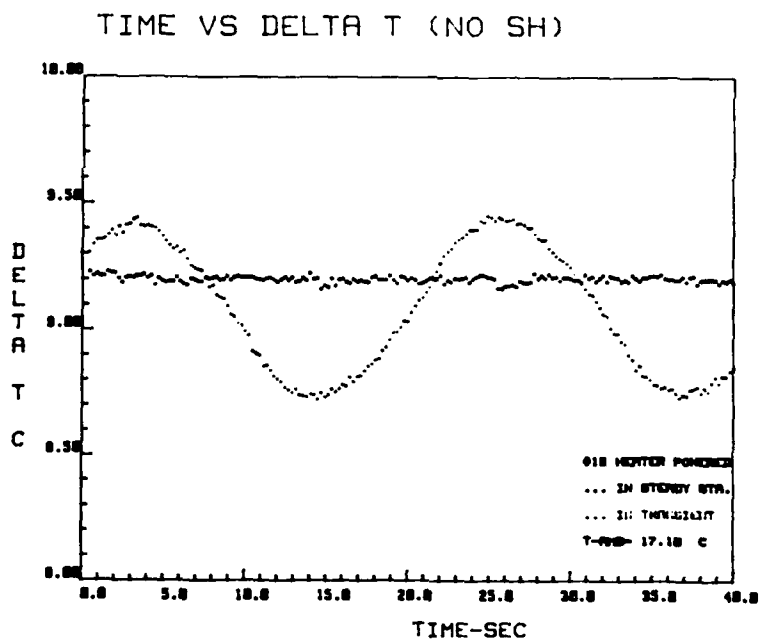
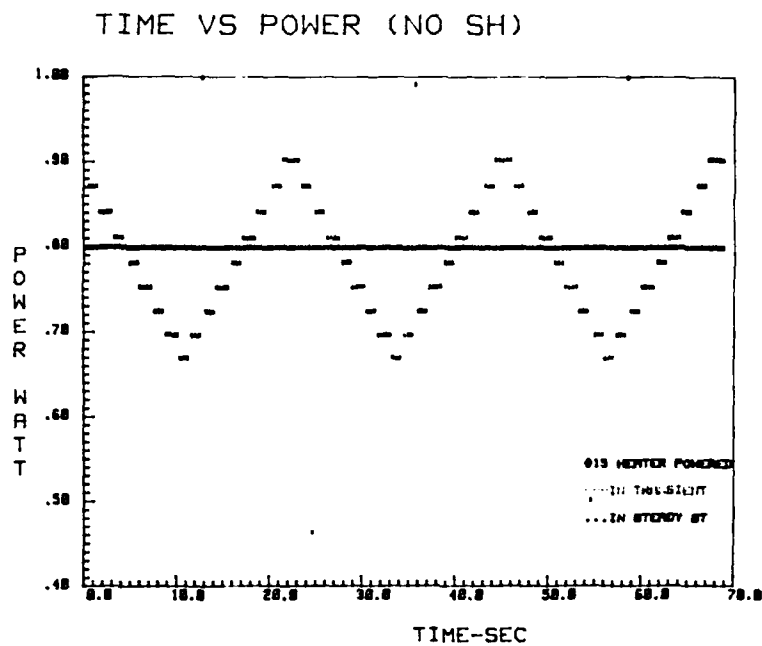


Figure 7. Oscillations in Surface Temperature of Bottom Heater Due To Input Power Pulsations at 0.8 W. Pulsation Amplitude and Period are 0.12 W and 20 sec

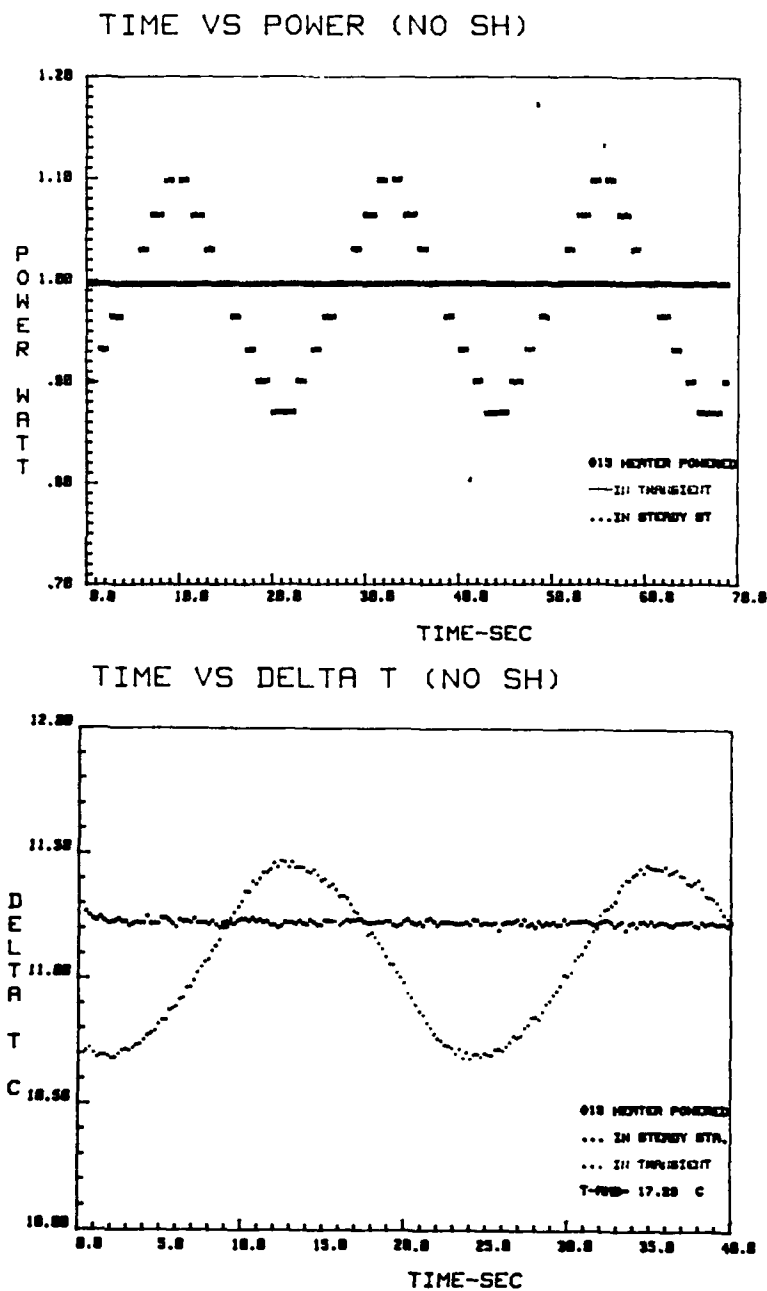


Figure 8. Oscillations in Surface Temperature of Bottom Heater Due To Input Power Pulsations at 1.0 W. Pulsation Amplitude and Period are 0.13 W and 20 sec

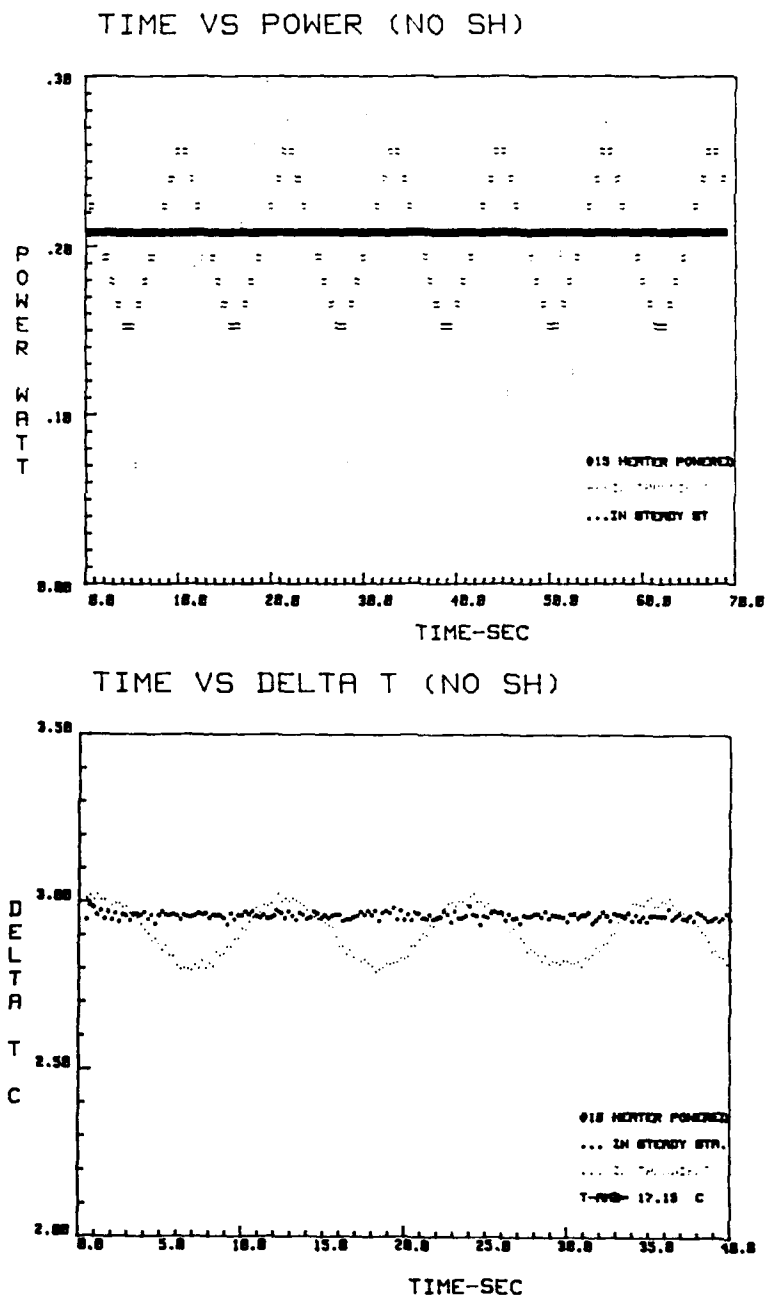


Figure 9. Oscillations in Surface Temperature of Bottom Heater Due To Input Power Pulsations with a Period of 10 sec. at 0.2 W. Pulsation Amplitude is 0.06 W.

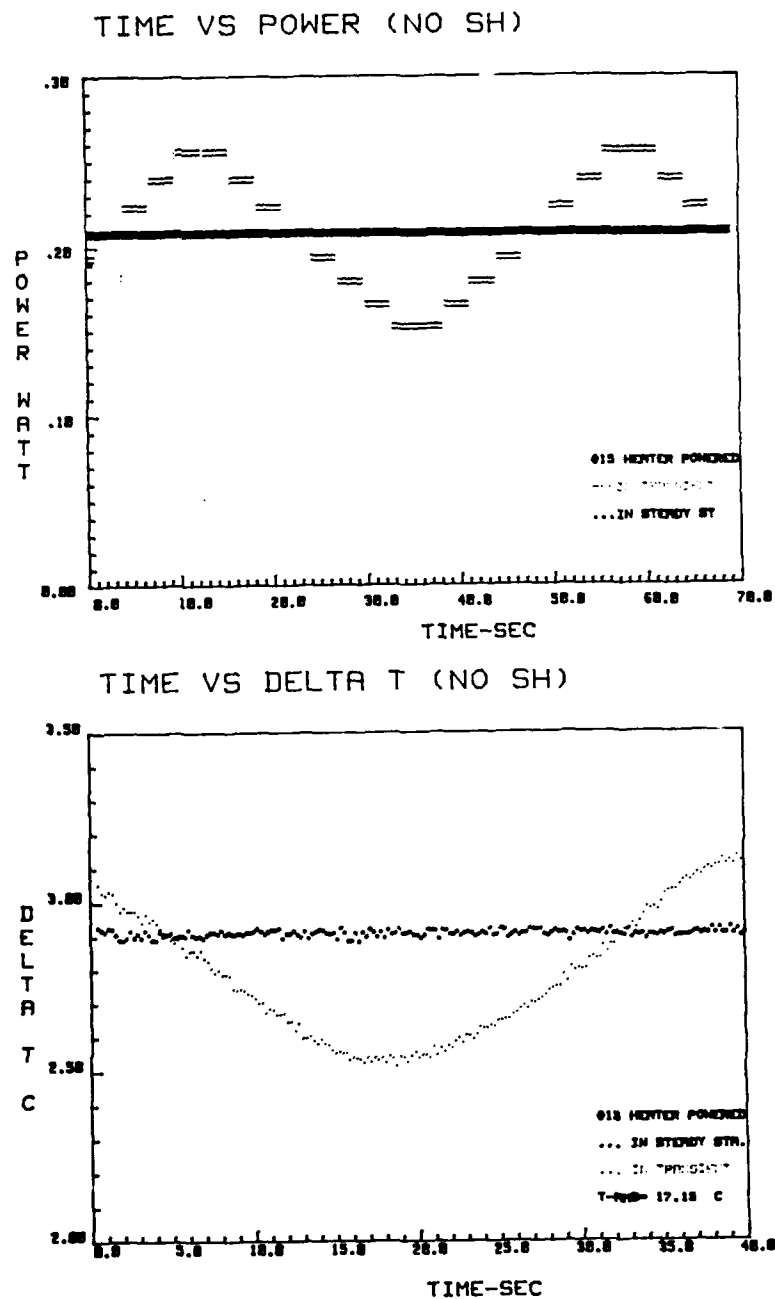


Figure 10. Oscillations in Surface Temperature of Bottom Heater Due To Input Power Pulsations with a Period of 40 sec. at 0.2 W. Pulsation Amplitude is 0.06W.

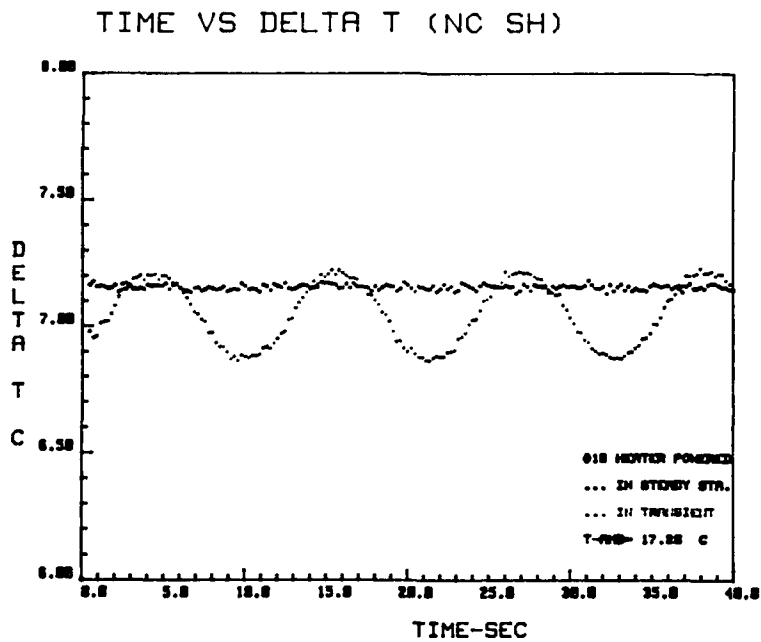
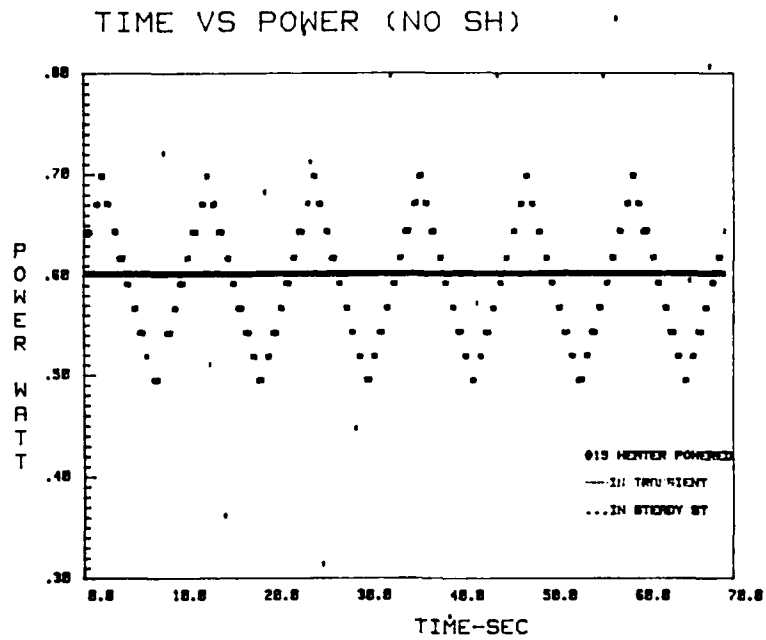


Figure 11. Oscillations in Surface Temperature of Bottom Heater Due To Input Power Pulsations with a Period of 10 sec. at 0.6 W. Pulsation Amplitude is 0.1 W.

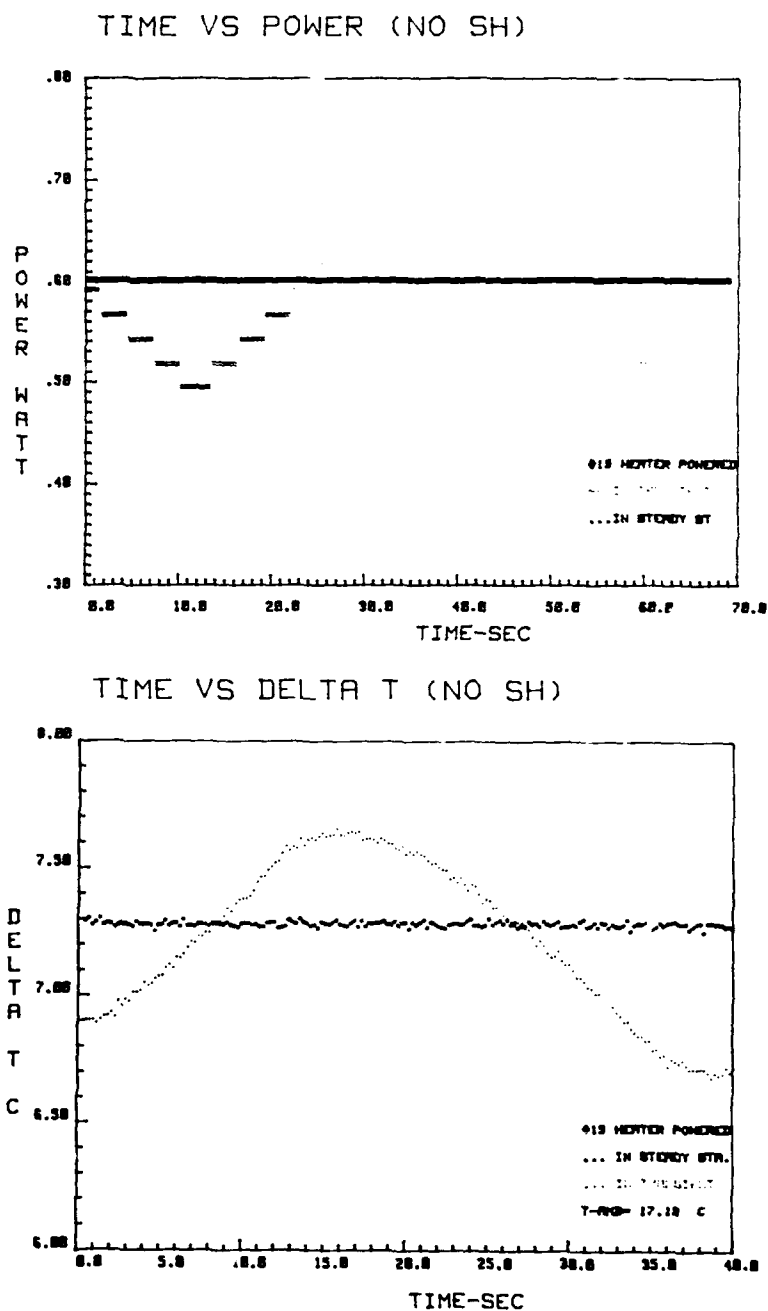


Figure 12. Oscillations in Surface Temperature of Bottom Heater Due To Input Power Pulsations with a Period of 40 sec. at 0.6 W. Pulsation Amplitude is 0.1 W.

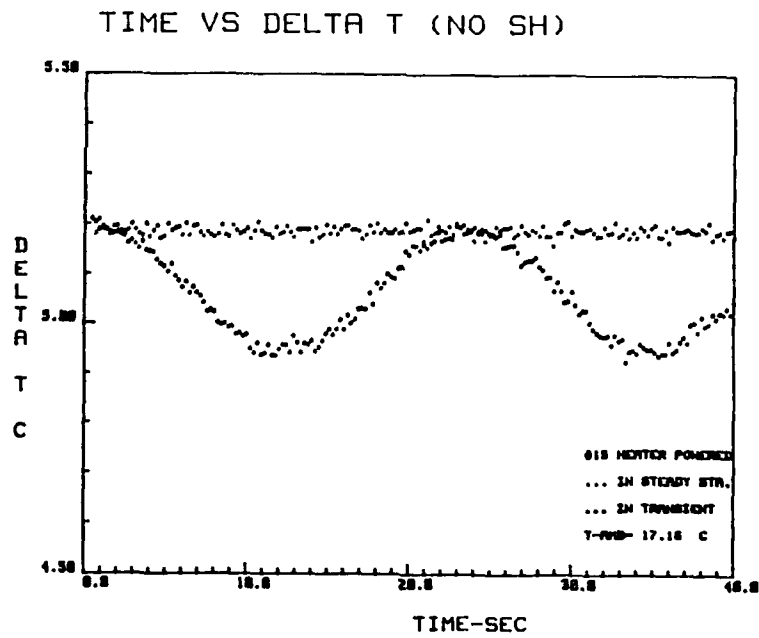
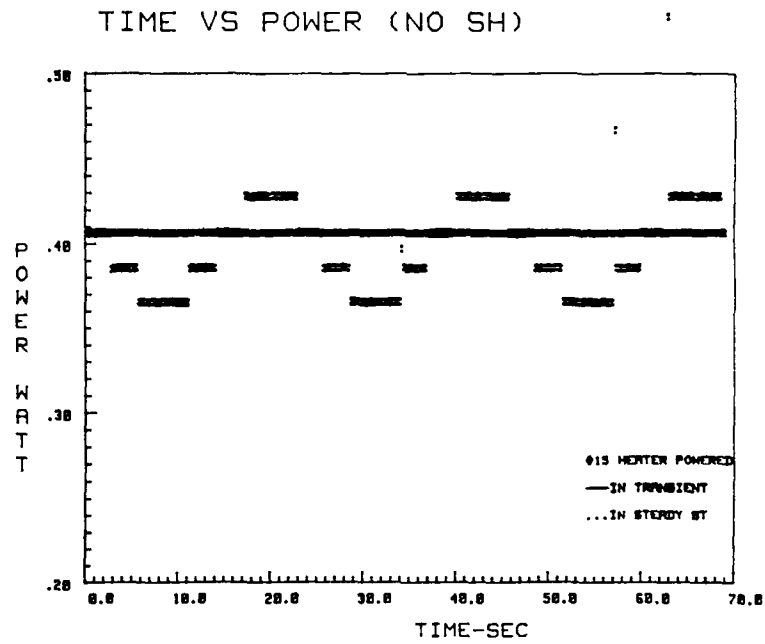


Figure 13. Oscillations in Surface Temperature of Bottom Heater Due To Input Power Pulsations with Mean Power of 0.4 W, Amplitude of 0.03 W and Period of 20 sec.

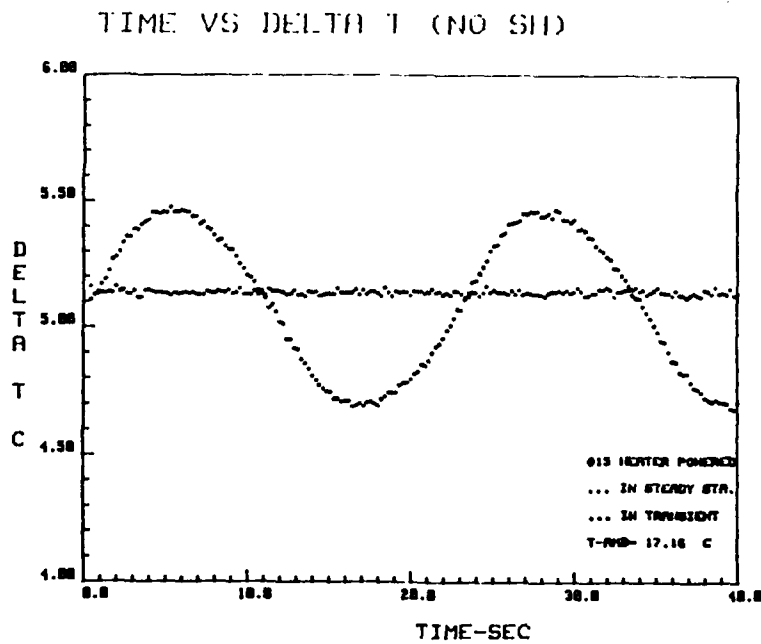
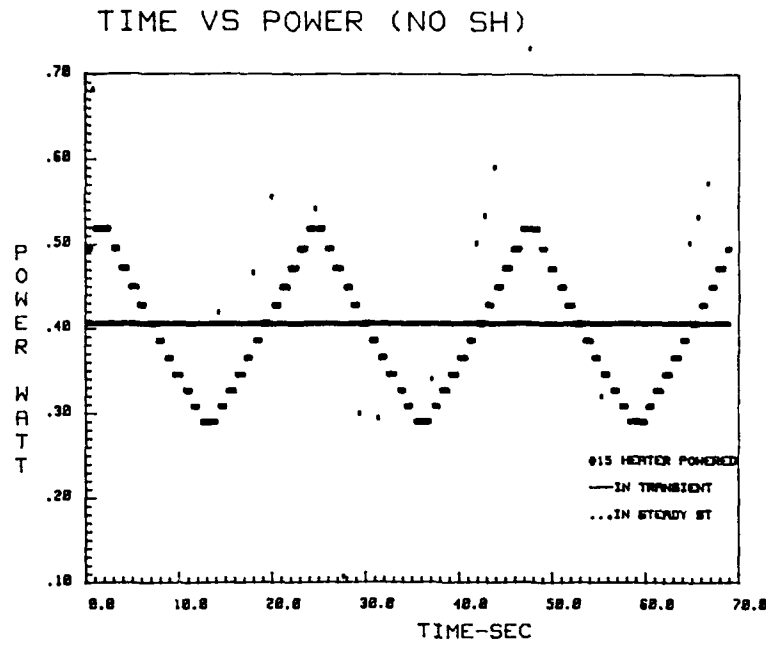


Figure 14. Oscillations in Surface Temperature of Bottom Heater Due To Input Power Pulsations with Mean Power of 0.4 W, Amplitude of 0.13 W and Period of 20 sec.

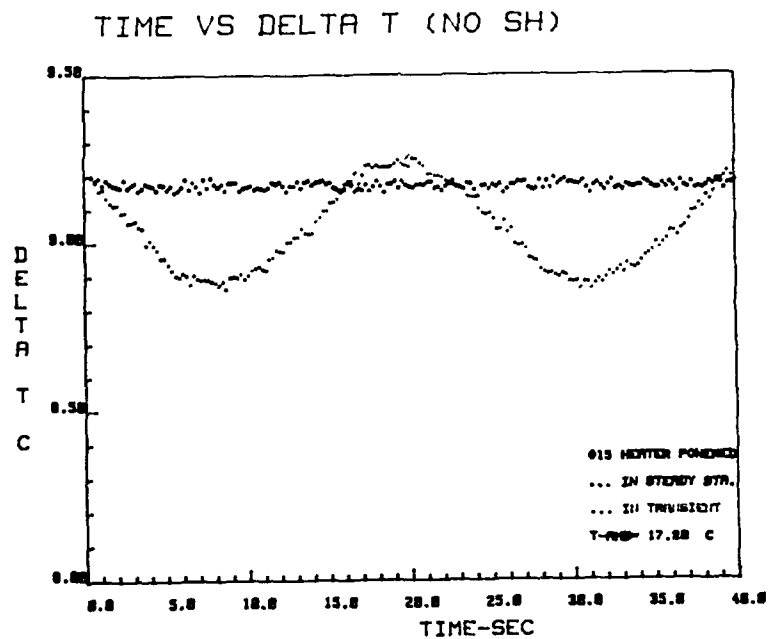
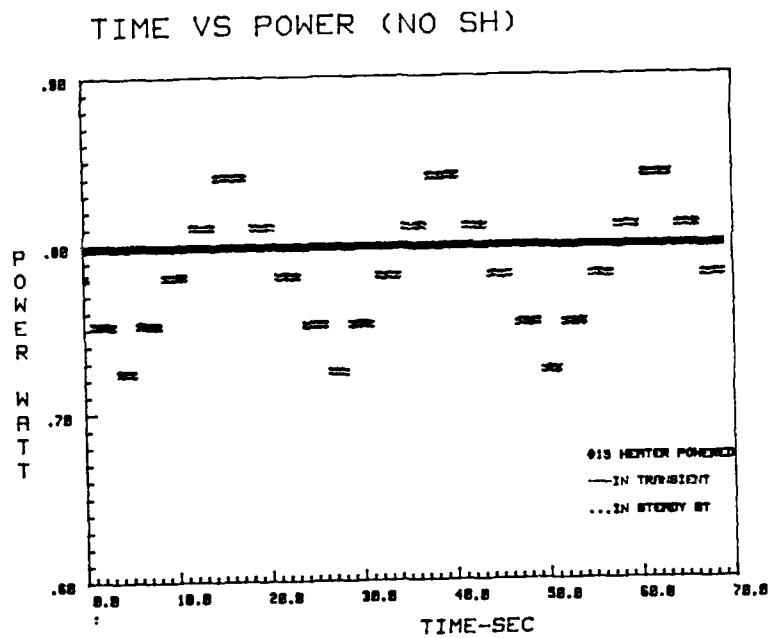


Figure 15. Oscillations in Surface Temperature of Bottom Heater Due To Input Power Pulsations with Mean Power of 0.8 W, Amplitude of 0.06 W and Period of 20 sec.

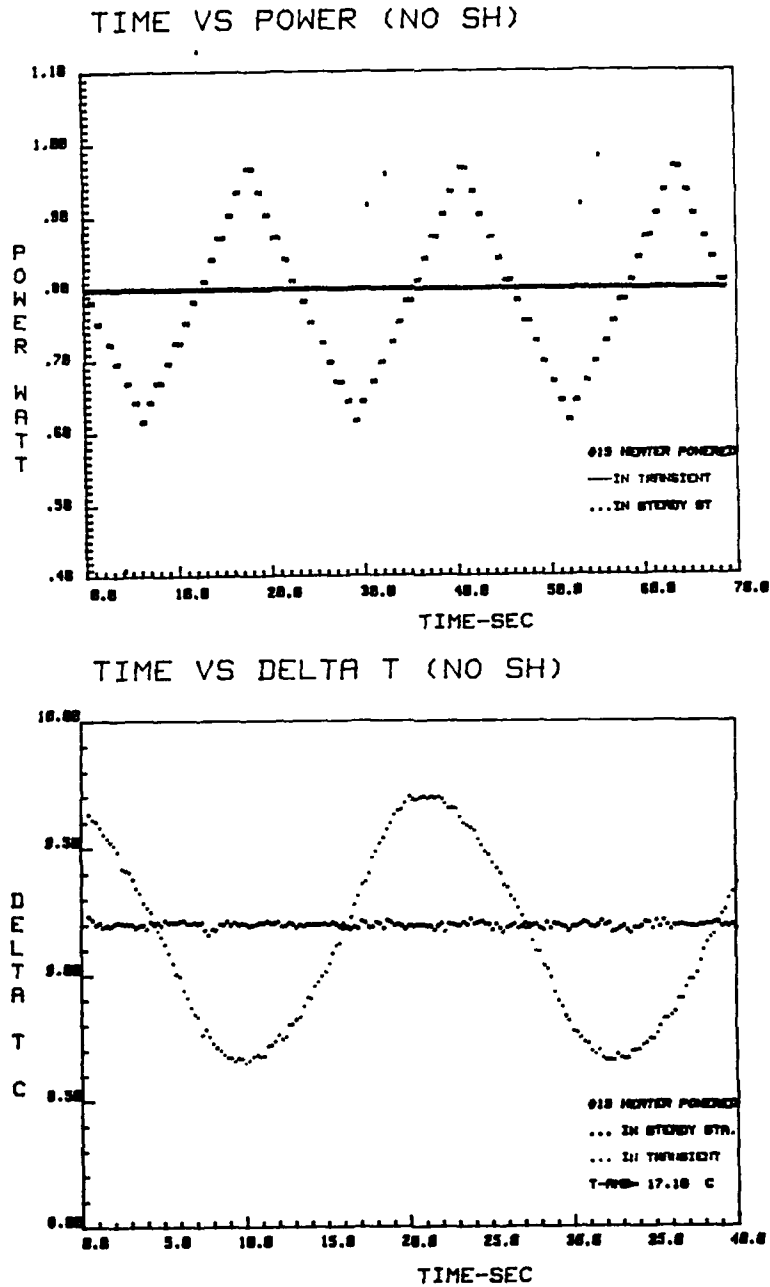


Figure 16. Oscillations in Surface Temperature of Bottom Heater Due To Input Power Pulsations with Mean Power of 0.8 W, Amplitude of 0.19 W and Period of 20 sec.

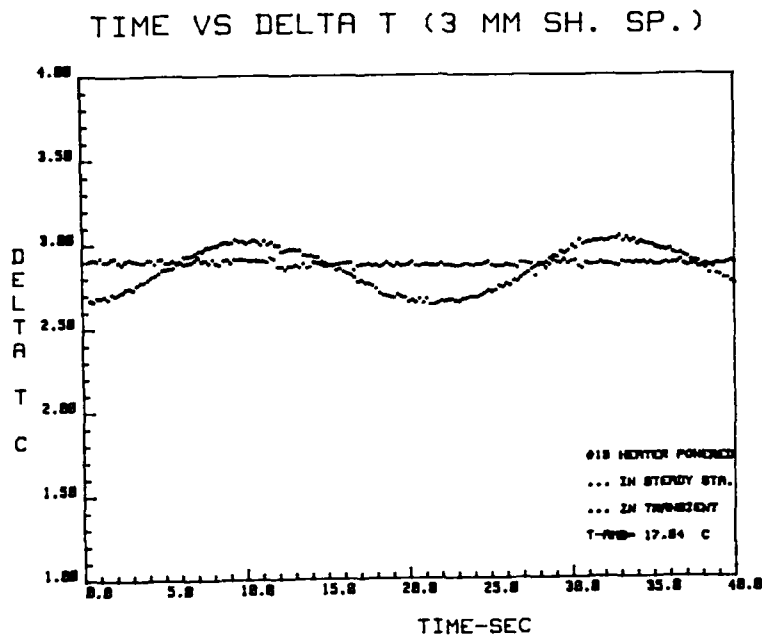


Figure 17. Oscillations in Surface Temperature of Bottom Heater Due To Input Power Pulsations with Mean Power of 0.2 W, Amplitude of 0.06 W and Period of 20 sec.

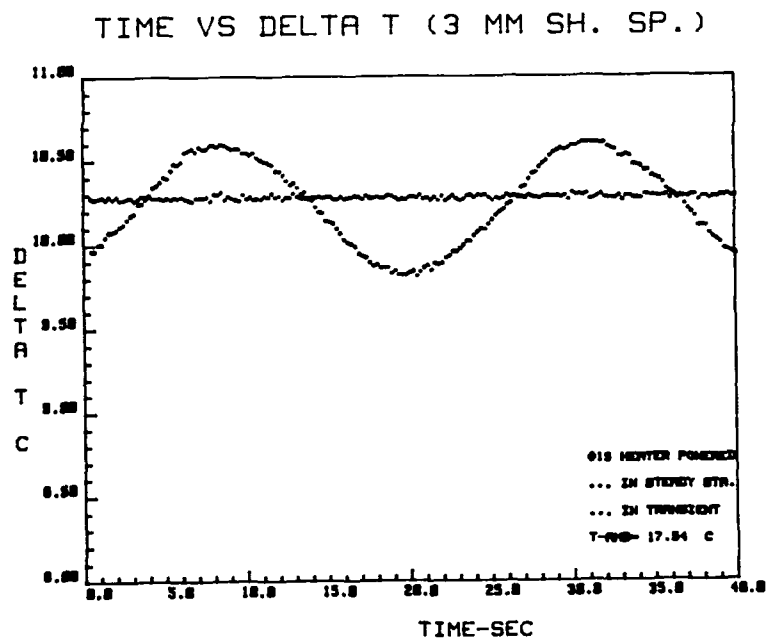


Figure 18. Oscillations in Surface Temperature of Bottom Heater Due To Input Power Pulsations with Mean Power of 1.0 W, Amplitude of 0.13 W and Period of 20 sec.

B. SINGLE COLUMN DATA

In another set of experiments the effects of transient power, applied to the heater at the bottom of the central column were examined. The remaining fourteen heaters in the column were steadily powered. The main point of interest was to look for changes in the heat transfer characteristics compared with those existing with steady power to all heaters. The same experimental procedure that is followed in the previous section is used for powering the bottom heater. The steady and transient temperature data were taken for five power levels, ranging from 0.2 W to 1.0 W both with and without a shroud. The surface temperatures of heaters 1st, 10th and 13th were monitored once steady power of bottom heater was switched to the periodic form. Temperature measurements were made with a sampling frequency of 300/335 Hz. over a period of 335 seconds.

1. Measurements In The Absence of Shroud

Figures 19-23 show ΔT versus x/L at steady input power levels of 0.2 W, 0.4 W, 0.6 W, 0.8 W and 1.0 W respectively. From the plots of data, the trend of increasing surface temperature along the test surface is readily apparent. It is also seen that at a given location, surface temperature increases with rising power level.

The steady temperature levels were used to determine the non-dimensional heat transfer characteristics. Rayleigh and Nusselt numbers were calculated as:

$Ra = (g\beta q l^3) / (\alpha k_f \rho)$, $Nu = h l / k_f$. Figures 24 and 25 are plots of Nu versus Ra for 0.2 W and 0.8 W respectively. The local values of h indicate a decreasing trend moving from the bottom heater to the top. It is also obvious that h values increase with rising power level at a given location due to the stronger flow.

The transient temperature data for the bottom heater over a period of 40 sec. were the same as for the single heater element examined in the previous section. Figures

26 and 27 are the temperatures of 1st, 10th and 13th heaters, over a period of 335 sec. for 0.4 W and 0.8 W input power levels respectively. As seen from the figures, oscillation in surface temperatures of downstream heaters, when power to the bottom heater is oscillated with time are barely noticeable.

2. Measurements With Shroud

In the previous section, it was found that the effects of the shroud on the heat transfer from the single heater element were not apparent. In this section, the effect of shroud is investigated with the entire central column powered. Surface temperature measurements of heaters were recorded at five different power levels for 3 mm shroud spacing. The results are compared with the unshrouded measurements.

The temperature rise above ambient for each heater at average power levels of 0.2 W and 0.8 W for 3 mm shroud spacing are seen in Figures 28 and 29. From these plots temperature values higher than the unshrouded case measurements are seen beyond the sixth heater element from the bottom. When the power levels increase, differences in ΔT values also increase compared to the unshrouded case. These measurements are in agreement with Knight [Ref. 13] and Gaiser [Ref. 10]. While the thermal layer near the bottom component is thin enough not to be effected by the presence of the shroud, the same is not true further downstream.

26 and 27 are the temperatures of 1st, 10th and 13th heaters, over a period of 335 sec. for 0.4 W and 0.8 W input power levels respectively. As seen from the figures, oscillation in surface temperatures of downstream heaters, when power to the bottom heater is oscillated with time are barely noticeable.

2. Measurements With Shroud

In the previous section, it was found that the effects of the shroud on the heat transfer from the single heater element were not apparent. In this section, the effect of shroud is investigated with the entire central column powered. Surface temperature measurements of heaters were recorded at five different power levels for 3 mm shroud spacing. The results are compared with the unshrouded measurements.

The temperature rise above ambient for each heater at average power levels of 0.2 W and 0.8 W for 3 mm shroud spacing are seen in Figures 28 and 29. From these plots temperature values higher than the unshrouded case measurements are seen beyond the sixth heater element from the bottom. When the power levels increase, differences in ΔT values also increase compared to the unshrouded case. These measurements are in agreement with Knight [Ref. 13] and Gaiser [Ref. 10]. While the thermal layer near the bottom component is thin enough not to be effected by the presence of the shroud, the same is not true further downstream.

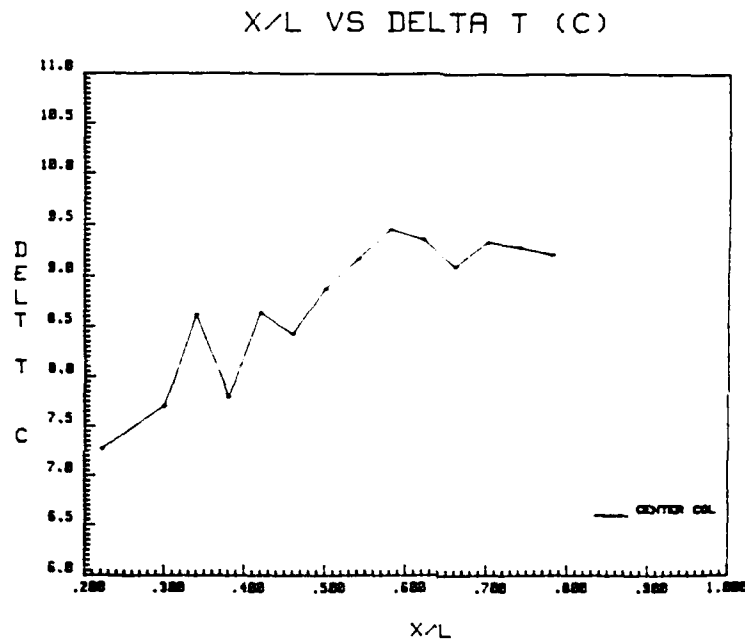


Figure 21. x/L versus ΔT at 0.6 W Input Power

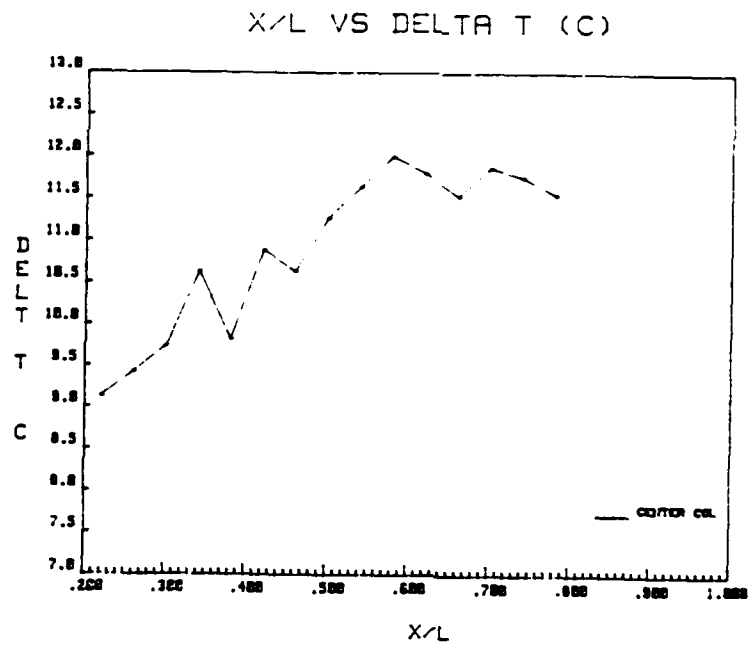


Figure 22. x/L versus ΔT at 0.8 W Input Power

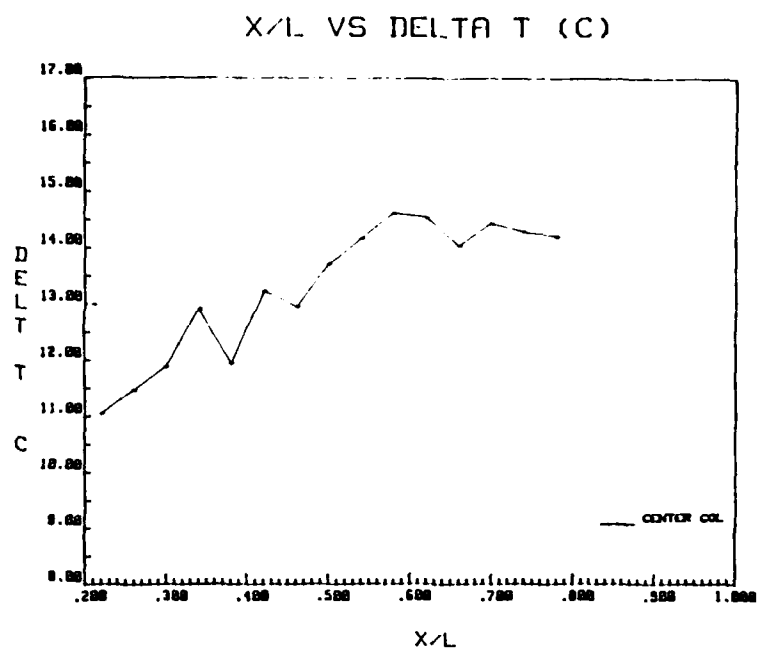


Figure 23. x/L versus ΔT at 1.0 W Input Power

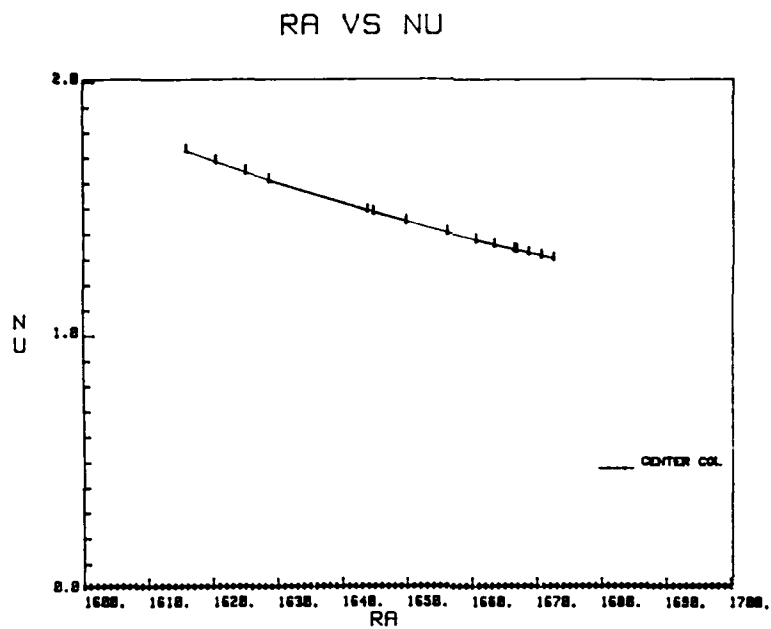


Figure 24. Nu versus Ra at 0.2 W

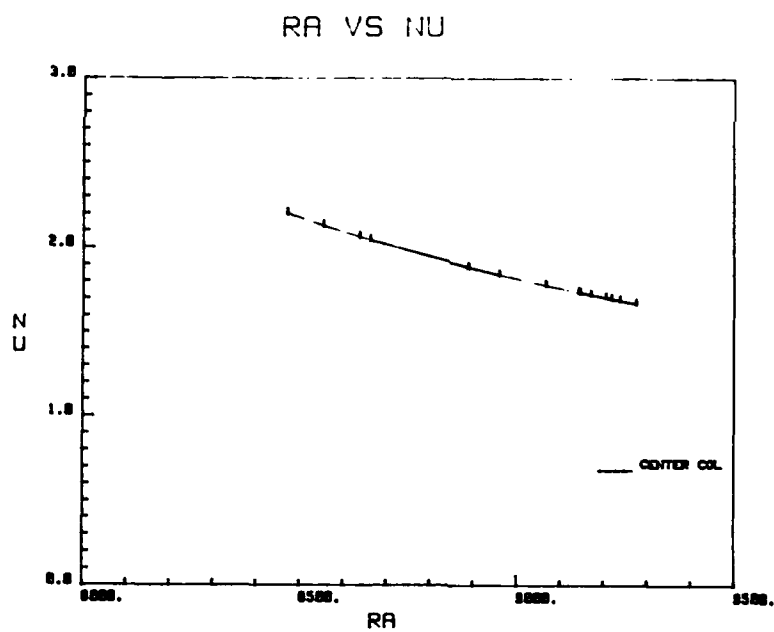


Figure 25. Nu versus Ra at 0.8 W

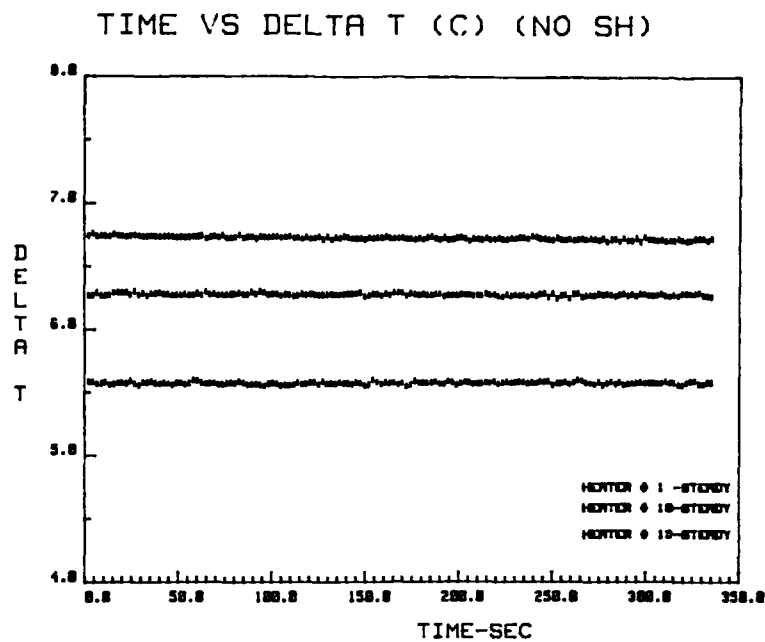


Figure 26. Monitoring The Surface Temperatures of Selected Heaters at 0.4 W When Input Power To The Bottom Heater Oscillated. Oscillation Amplitude and Period are 0.07 W and 20 sec. respectively.

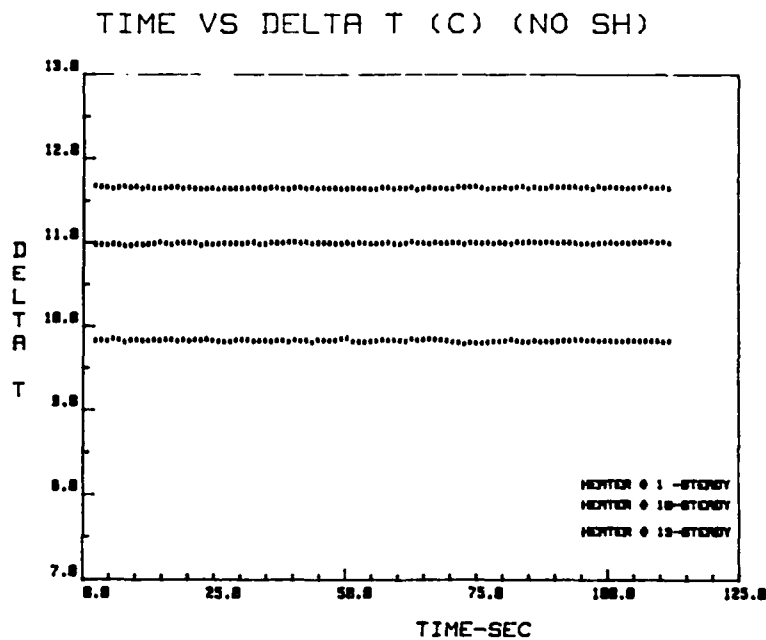


Figure 27. Monitoring The Surface Temperatures of Selected Heaters at 0.8 W When Input Power To The Bottom Heater Oscillated. Oscillation Amplitude and Period are 0.07 W and 20 sec. respectively.

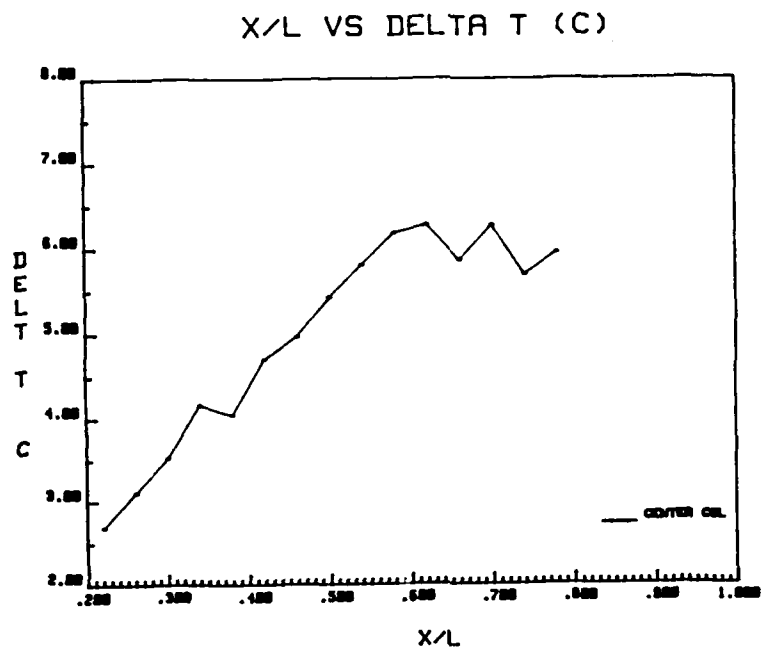


Figure 28. x/L versus ΔT at 0.4 W With 3 mm Shroud Spacing

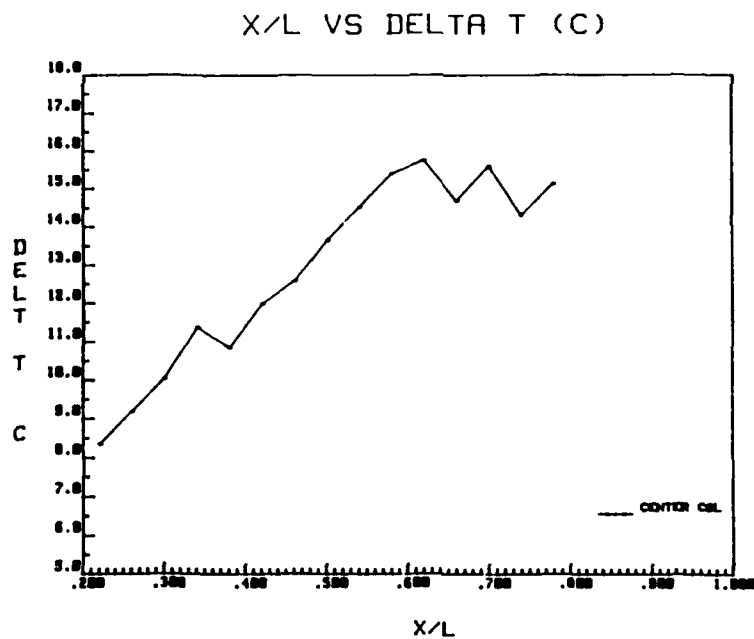


Figure 29. x/L versus ΔT at 0.8 W With 3 mm Shroud Spacing

C. DATA WITH ALL THREE COLUMNS POWERED

A third set of experiments was undertaken to examine the effects of placing flanking columns of heaters on each side of the central column. The three column results are discussed next. In addition to the measurements for the central column, the surface temperatures of top and bottom heaters of both side columns were also monitored for 335 sec. with a sampling frequency of 300/335 Hz. These transient measurements were repeated for average power levels ranging from 0.2 W to 1.0 W with 3mm shroud spacing and also without shroud. Additional runs were performed with steady power inputs, within the same power range and shroud spacings of 6 and 9 mm.

1. Measurements In The Absence of Shroud

The surface temperatures in each of the three columns are plotted to indicate changes in convective heat transfer characteristics as compared with the single column case. Figures 30 and 31 are ΔT versus x/L plots at steady power levels of 0.2 W and 0.8 W respectively. From these plots it is seen that at any x/L the central column has slightly higher ΔT values when compared to the right and left columns. Referring back to Figures 19 and 23 for a single column, it is apparent that the ΔT values for central column components with all three columns powered are similar to the values obtained for single column powered case. Comparing the heat transfer coefficients for these experiments with the single column values it was seen that the three column data produced almost the same values of h .

As was done with the single column, the surface temperature of the bottom heater of the central column was monitored for 40 sec. with a sampling frequency of 180/40 Hz, after modulating its input power with a time period of 20 sec. Once again the temperatures of the three heaters above it and the heater at the top of each column were also monitored for 335 sec. with a sampling frequency of 300/335 Hz. Figures 32-34 are plots of ΔT versus time for mean power 0.2 W, amplitude 0.06 W and Figures

35-37 for average power 0.8 W, amplitude 0.12 W. From the figures, no oscillation in the surface temperature in any heater indicates the damping of the effect of the input power variation in the bottom heater is observed. It is also noted that the surface temperature oscillation of bottom heater due to periodic power, follows the same pattern as for a single heater.

2. Measurements With Shroud

Measured heater surface temperatures are presented for the central column in Figures 38-40 at various shroud spacings and power levels. It is seen that the shroud has a significant effect on the heater temperatures only for small spacings. For spacings greater than 6 mm, the heater temperatures are almost equal to the unshrouded test case. Figure 41 compares the surface temperatures for 3 mm shroud spacing at various power levels. Figure 42 compares the measured surface temperatures without shroud with the values for 3 mm shroud spacing at 0.4 W and 0.8 W power levels. From the figure it is seen that as the shroud spacing decreases, surface temperatures of central column heaters are increased. Figure 43 shows the surface temperatures of all heaters for 3 mm shroud spacing at 0.4 W. From the figure it is seen that for this shroud spacing, surface temperatures of the central column heaters are higher than the measured values for the side columns at the same x/L . Fluid entrainment with shroud in place is impeded in the direction normal to the test surface. Lateral fluid movement brings warmer fluid from the flanking columns towards the central column. This results in an increase in temperature of the central column heaters.

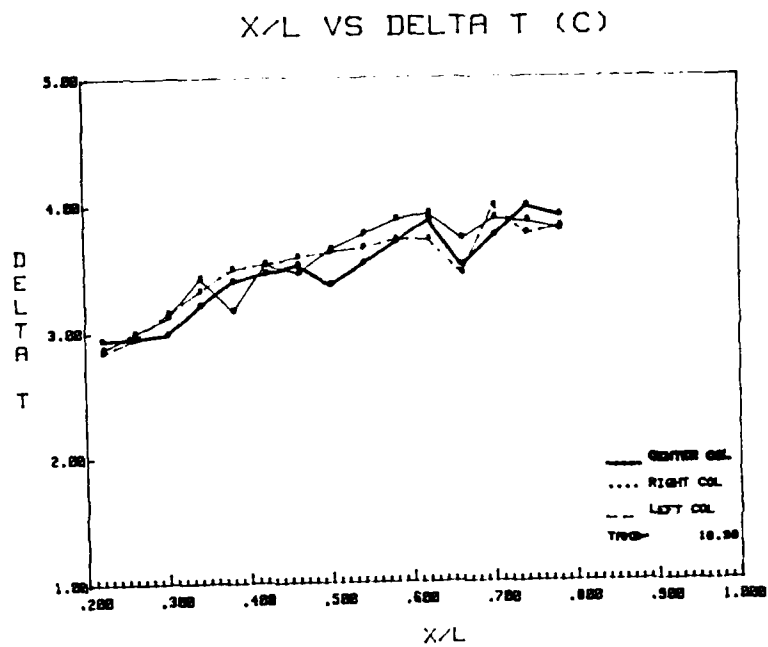


Figure 30. x/L versus ΔT at 0.2 W Input Power

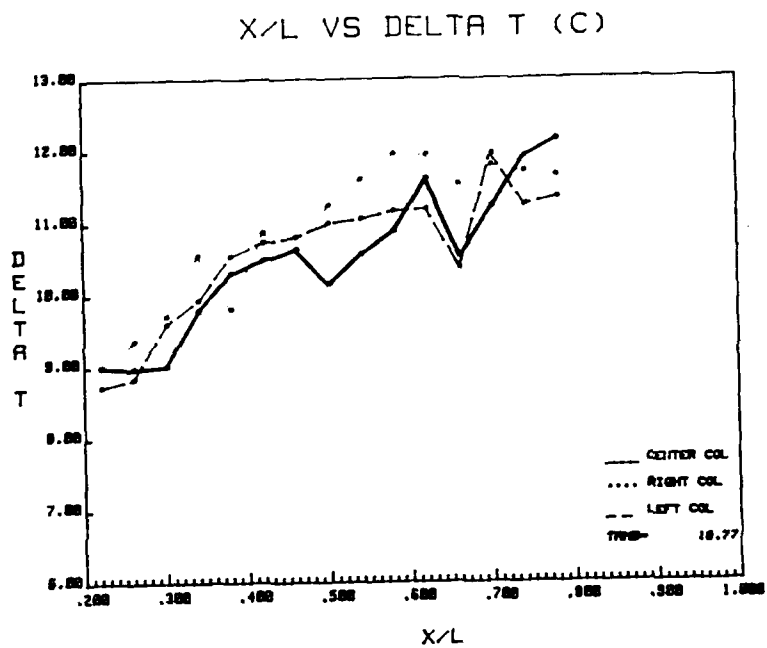


Figure 31. x/L versus ΔT at 0.8 W Input Power

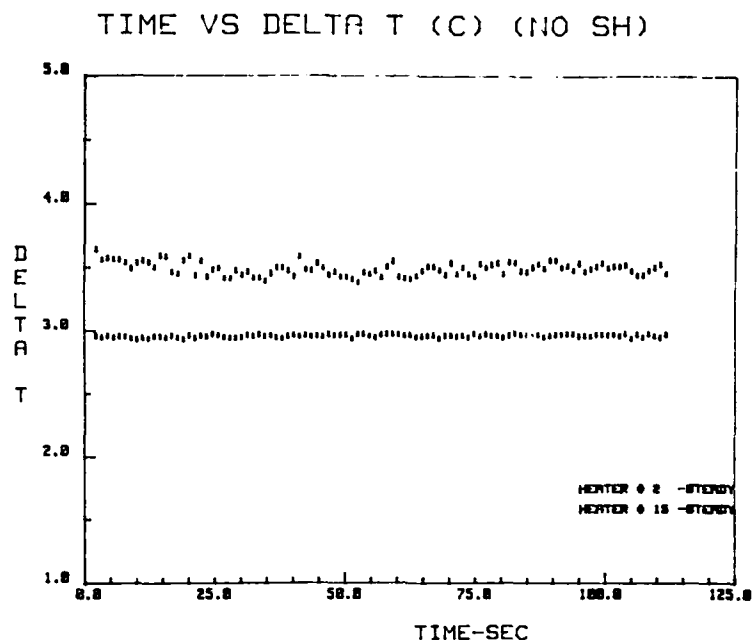


Figure 32. Monitoring The Surface Temperatures of Selected Heaters at 0.2 W When Input Power To The Bottom Heater Oscillated. Oscillation Amplitude and Period are 0.06 W and 20 sec. respectively.

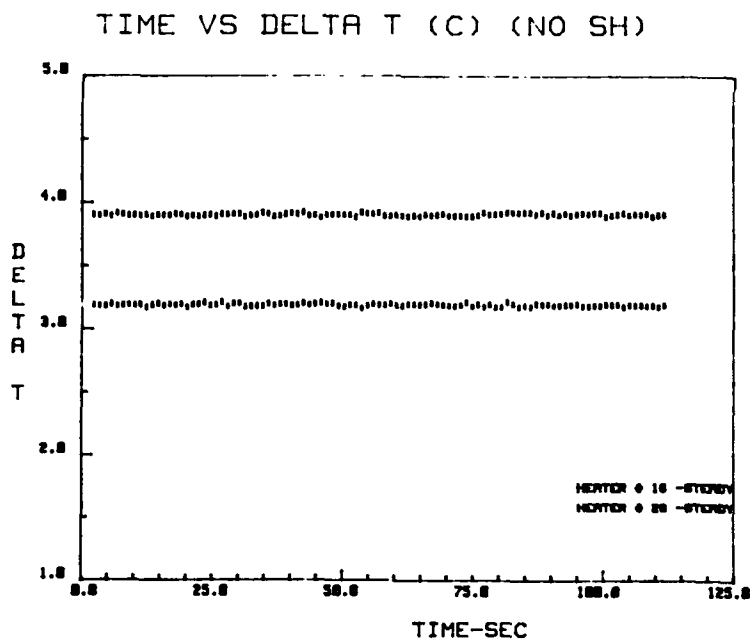


Figure 33. Monitoring The Surface Temperatures of Selected Heaters at 0.2 W When Input Power To The Bottom Heater Oscillated. Oscillation Amplitude and Period are 0.06 W and 20 sec. respectively.

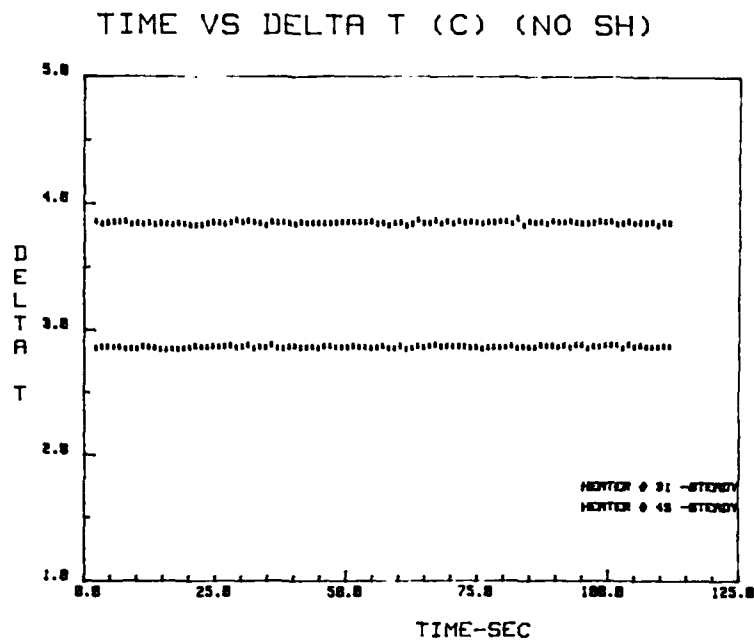


Figure 34. Monitoring The Surface Temperatures of Selected Heaters at 0.2 W When Input Power To The Bottom Heater Oscillated. Oscillation Amplitude and Period are 0.06 W and 20 sec. respectively.

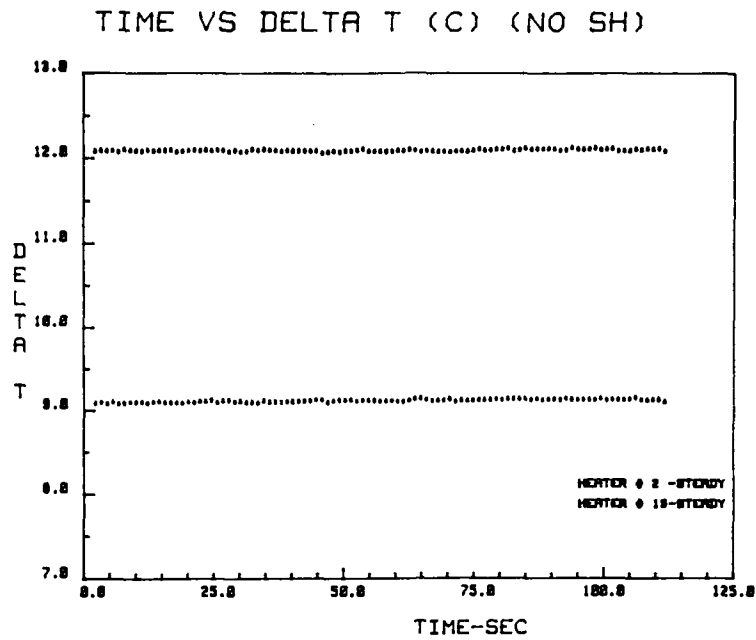


Figure 35. Monitoring The Surface Temperatures of Selected Heaters at 0.8 W When Input Power To The Bottom Heater Oscillated. Oscillation Amplitude and Period are 0.12 W and 20 sec. respectively.

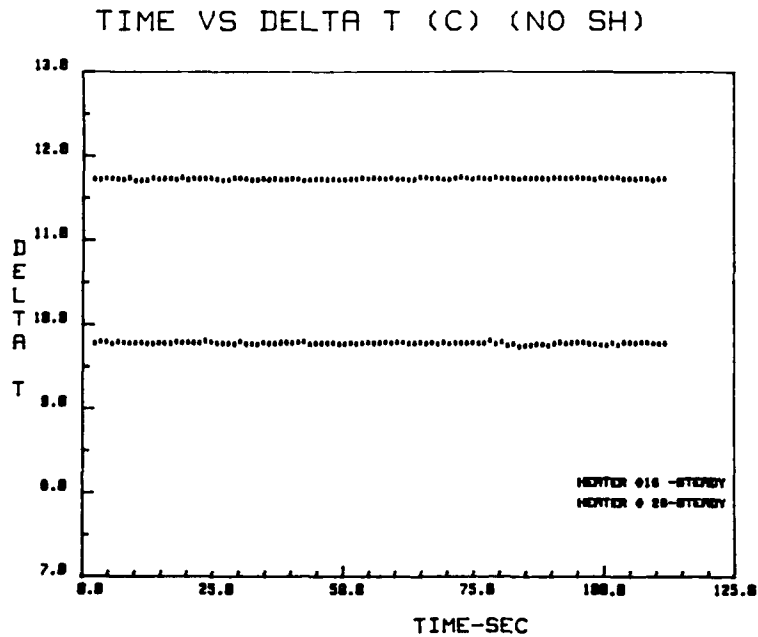


Figure 36. Monitoring The Surface Temperatures of Selected Heaters at 0.8 W When Input Power To The Bottom Heater Oscillated. Oscillation Amplitude and Period are 0.12 W and 20 sec. respectively.

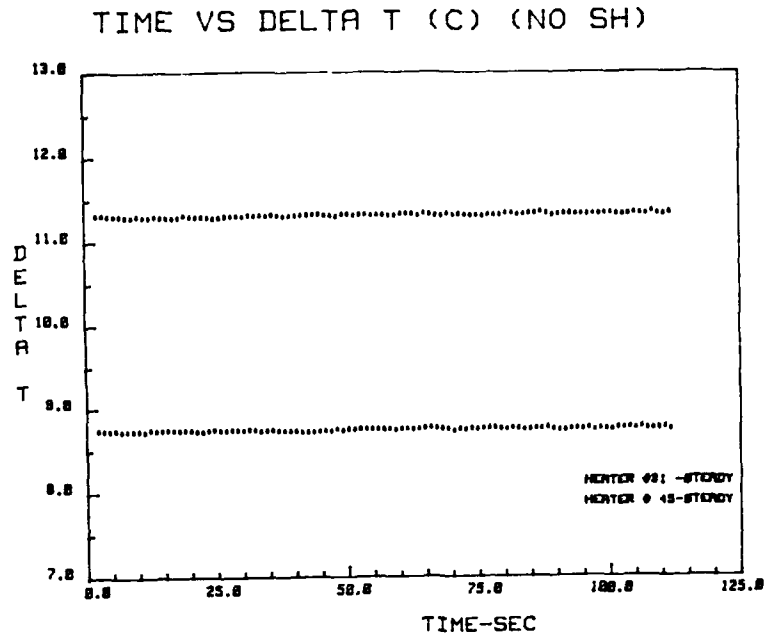


Figure 37. Monitoring The Surface Temperatures of Selected Heaters at 0.8 W When Input Power To The Bottom Heater Oscillated. Oscillation Amplitude and Period are 0.12 W and 20 sec. respectively.

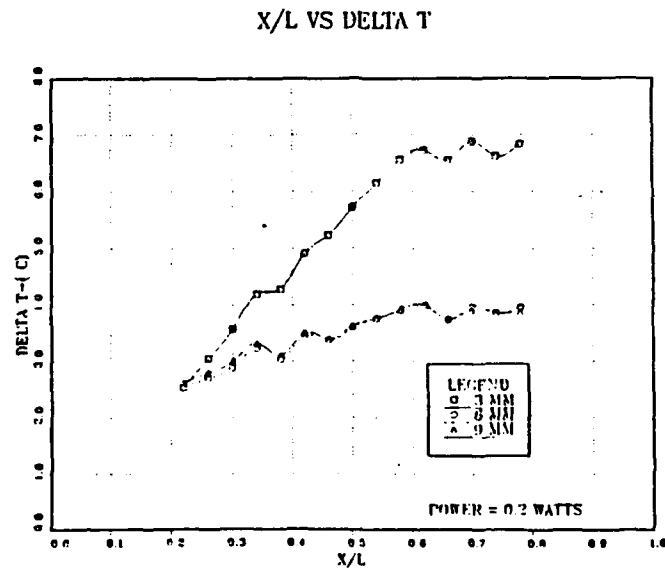


Figure 38. x/L versus ΔT for Different Shroud Spacings At 0.2 W

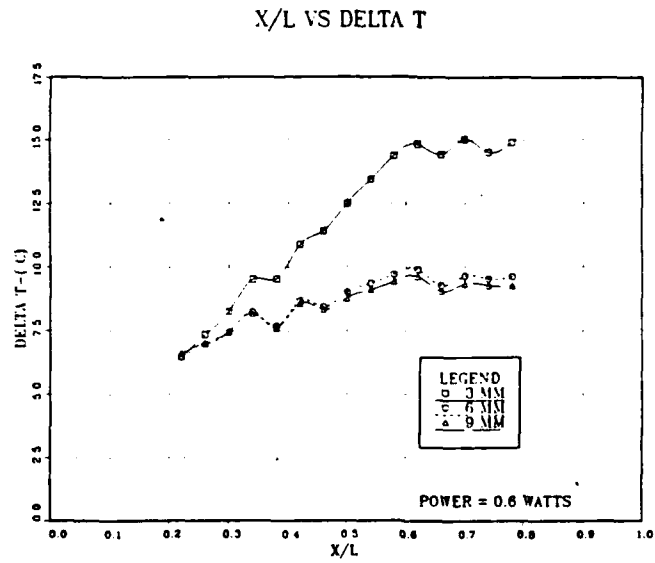


Figure 39. x/L versus ΔT for Different Shroud Spacings At 0.6 W

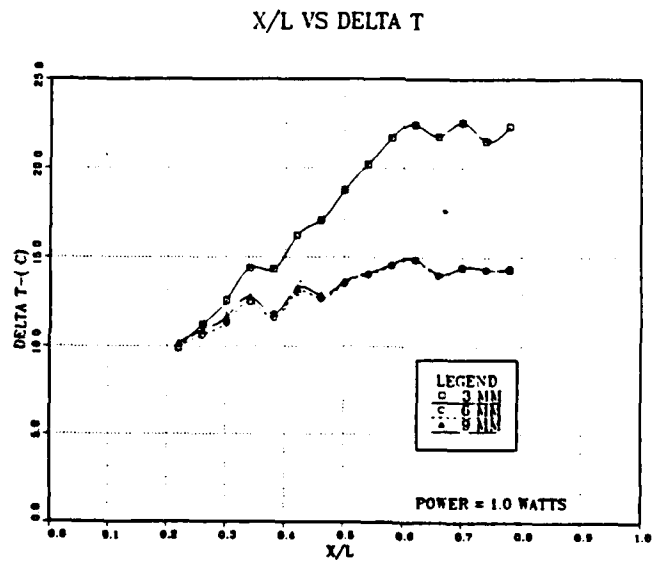


Figure 40. x/L versus ΔT for Different Shroud Spacings At 1.0 W

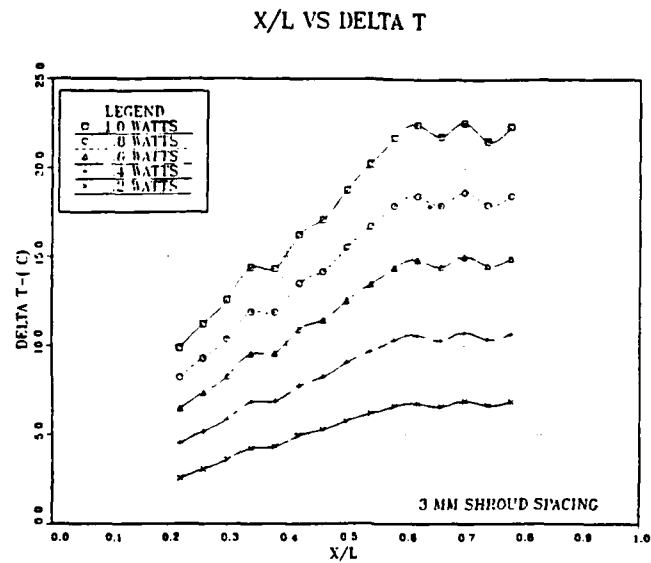


Figure 41. x/L versus ΔT for 3 mm Shroud Spacing At Various Power Levels

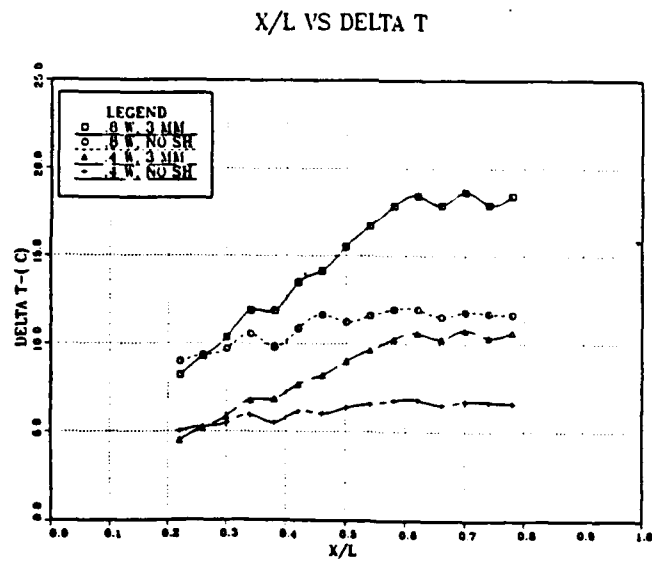


Figure 42. Comparison of Surface Temperatures Measured Without And With A Shroud at 3 mm For 0.4 W and 0.8 W

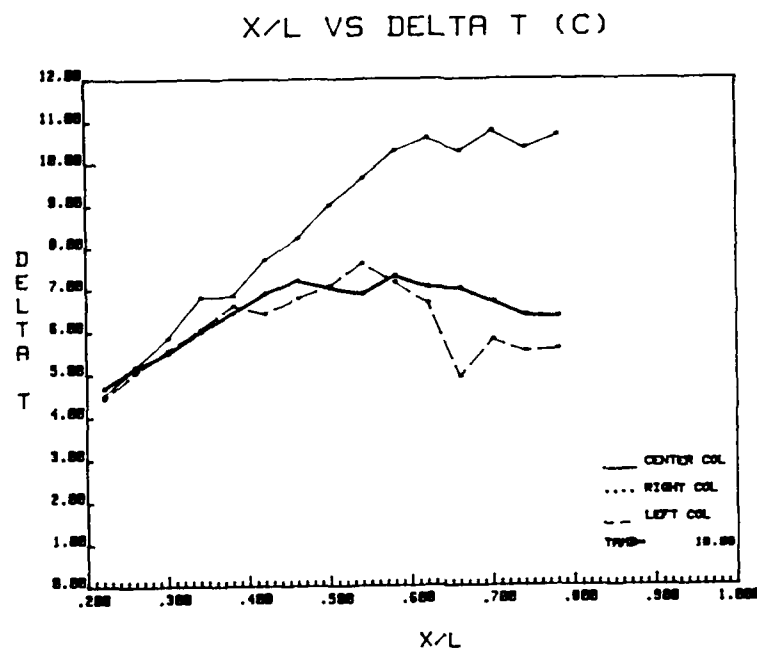


Figure 43. Effect of Shroud on Surface Temperatures of Heaters on Different Columns of Test Surface with The Same x/L

IV. NUMERICAL MODEL AND COMPARISON WITH MEASUREMENTS

Based on the experimental results presented in the previous chapter it is clear that in the absence of shroud the lateral fluid entrainment is not very strong. With only a single component powered, the transport away from the ends can then be modelled as two dimensional. In the following, a computational model of natural convection transport from a single flush heater is presented.

A. MATHEMATICAL FORMULATION

The schematic sketch of the configuration numerically investigated is shown in Figure 44. The flow is assumed to be two dimensional, resulting from a heat source, flush mounted on a vertical substrate and located at the middle of the surface. The shaded region represents the substrate, and the darker region in it represents the heater. The heater, the substrate and the fluid have constant thermophysical properties. The vertical coordinate x is measured upward from the base of substrate and u is the velocity component in this direction. The y coordinate is measured horizontally from the surface and v is the velocity component in the same direction. Isothermal impermeable enclosure walls with no-slip i.e $u = v = T = 0$ are prescribed as boundary conditions. The governing equations assuming no viscous dissipation and pressure energy terms and the Boussinesq approximations to be true, are:

FLUID REGION :

$$\frac{\partial (\rho_f)}{\partial t} + \frac{\partial (\rho_f u)}{\partial x} + \frac{\partial (\rho_f v)}{\partial y} = 0$$

$$\begin{aligned} \frac{\partial (\rho_f u)}{\partial t} + \frac{\partial (\rho_f u^2)}{\partial x} + \frac{\partial (\rho_f u v)}{\partial y} = & \mu \left(\frac{\partial^2 u}{\partial x^2} + \frac{\partial^2 u}{\partial y^2} \right) \\ & + \rho_f g \beta (T - T_{amb}) - \frac{\partial p}{\partial x} \end{aligned}$$

$$\frac{\partial (\rho_f v)}{\partial t} + \frac{\partial (\rho_f u v)}{\partial x} + \frac{\partial (\rho_f v^2)}{\partial y} = \mu \left(\frac{\partial^2 v}{\partial x^2} + \frac{\partial^2 v}{\partial y^2} \right) - \frac{\partial p}{\partial y}$$

$$\frac{\partial (\rho_f c_p T)}{\partial t} + \frac{\partial (\rho_f c_p u T)}{\partial x} + \frac{\partial (\rho_f c_p v T)}{\partial y} = k_f \left(\frac{\partial^2 T}{\partial x^2} + \frac{\partial^2 T}{\partial y^2} \right)$$

SUBSTRATE :

$$\frac{\partial (\rho_s c_p T)}{\partial t} = k_s \left(\frac{\partial^2 T}{\partial x^2} + \frac{\partial^2 T}{\partial y^2} \right)$$

HEATER REGION :

$$\frac{\partial (\rho_H c_p T)}{\partial t} = k_H \left(\frac{\partial^2 T}{\partial x^2} + \frac{\partial^2 T}{\partial y^2} \right) + q'''$$

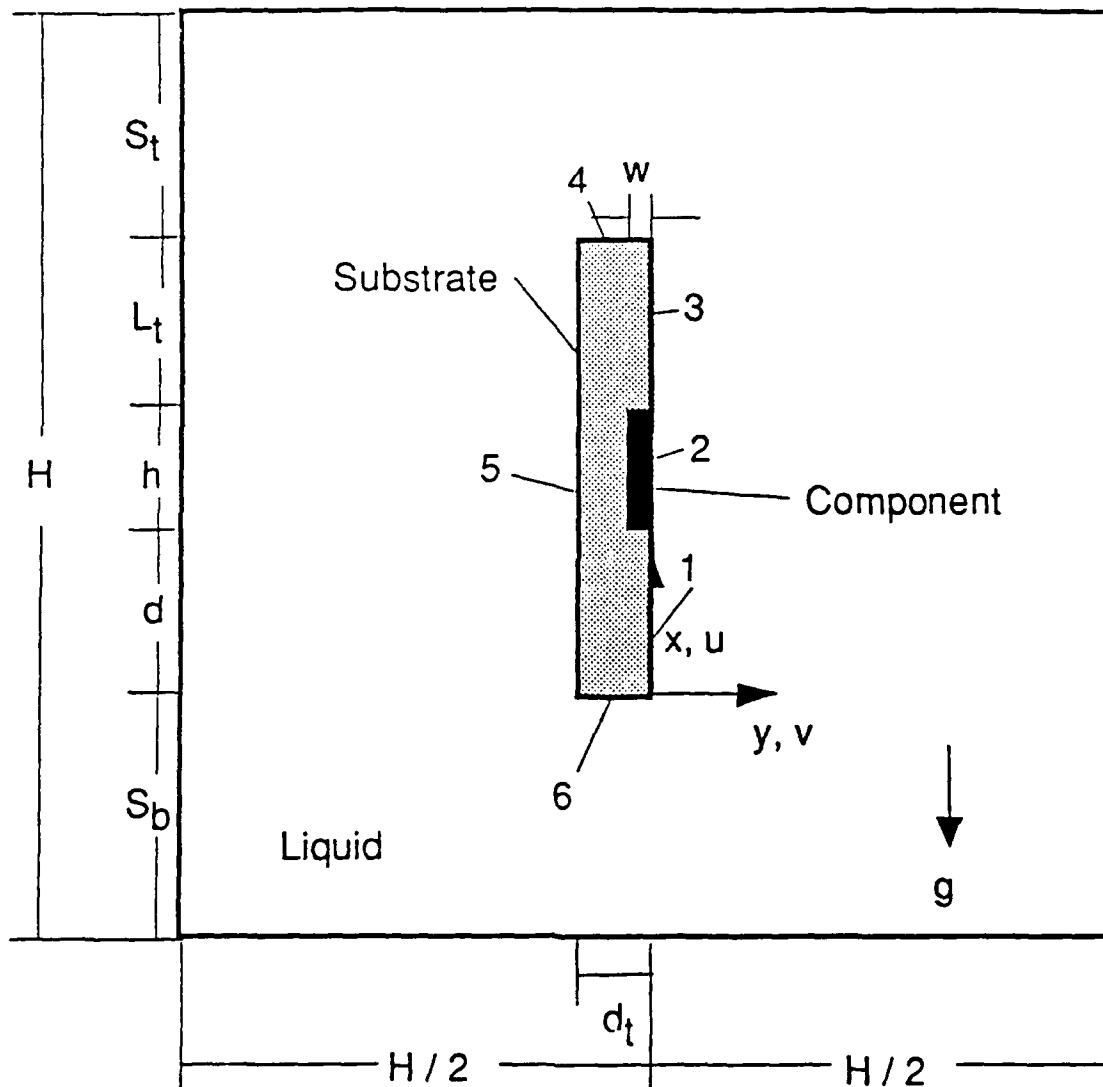


Figure 44. Numerical Model (After Haukeness [Ref. 10])

B. COMPUTATIONAL PROCEDURE

The information contained in the differential equations is discretized which makes it possible to replace the governing partial differential equations with algebraic equations, which can be solved with relative ease. A finite difference scheme is used for discretizing the equations. The calculation domain is divided into a number of control volumes such that there is one control volume surrounding each grid point. The temperature and pressure components are located at the main grid points. The location of the velocity components is staggered and defined on the control volume faces. The power law profile that provides a very good fit to the exact expression, is used for the spatial variation of the dependent variables between grid points. The harmonic mean formulation that provides physically meaningful results even with large changes in material properties is followed for the calculation of the interface diffusivities. The details of the discretization process can be found in Patankar [Ref. 14].

The discretized, nominally linear equations are solved by line-by-line TDMA (Tri-Diagonal Matrix Algorithm) method in which the coefficients are iteratively recalculated and the process repeated until convergence. Convergence is based on a balance of the rate of energy generated in the heater and the rate of energy leaving the enclosure walls. The SIMPLER (SIMPLE-Revised) algorithm that employs two different equations: one for the task of correcting the velocities, the other for obtaining a new pressure field, is followed during solution as outlined in [Ref. 14]. Even though separate equations are written for solid and fluid regions, numerically the solid region in the momentum equation is simulated by specifying a very large viscosity. The heat source term and property values in the energy equation are specified appropriately in the various regions. As a result, only one momentum and one energy equation are solved throughout the computational domain.

Numerical computations were performed on 48x56 control volumes. Different time steps were tried ranging from 0.1 sec. to 5.0 sec. to determine their effect on the solutions. Calculations for the modulated power input were started with u, v and T values, determined previously for a steady case with the same average power. The initial profiles were obtained by running the transient code with a very large time step.

The computations were performed initially on a IBM-370/3033 computer and later on an Amdahl Computer. Appendix 1 shows the problem dependent portion of the finite difference program used to obtain the numerical results.

C. COMPARISON OF COMPUTATIONS WITH EXPERIMENTAL MEASUREMENTS

Numerical investigation of transient heat transfer consisted of two parts. For the first, initial transient response due to sudden step power input was studied. Figures 45 and 46 show representative transient flow and temperature contour developments for 8.69 W/m step input. We note that for the heater size used in the experiments this power input corresponds to 0.2 W. The figures from left to right show the contours at 10, 44, 80 and 120 seconds following start of heating. At 10 sec. the isotherms are almost parallel to the heater indicating a diffusion dominated response. A single clockwise cell exists next to the heater. In the second and third figures, the secondary cell appears and grows. Flow becomes relatively faster and spreads further away. Also at 120 sec. the flow begins to resemble the fully developed condition seen in Figure 54 for the same input power.

For the second part of numerical study, the transient response following a periodic input power into the heater was studied. The amplitude and time period of imposed power oscillations were varied. Time steps from 0.1 sec. to 5.0 sec. were investigated. Surface temperatures calculated for different time steps are presented in Table 3. Transient variations of surface temperatures for different time steps are displayed in Figures 47 - 50. The surface temperature patterns are similar for all time steps. The highest difference in calculated temperature values was 2.25 %, when 5.0 sec. time step was used instead of 0.1 sec. Difference in calculated surface temperatures was smaller than 0.45 %, if calculations were performed with 0.5 sec. time step rather than 0.1 sec. In order to optimize the computation times without compromising significantly on the accuracy, all numerical calculations were carried out with a time step of 0.5 sec.

Numerical computations were also performed for two different sets of heating element properties since the actual element properties in the experiments were not easily

quantifiable. In the experiment, the composite heater element consisted of an inconel ribbon attached to a kapton substrate. In order to cover the range of property variations between the two materials, the computations were repeated, with the properties of inconel and of plastic separately for the heater [Ref. 15]. Figures 51 and 52 show the numerically calculated surface temperatures with time for average power levels of 0.2 W and 1.0 W for plastic heater and Figure 53 for inconel heater at 1.0 W average power level. While the mean temperatures in Figure 53 are lower than in Figure 52, the amplitudes of temperature oscillations remain approximately the same.

Table 3. EFFECT OF SELECTING DIFFERENT TIME STEPS ON COMPUTED QUANTITIES

TIME_(sec.)	Surface Temperatures (°C) Calculated by Taking Time Steps (sec.) of :			
	0.1	0.5	1.0	5.0
0.1	2.1271	-	-	-
0.5	2.1186	2.1179	-	-
1.0	2.1094	2.1081	2.1072	-
2.0	2.0955	2.0930	2.0910	-
5.0	2.0866	2.0806	2.0756	2.0394
10.0	2.1615	2.1512	2.1412	2.0660
15.0	2.2149	2.2104	2.2074	2.1848
20.0	2.1474	2.1484	2.1522	2.1802

Table 4. THERMOPHYSICAL PROPERTIES OF MATERIALS IN HEATER ELEMENT

Thermophysical Property	MATERIAL	
	Inconel	Plastic
c_p (J/kg-K)	439.0	1500.0
k (W/m-K)	11.7	0.2
ρ (kg/m ³)	8510.0	1180.0

Streamlines

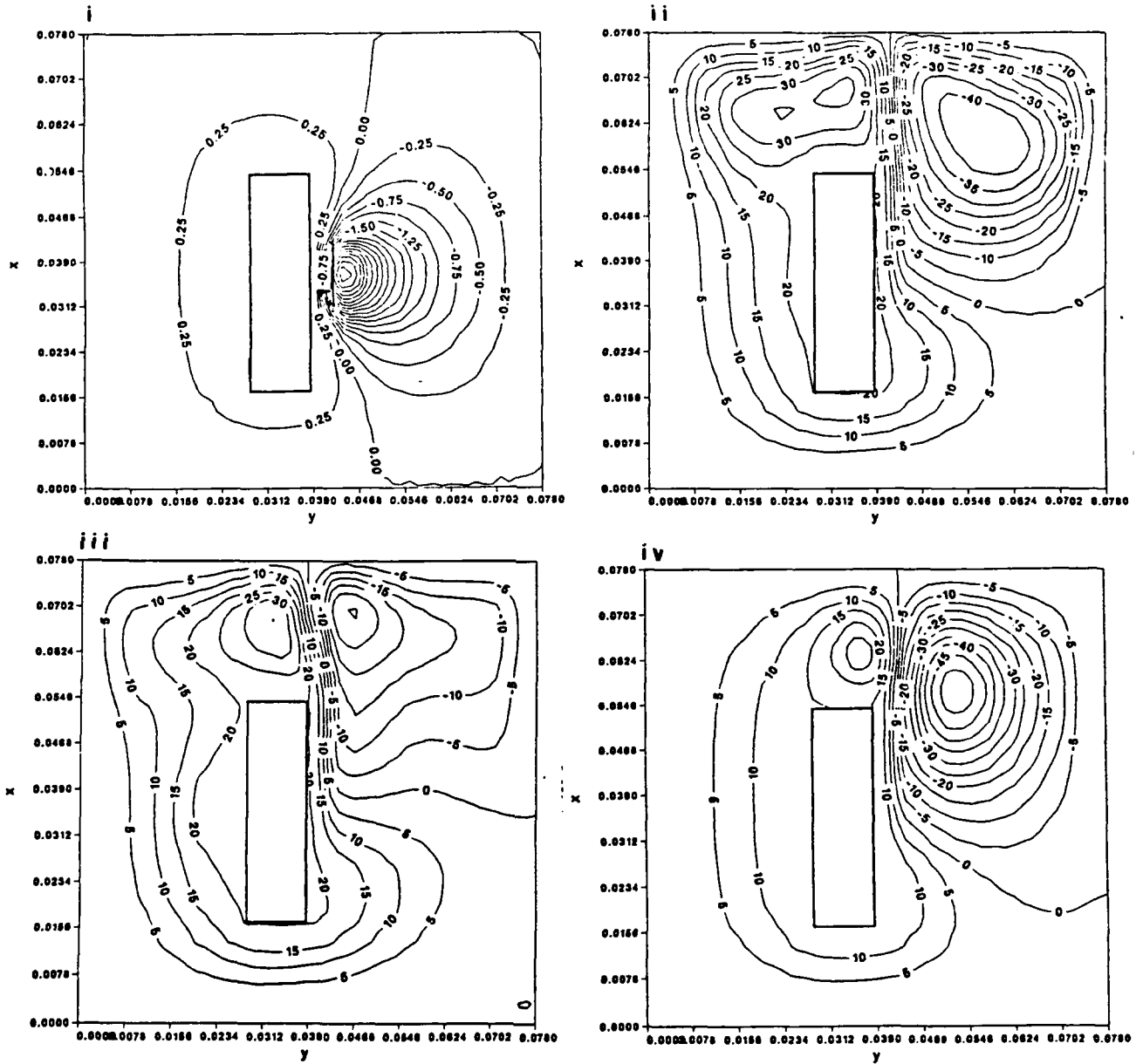


Figure 45. Development of Flow During Initial Transient Due To 0.2 W Step Input Power. The Figures are at (i)10, (ii)44, (iii)80 and (iv)120 seconds.

Temperature Contours

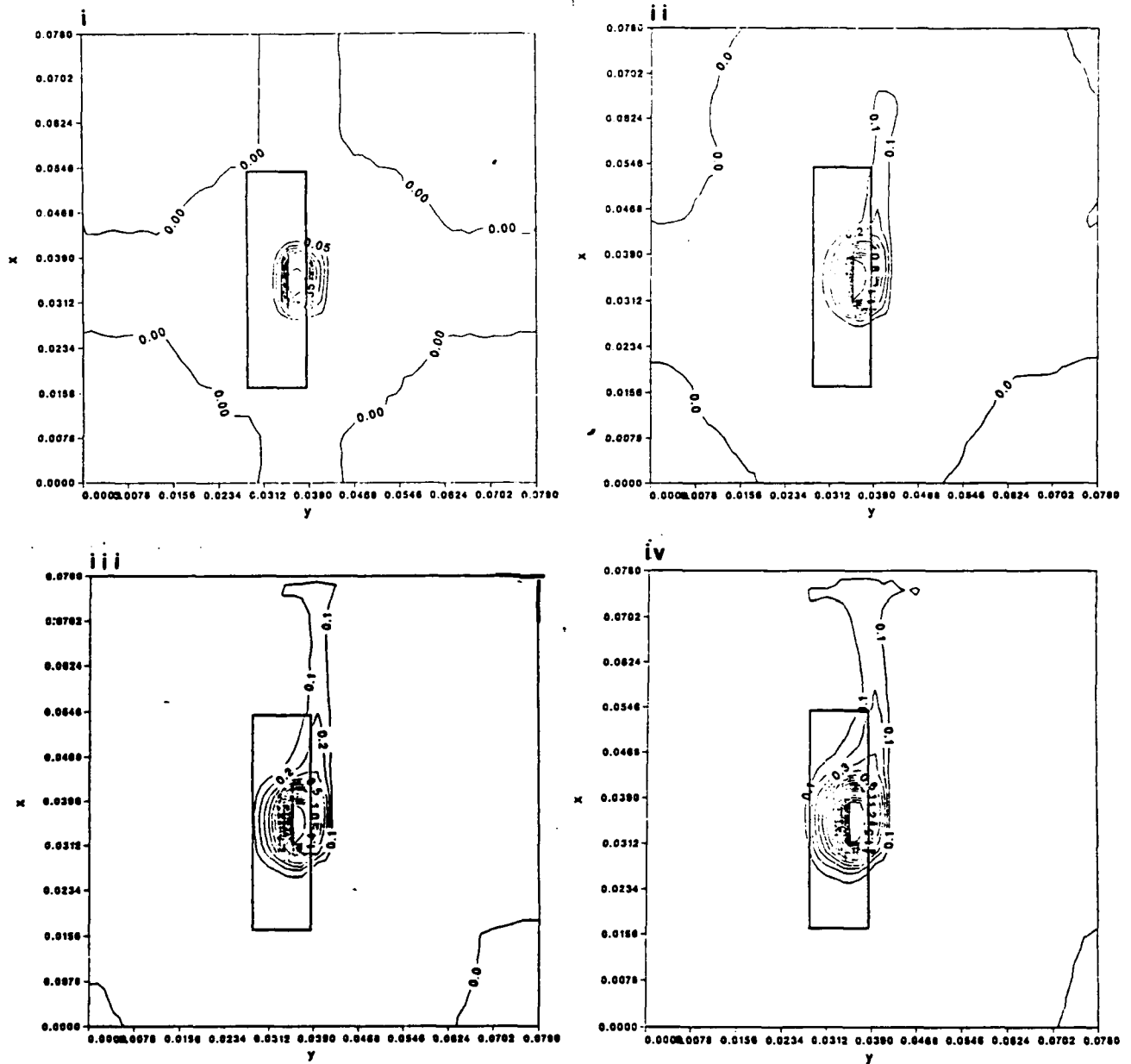


Figure 46. Development of Temperature Contours Due To 0.2 W Step Input Power. The Figures are at (i)10, (ii)44, (iii)80 and (iv)120 seconds.

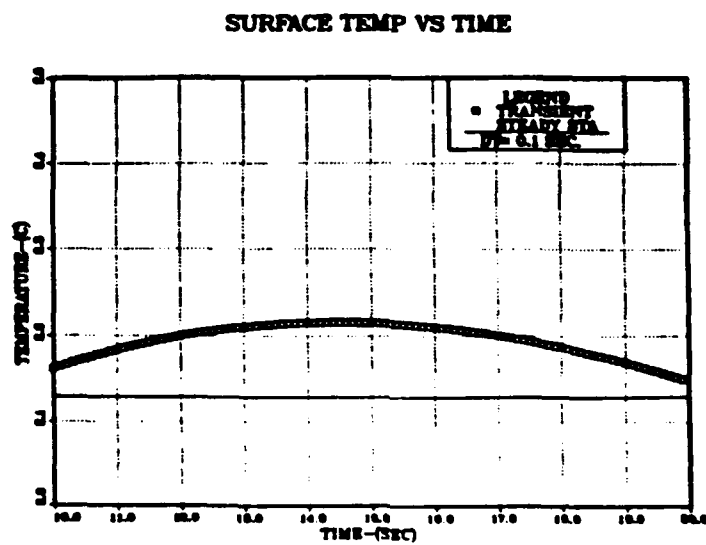
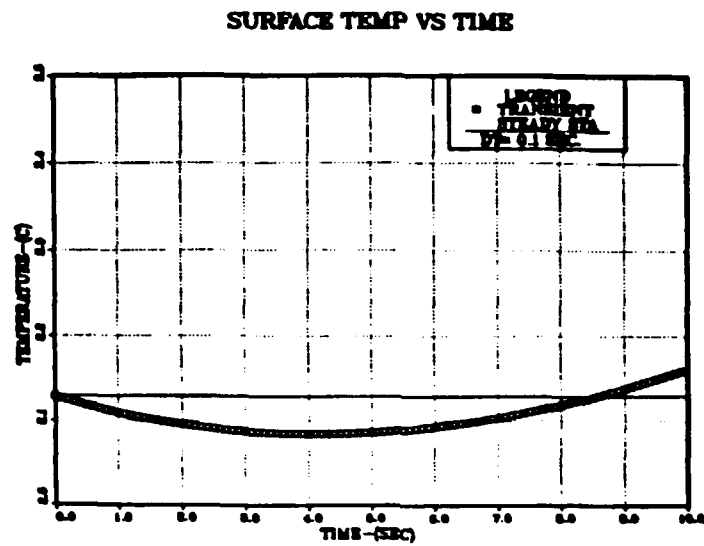


Figure 47. Surface Temperature Calculated with Time Step of 0.1 sec.

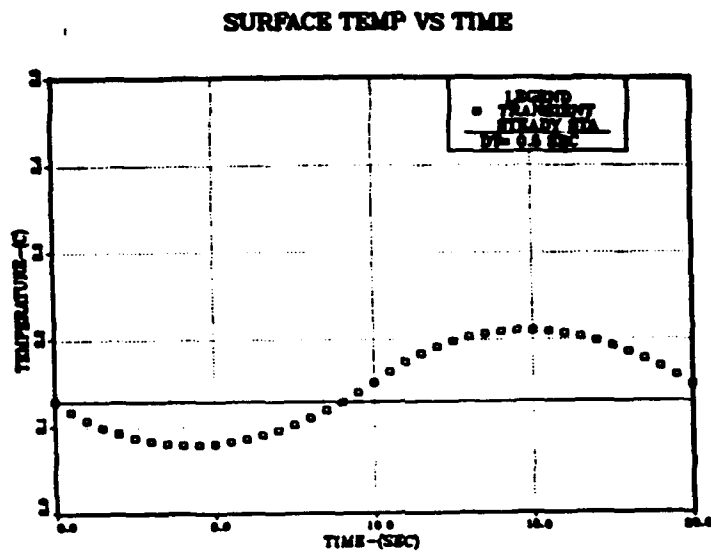


Figure 48. Surface Temperature Calculated with Time Step of 0.5 sec.

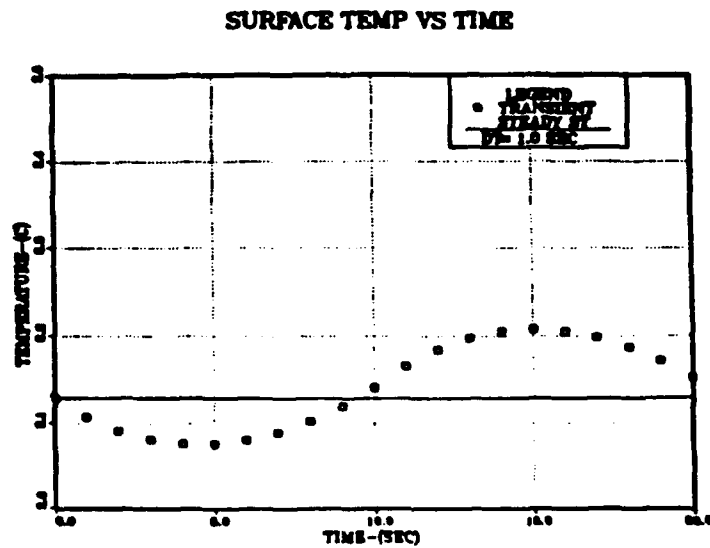


Figure 49. Surface Temperature Calculated with Time Step of 1.0 sec.

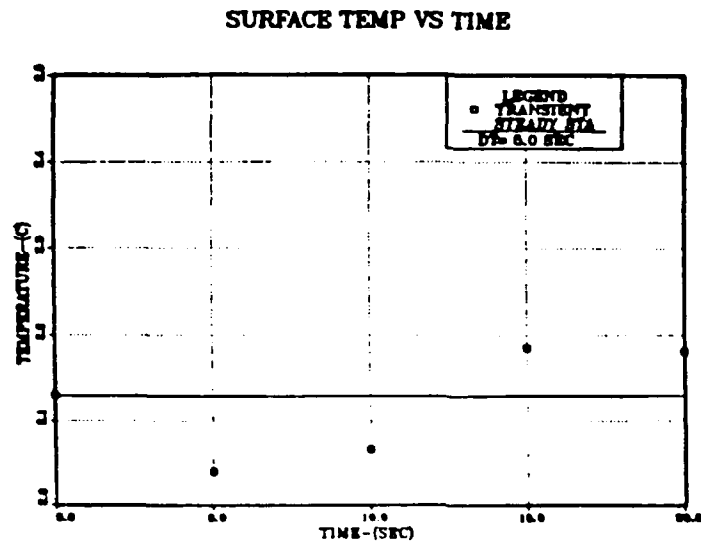


Figure 50. Surface Temperature Calculated with Time Step of 5.0 sec.

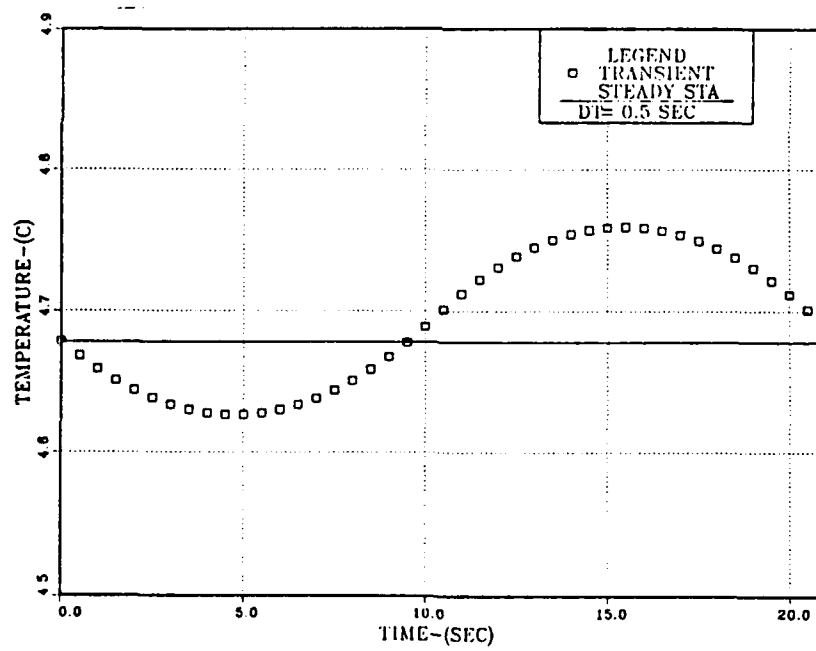


Figure 51. Surface Temperature Calculated with the Properties of Plastic at 0.2 W Average Input Power

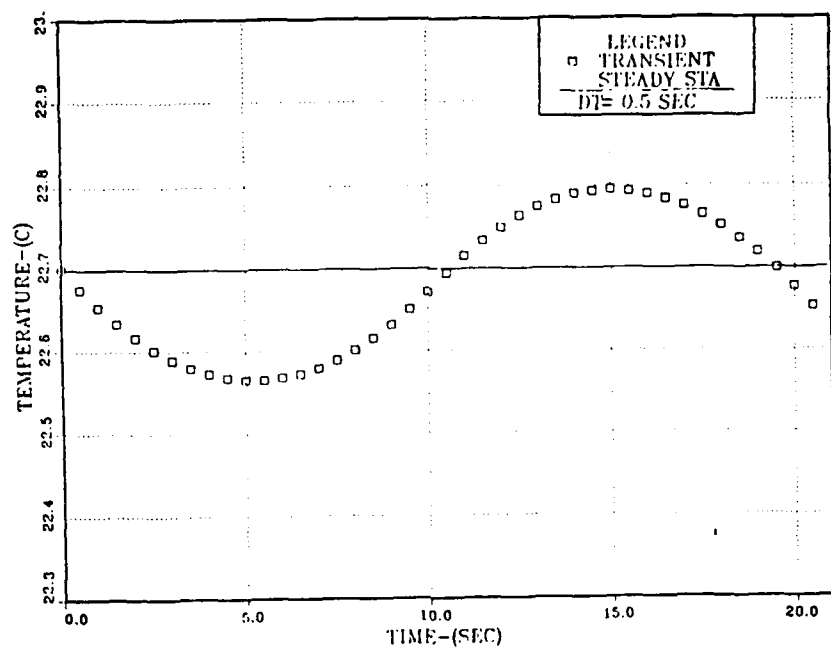


Figure 52. Surface Temperature Calculated with the Properties of Plastic at 1.0 W Average Input Power

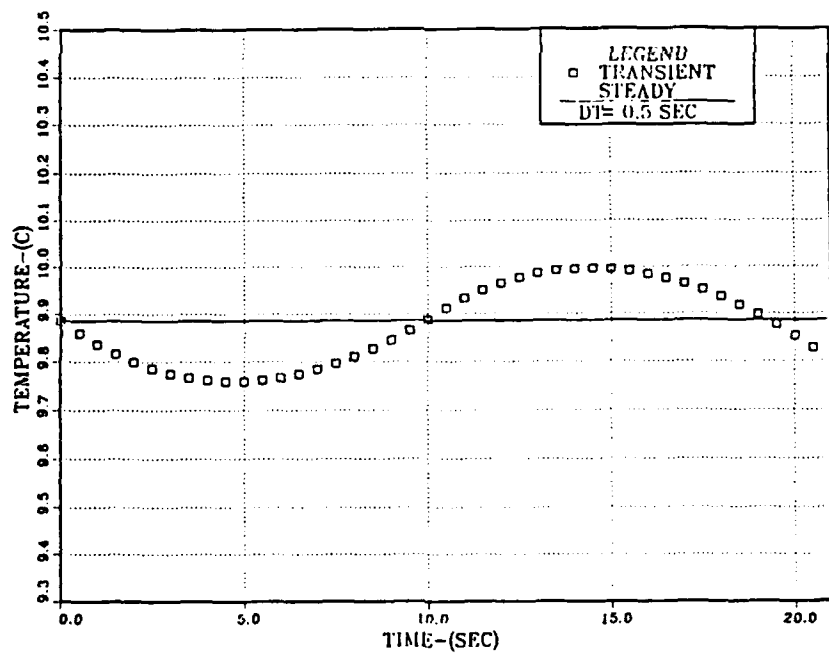


Figure 53. Surface Temperature Calculated with the Properties of Inconel at 1.0 W Average Input Power

COMPARISON

The bottom heater in the central column (Section AA in Fig.4) was chosen for a comparison with numerical results. For 0.2 W average power input with 0.06 W amplitude and 20 sec. pulsations, the steady periodic temperature response, calculated at the back of the model heater, was 27 % lower than the measured for an inconel heater and 38 % higher than the measured value for a plastic heater. The oscillation amplitudes in calculated surface temperatures agreed within approximately 33 % with the experimentally measured values. For the 1.0 W average power case, the calculated surface temperature of an inconel heater was 13 % lower than the experimentally measured value. The calculated value for a plastic heater was 51 % higher than the measured one. The amplitudes of oscillations in calculated surface temperatures agreed within 33 % with the experimental values.

The percent differences, presented in the following between numerically calculated and experimentally measured surface temperatures, are for the case when the heater material is assumed to be inconel. Figures 54 and 55 show the corresponding temperature contours and streamlines for the average power input levels of 0.2 W and 1. W. The effect of change in the period of the input power pattern was also examined numerically. Figures 56 and 57 show the surface temperature variation with time for 0.2 W average power with different periods. The trend for increasing period of the measured temperature response due to increase in period of applied power is evident. When compared to the experimentally measured values, the calculated temperature oscillation amplitudes were almost 33 % lower for all power levels. Figures 58-60 show the effects of the period of applied power for a higher average power level of 0.6 W.

The effect of change in the amplitude of the applied power variation was also investigated. Computations revealed increasing differences between peak values of calcu-

lated heater surface temperatures due to increase in amplitude of applied power. The calculated surface temperatures versus time for 0.4 W and 0.8 W average power levels with changing amplitudes are presented in Figures 61 and 62. The corresponding temperature contours and streamlines are plotted in Figures 63 and 64. The calculated steady mean temperature was almost 21 % lower for 0.4 W and 13 % lower for 0.8 W compared to the experimentally measured values. The calculated oscillation amplitudes in surface temperatures agreed only within 67 % with the experimental values for both power levels.

This difference can be ascribed to the larger thickness of the heater model than the actual value. The actual thickness was about .195 mm. However a very fine grid will be required if this size is to be taken in the model. As the thickness of the heater in the computational model was reduced, the oscillation amplitudes increase. This trend is presented in Figure 66 with the depth of the heater reduced to half of the previous value. If the actual properties of heater element which are combination of inconel and kapton properties were available, it is obvious that the agreement with the experiment will improve. The experimentally measured temperature values are bracketed by the computations, as expected.

Additional computations were performed with k values between inconel and plastic to achieve better agreement between the model and experiments. Figure 65 shows the surface temperatures calculated with $k_H = 1.45 \text{ W/m}^\circ\text{C}$. It is seen that calculated values are reasonably close to the experimental values. A particular run was performed with $k = 1.0 \text{ W/m-K}$ and heater thickness of .195 mm. Computed results are presented in Figure 67. For these choices of thermophysical properties and component dimensions close agreement is seen with the experimental data in Figure 4.

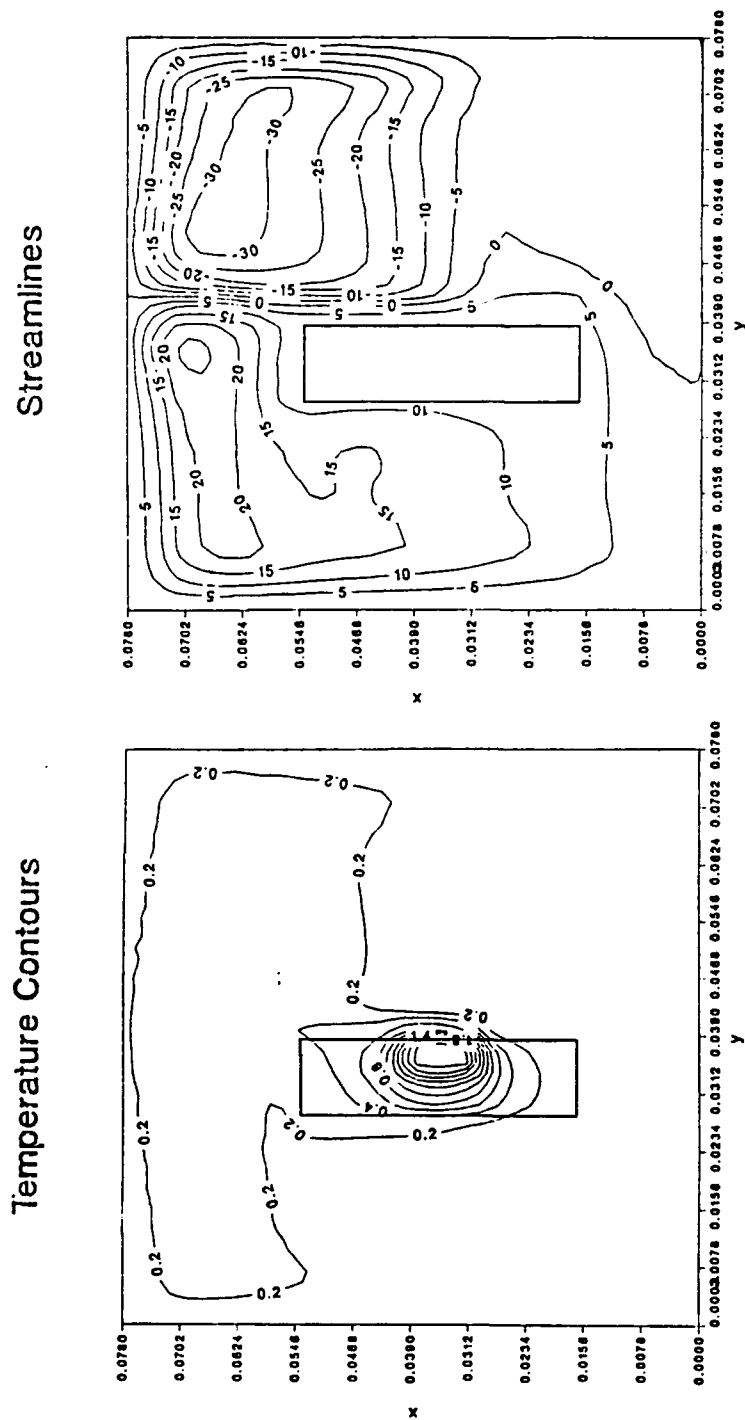
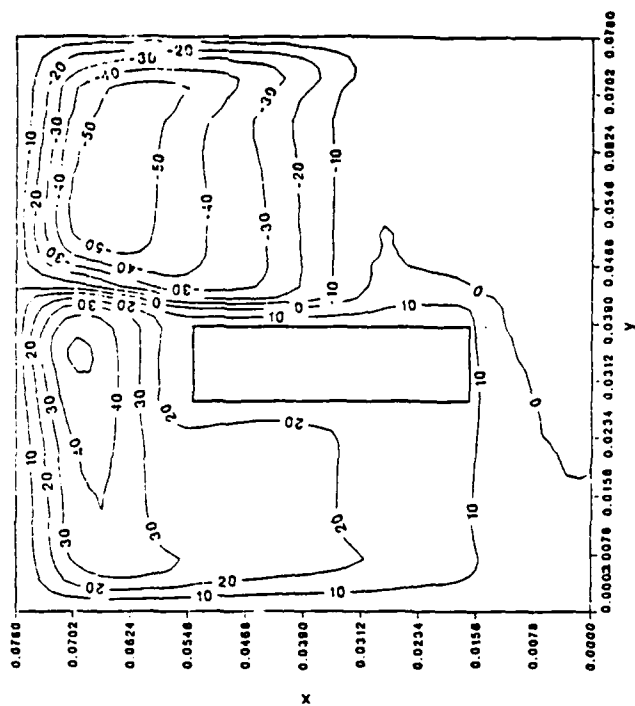


Figure 54. Temperature Contours and Streamlines with An Inconel Heater for Mean Power of 0.2 W, Amplitude of 0.06 W, Period of 20 sec at 15th sec

Streamlines



Temperature Contours

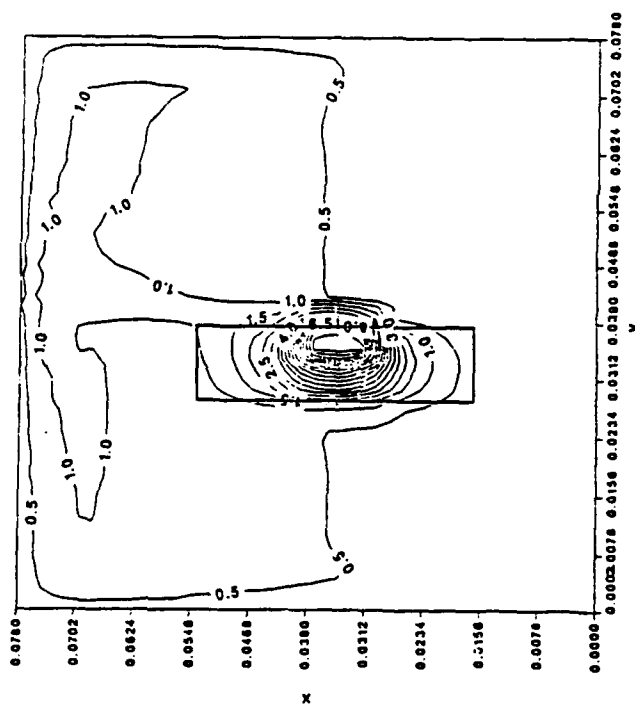


Figure 55. Temperature Contours and Streamlines with An Inconel Heater for Mean Power of 1.0 W, Amplitude of 0.13 W, Period of 20 sec at 15th sec

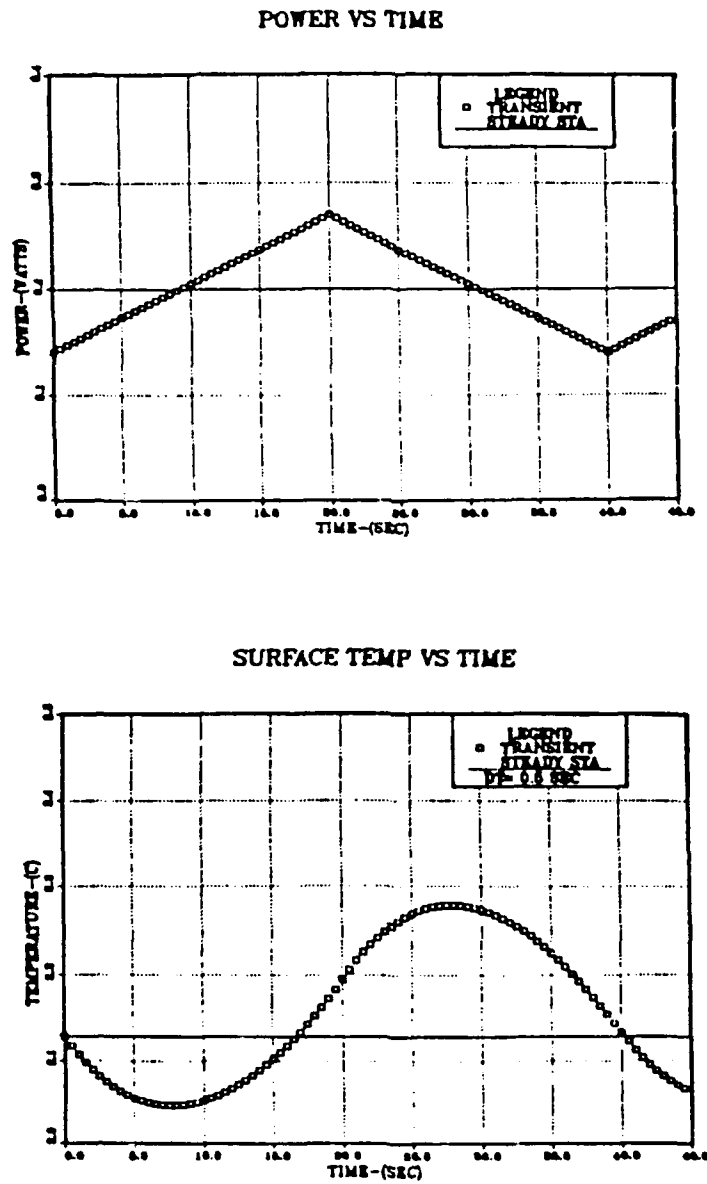


Figure 56. Surface Temperature Due to Power Pulsation with a Period of 40 sec.
for 0.2 W Average Power and Amplitude of 0.06 W.

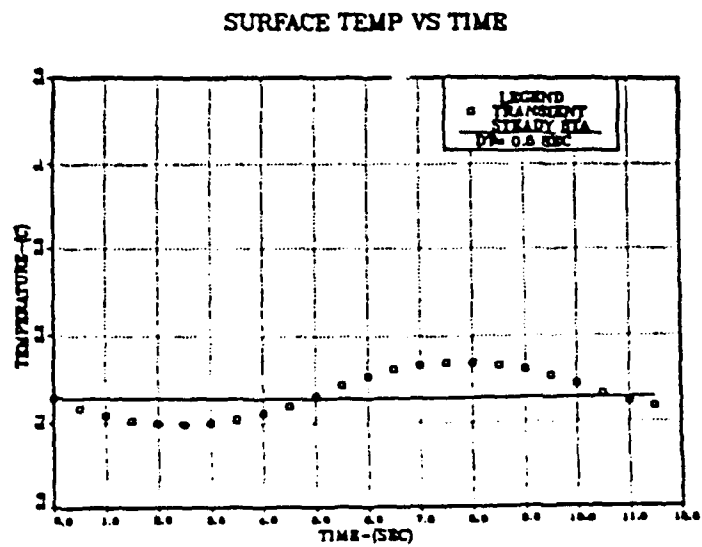
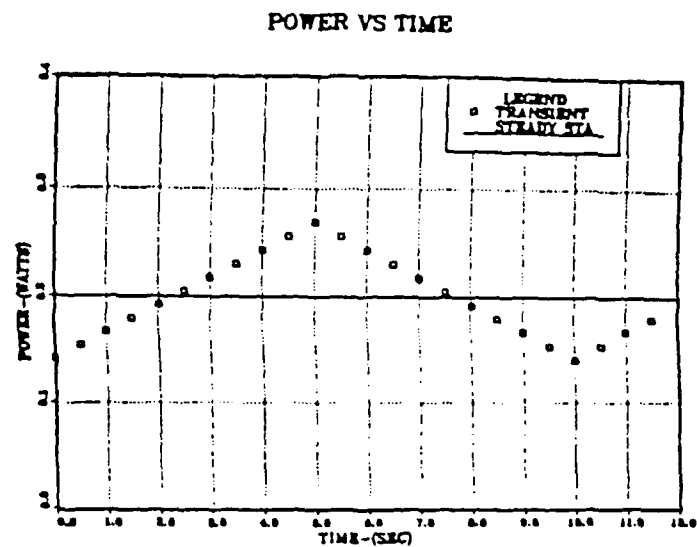


Figure 57. Surface Temperature Due to Power Pulsation with a Period of 10 sec.
for 0.2 W Average Power and Amplitude of 0.06 W

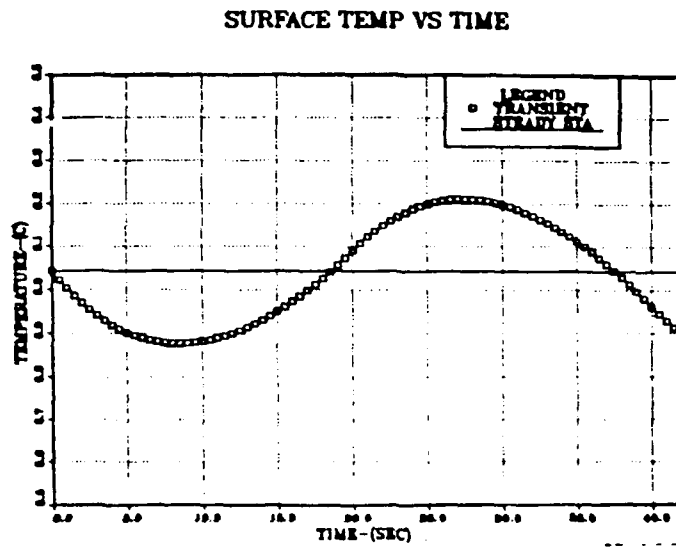


Figure 58. Surface Temperature Due to Power Pulsation with a Period of 40 sec.
for 0.6 W Average Power and Amplitude of 0.1 W

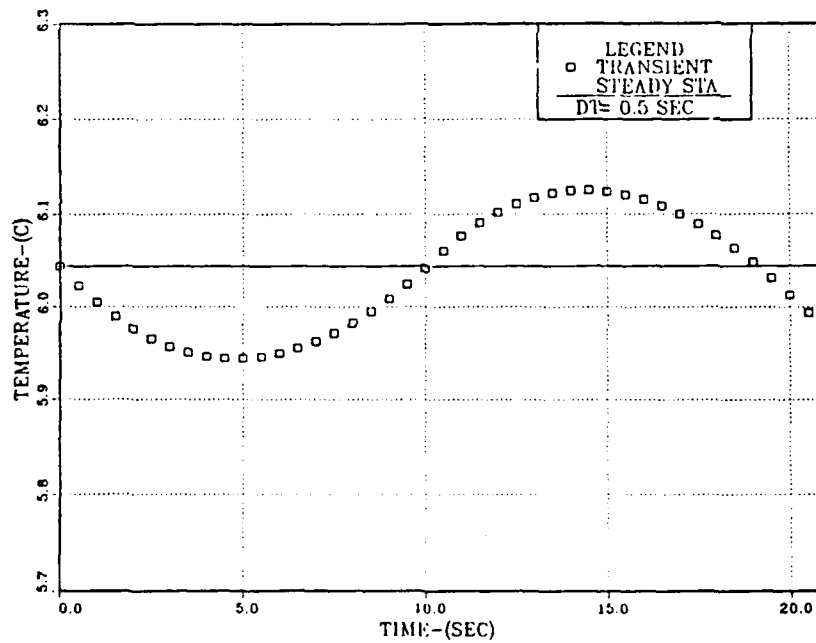


Figure 59. Surface Temperature Due to Power Pulsation with a Period of 20 sec.
for 0.6 W Average Power and Amplitude of 0.1 W

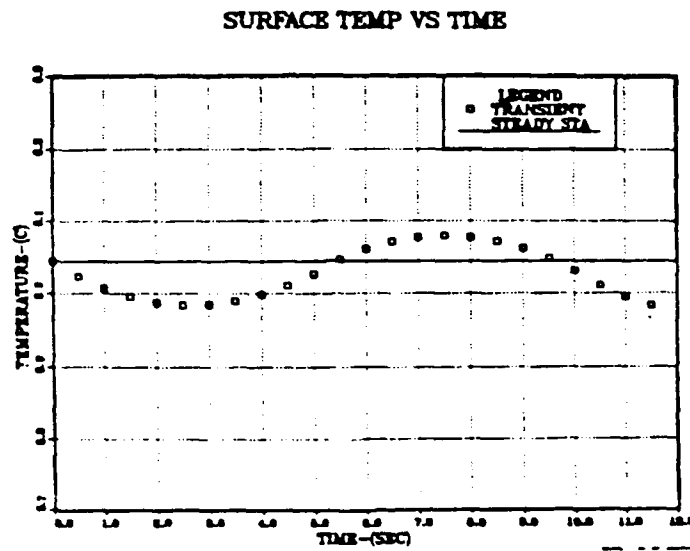


Figure 60. Surface Temperature Due to Power Pulsation with a Period of 10 sec.
for 0.6 W Average Power and Amplitude of 0.1 W

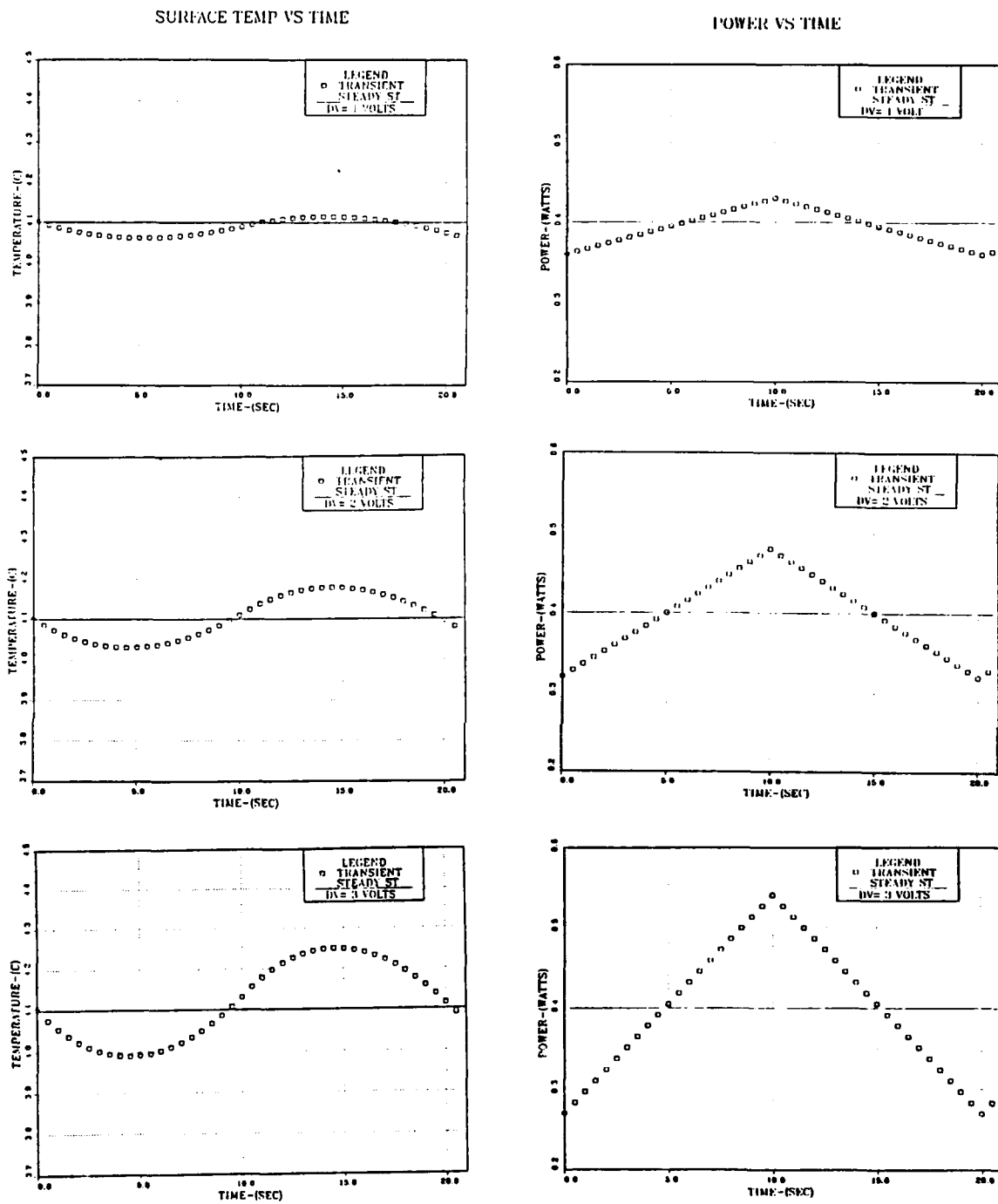


Figure 61. Surface Temperature Due to Power Pulsation with Different Amplitudes for 0.4 W Average Power

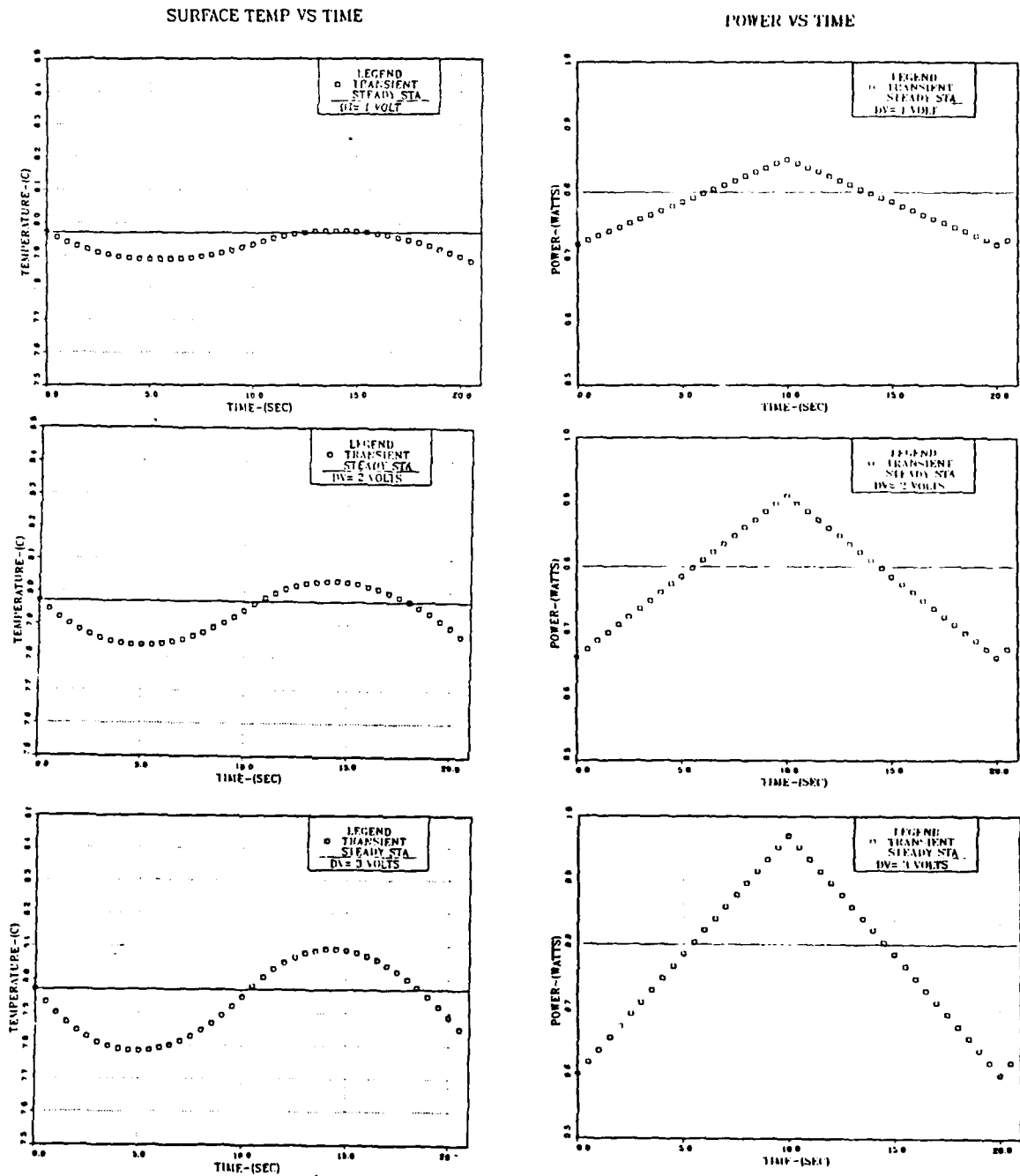


Figure 62. Surface Temperature Due to Power Pulsation with Different Amplitudes for 0.8 W Average Power

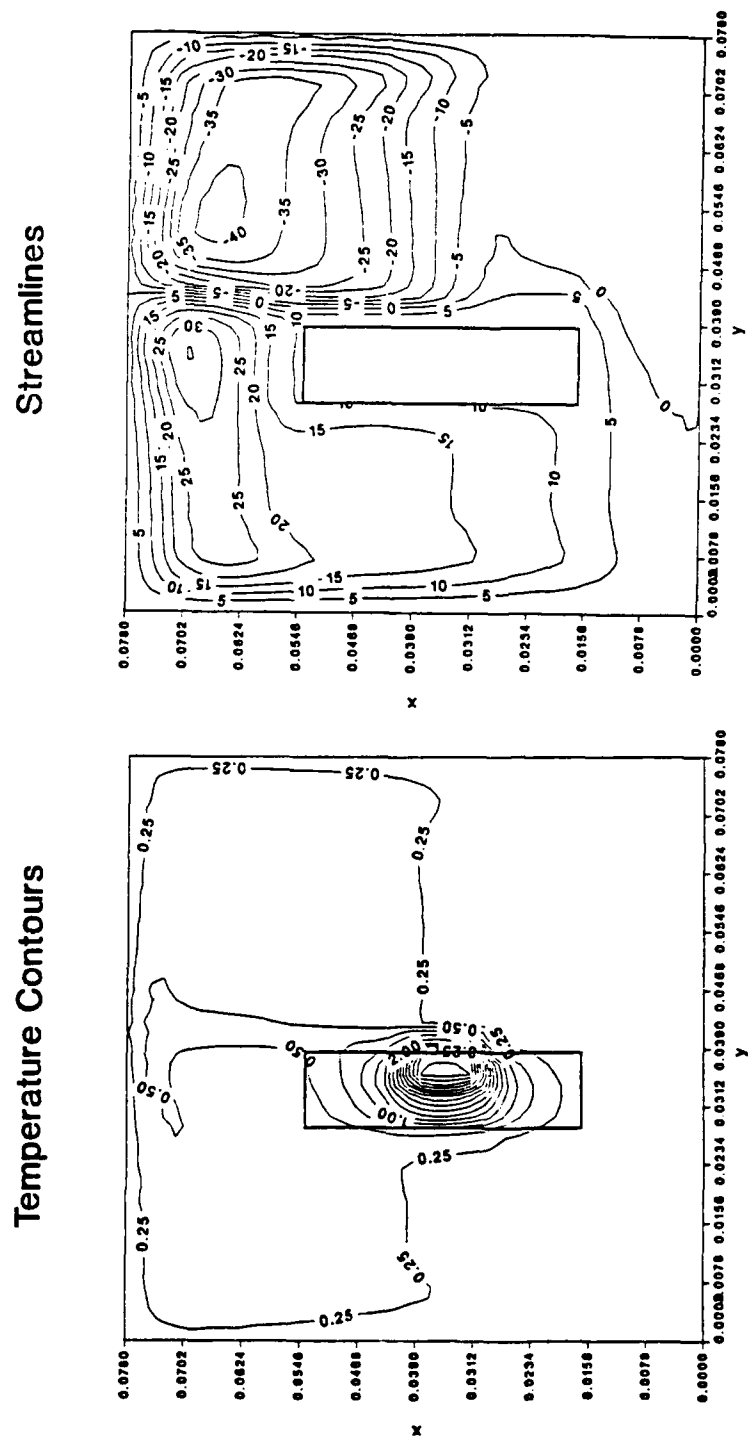


Figure 63. Temperature Contours and Streamlines for 0.4 W Average Power, 0.07 W Amplitude and 20 sec. Period of Oscillation

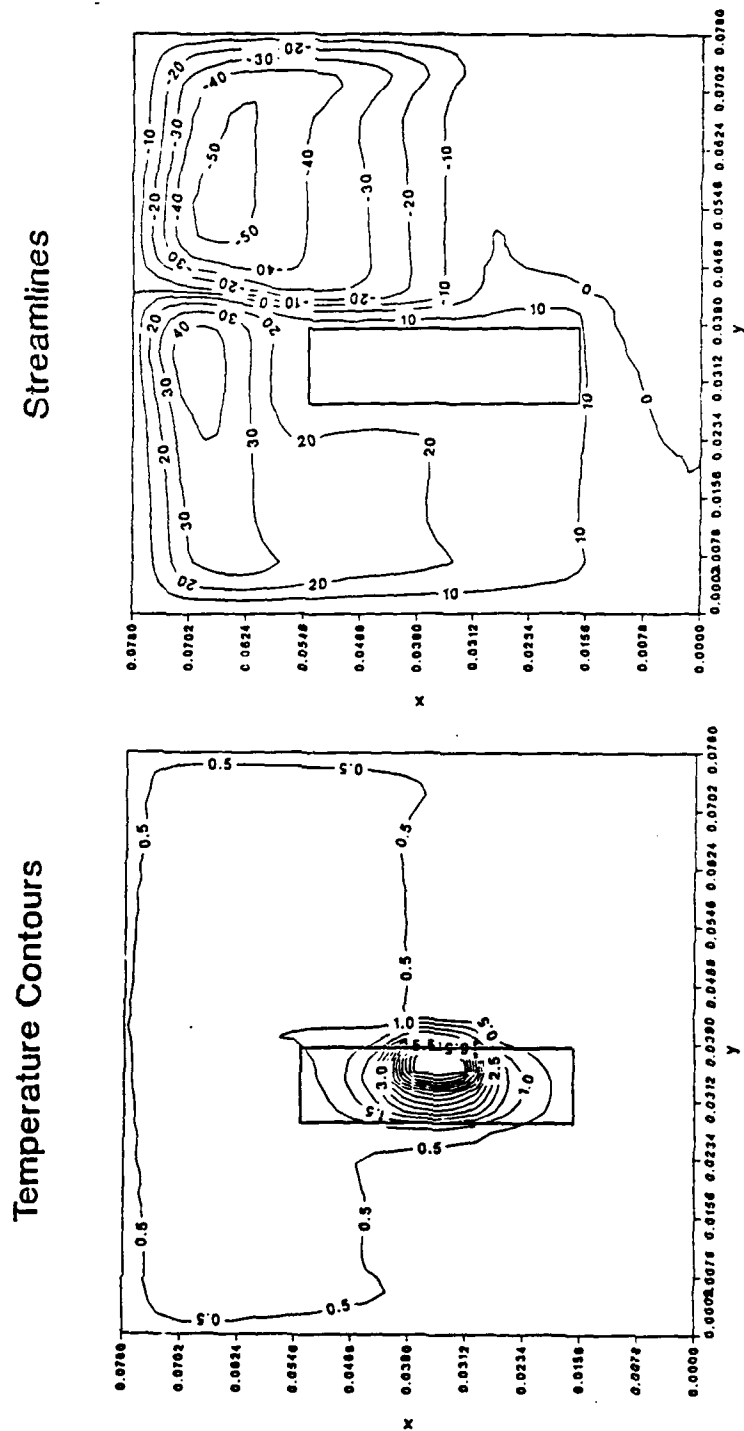


Figure 64. Temperature Contours and Streamlines for 0.8 W Average Power, 0.12 W Amplitude and 20 sec. Period of Oscillation

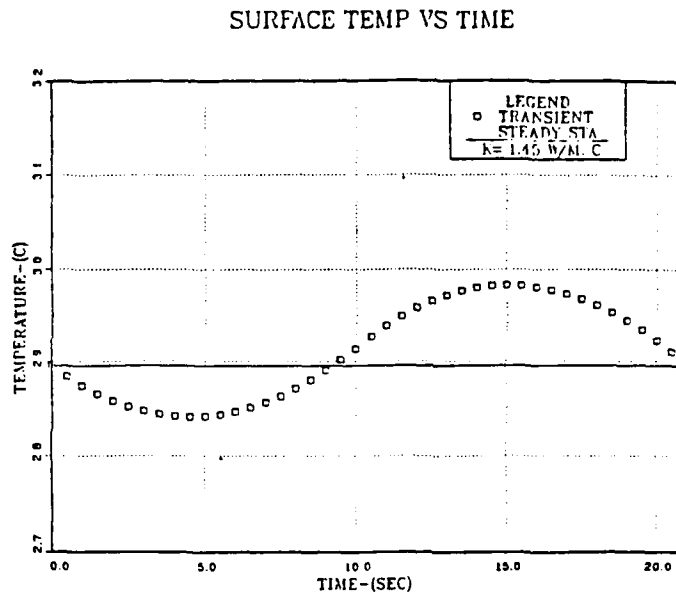


Figure 65. Effects of Thermophysical Properties on Calculated Temperatures

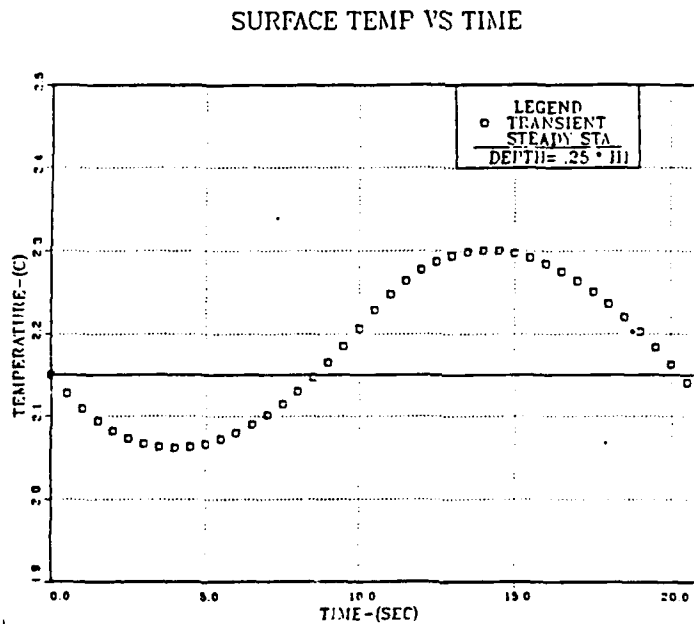


Figure 66. Effects of Heater Dimensions on Calculated Temperatures

SURFACE TEMP VS TIME

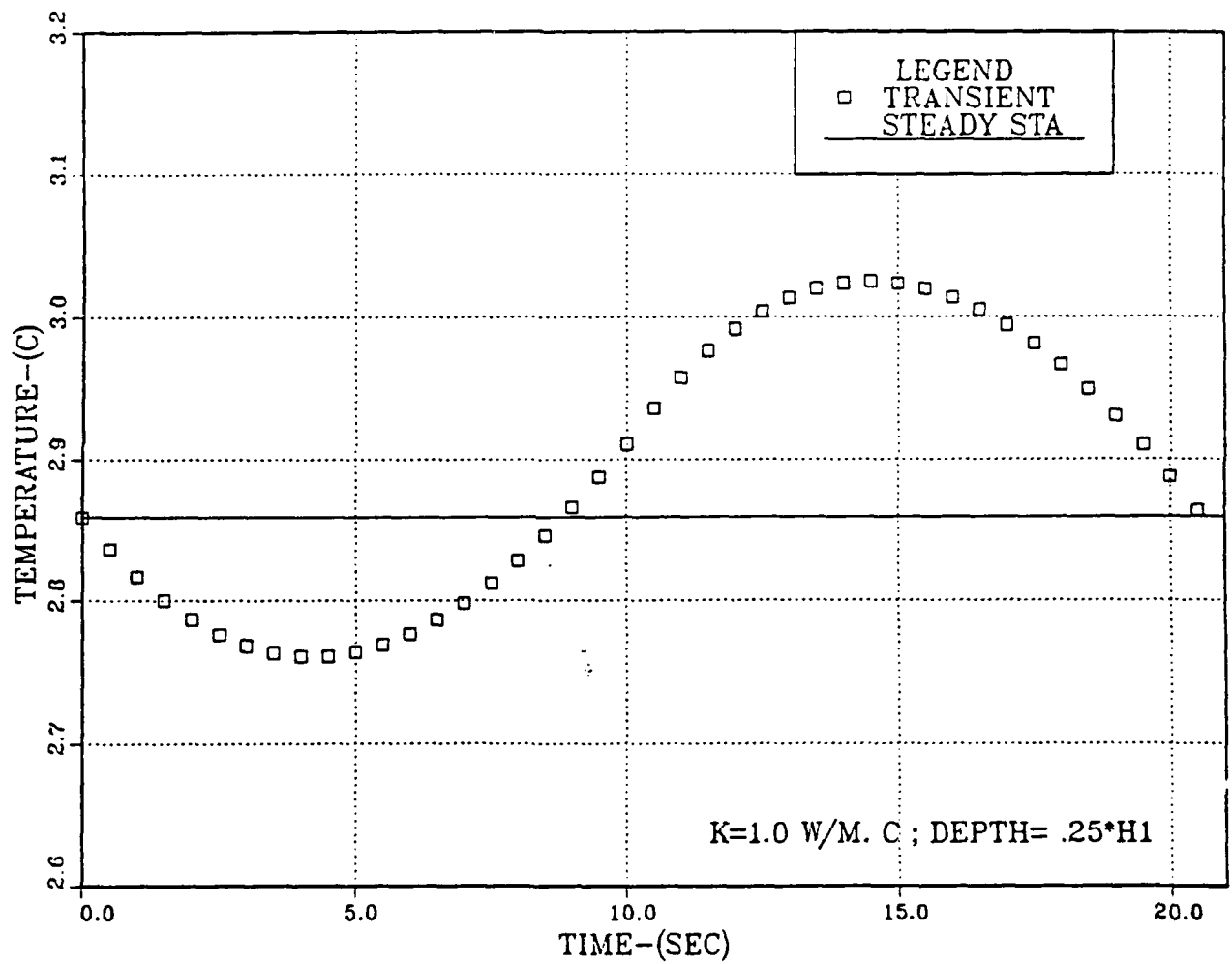


Figure 67. Surface Temperature vs Time

V. CONCLUSIONS

Following conclusions are drawn based on this experimental and numerical study about the heat transfer effects of input power pulsations.

The experiments:

The oscillation amplitudes in surface temperature increase with an increase in both the amplitude and the time period of the applied power. The period of temperature oscillation remains almost the same for all shroud spacings at a particular power level. It was observed that the effects of periodic power, applied to the heater at the bottom of the central column are barely noticeable on the heat transfer characteristics of the other steadily powered heaters in the column. There is no noticeable oscillation in surface temperatures of downstream heaters when power to the bottom heater oscillates in time. With all three columns powered under steady conditions and with a shroud in place, the central column heaters at any x/L have slightly higher ΔT values when compared to the right and left columns. For spacings greater than 6 mm, the heater temperatures are almost equal to the unshrouded test case. These conclusions regarding the steady response are in agreement with Knight [Ref. 13] and Gaiser [Ref. 10].

The computations:

Numerical computations of the transient response due to both a sudden step power input and a periodic power input were conducted. Transient flow and temperature profiles were obtained. Computations were performed for two different heating element properties since the actual element in the experiments was a composite and its properties were not easily quantifiable. Thermophysical properties of the heating element and its thickness had a pronounced effect on calculated temperatures. As the thickness of the heater element was reduced, the temperature oscillation amplitudes increased. Once the

variations in the thermophysical properties and appropriate thickness of the heating element were taken into account in the numerical study, the predicted temperatures were in reasonable agreement with measurements.

VI. RECOMMENDATIONS

In continuation of this study it is recommended that the following aspects be further investigated:

- The effects of pulsating power inputs to more than one heater on the heat transfer from the other steadily powered heaters should be considered.
- Investigate heat transfer enhancement due to possible turbulence effects caused by high amplitude power pulsations at relatively high average power levels.
- Use a multiple heater numerical model to determine heater interaction effects.
- Analyze transient conditions for both one and multiple heater numerical models in the presence of a shroud.
- Numerically study the effects of thermophysical properties of substrate on the amplitudes of oscillations of surface temperature.

APPENDIX A. SUBROUTINE USER

```

SUBROUTINE USER
  LOGICAL LSOLVE,LPRINT,LBLK,LSTOP,LSWICH
  COMMON F(66,66,10),P(66,66),RHO(66,66),GAM(66,66),CON(66,66),
  1 AIP(66,66),AIM(66,66),AJP(66,66),AJM(66,66),AP(66,66),
  2 X(66),XU(66),XDIF(66),XCV(66),XCVS(66),
  3 Y(66),YV(66),YDIF(66),YCV(66),YCVS(66),
  4 YCVR(66),YCVRS(66),ARX(66),ARXJ(66),ARXJP(66),
  5 R(66),RMN(66),SX(66),SXMN(66),XCVI(66),XCVIP(66)
  COMMON DU(66,66),DV(66,66),FV(66),FVP(66),
  1 FX(66),FXM(66),FY(66),FYM(66),PT(66),QT(66),
  COMMON/INDX/NF,NFMAX,NP,NRHO,NGAM,L1,L2,L3,M1,M2,M3,
  1IST,JST,ITER,LAST,RELAX(13),TIME,DT,XL,YL,
  ZIPREF,JPREF,LSOLVE(10),LPRINT(13),LBLK(10),MODE,NTIMES(10),RHOCON
  COMMON/CHTL/LSTOP,LSWICH
  COMMON/SORC/SMAX,SSUM
  COMMON/COEF/FLOW,DIFF,ACOF
  COMMON/TRANS/CTIME,DELT,TLAST
  COMMON/OLD/ UOLD(66,66),VOLD(66,66),EOLD(66,66),IBODY(66,66)
  DIMENSION U(66,66),V(66,66),PC(66,66),COOL(66,66)
  DIMENSION T1(66,66),EN(66,66)
  EQUIVALENCE(F(1,1,1),U(1,1)),(F(1,1,2),V(1,1)),(F(1,1,3),PC(1,1))
  DIMENSION TH(66),THU(66),THDIF(66),THCV(66),THCVS(66),STO(66,66)
  EQUIVALENCE(X,TH),(XU,THU),(XDIF,THDIF),(XCV,THCV)
  1 , (XCVS,THCVS),(XL,THL)
  C*****
  DIMENSION E(66,66),T(66,66),COND(66,66),
  $TOLD(66,66),RHOOLD(66,66)
  EQUIVALENCE (F(1,1,4),E(1,1))
  EQUIVALENCE (F(1,1,5),T(1,1))
  EQUIVALENCE (F(1,1,10),COND(1,1))
  C
  ENTRY GRID
  C***** GRID PARAMETERS *****
  H1=0.0078
  WIDTH=0.023
  DEPTH=0.5*H1
  N1X=4
  N2X=12
  N3X=4
  N4X=4
  N5X=16
  N6X=8
  N1Y=6
  N2Y=8
  N3Y=12
  N4Y=12
  N5Y=18
  AL1=0.5*H1
  AL2=3.*H1
  AL3=1.*H1
  AL4=0.5*H1
  AL5=4.5*H1
  AL6=0.5*H1
  BL1=2.*H1
  BL2=2.*H1
  BL3=1.*H1
  BL4=2.*H1
  BL5=3.*H1
  DX1=AL1/N1X
  DX2=AL2/N2X
  DX3=AL3/N3X
  DX4=AL4/N4X
  DX5=AL5/N5X
  DX6=AL6/N6X
  DY1=BL1/N1Y
  DY2=BL2/N2Y
  DY3=BL3/N3Y
  DY4=BL4/N4Y
  DY5=BL5/N5Y
  XU(2)=0.0
  LFIRST=3

```

```

      LLAST=N1X+2
      DO 10 I=LFIRST,LLAST
      XU(I)=XU(I-1)+DX1
10    CONTINUE
      LFIRST=LLAST+1
      LLAST=LLAST+N2X
      DO 20 I=LFIRST,LLAST
      XU(I)=XU(I-1)+DX2
20    CONTINUE
      LFIRST=LLAST+1
      LLAST=LLAST+N3X
      DO 30 I=LFIRST,LLAST
      XU(I)=XU(I-1)+DX3
30    CONTINUE
      LFIRST=LLAST+1
      LLAST=LLAST+N4X
      DO 40 I=LFIRST,LLAST
      XU(I)=XU(I-1)+DX4
40    CONTINUE
      LFIRST=LLAST+1
      LLAST=LLAST+N5X
      DO 50 I=LFIRST,LLAST
      XU(I)=XU(I-1)+DX5
50    CONTINUE
      LFIRST=LLAST+1
      LLAST=LLAST+N6X
      DO 60 I=LFIRST,LLAST
      XU(I)=XU(I-1)+DX6
60    CONTINUE
      L1=LLAST
      XL=XU(LLAST)
      YV(2)=0.
      LFIRST=3
      LLAST=N1Y+2
      DO 11 I=LFIRST,LLAST
      YV(I)=YV(I-1)+DY1
11    CONTINUE
      LFIRST=LLAST+1
      LLAST=LLAST+N2Y
      DO 21 I=LFIRST,LLAST
      YV(I)=YV(I-1)+DY2
21    CONTINUE
      LFIRST=LLAST+1
      LLAST=LLAST+N3Y
      DO 31 I=LFIRST,LLAST
      YV(I)=YV(I-1)+DY3
31    CONTINUE
      LFIRST=LLAST+1
      LLAST=LLAST+N4Y
      DO 41 I=LFIRST,LLAST
      YV(I)=YV(I-1)+DY4
41    CONTINUE
      LFIRST=LLAST+1
      LLAST=LLAST+N5Y
      DO 51 I=LFIRST,LLAST
      YV(I)=YV(I-1)+DY5
51    CONTINUE
      M1=LLAST
      YL=YV(LLAST)
      RETURN
C
      ENTRY START
      NHTRX=N1X+N2X+N3X+2
      NHTRY=N1Y+N2Y+2
      NHTRX1=NHTRX+N4X-1
      NHTRY1=NHTRY+N3Y-1
      NBOSTX=N1X+N2X+2
      NBOFNX=N1X+N2X+N3X+N4X+1
      NBOSTY=N1Y+2
      NBOFNY=N1Y+N2Y+N3Y+N4Y+1
      PRINT *, 'INPUT LAST TIME VALUE IN SEC. AND'
      PRINT *, 'TIME STEP INTERVAL'

```

```

READ *,TLAST,DELT
PERI=20.0
DT=DELT
CTIME=0.0
DTIME=0.0
PRINT *, 'INPUT DESIRED TIME FOR CONTOUR PLOTTING IN SEC. '
READ *,TRINT
REWRITE(8)
READ(8) LTM
DO 3000 I=1,L1
3000 READ (8) (U(I,J),J=1,M1)
DO 3001 I=1,L1
3001 READ (8) (V(I,J),J=1,M1)
DO 3002 I=1,L1
3002 READ (8) (E(I,J),J=1,M1)
DO 3003 I=1,L1
3003 READ (8) (F(I,J,5),J=1,M1)
DO 3004 I=1,L1
3004 READ (8) (P(I,J),J=1,M1)
DO 3005 I=1,L1
3005 READ (8) (STG(I,J),J=1,M1)
CP=4178.
CPS=1500.
CPHTR=439.
RHOE=995.
RHOS=1180.
RHOH=8510.
BETA=319.25E-6
G=9.807
Q1=6.
ALFA=0.6
ALFAM=0.4
DYNVIS=774.2E-6
CONFLD=0.6027
CONPLX=0.20
CONHTR=11.7
PI=3.14159256
PR=DYNVIS*CP/CONFLD
WRITE(*,*) 'PR=',PR
RETURN

C
C
C
ENTRY SETTIM
PRINT *, 'CTIME=', 'DTIME=',DTIME
IF(DTIME.LT.10.1) THEN
EIN=(.36+0.07*DTIME/10.)/WIDTH
ELSE
EIN=(.430-(DTIME-10.)*.07/10.)/WIDTH
ENDIF
ENGEN=EIN/(DEPTH*H1)
POW=ENGEN*WIDTH*DEPTH*H1
IPRTIM=0
WRITE (1,*) CTIME,E(NHTRX+1,NHTRY+6),POW
IF((DTIME.GT.9.95).AND.(DTIME.LT.10.05)) IPRTIM=1
IF(DTIME.GT.(PERI-.1)) THEN
DTIME=0.
IPRTIM=1
ENDIF
IF (IPRTIM.EQ.1) THEN
DSUM=0.0
POWER=0.0
POWER1=0.0
DTOT=0.0
DO 504 I=2,L2
POWER=CONFLD*(XU(I+1)-XU(I))*E(I,2)/((YV(3)-YV(2))/2.)
POWER1=CONFLD*(XU(I+1)-XU(I))*E(I,M2)/((YV(M1)-YV(M2))/2.)
DSUM=POWER+POWER1+DSUM
504 CONTINUE
DSUM1=0.0
POWER2=0.0
POWER3=0.0

```



```

DO 506 J=2,M2
  POWER2=CONFLD*(YV(J+1)-YV(J))*E(2,J)/((XU(3)-XU(2))/2.)
  POWER3=CONFLD*(YV(J+1)-YV(J))*E(L2,J)/((XU(L1)-XU(L2))/2.)
  DSUM1=DSUM1+POWER2+POWER3
506 CONTINUE
  WRITE(*,*) 'ENERGY IN=',EIN
  WRITE(*,*) 'ENERGY OUT=',DSUM+DSUM1
  WRITE(*,*) 'CURRENT TIM=',CTIME
  ENDIF
  FARK=TRINT-CTIME
  IF (TRINT.EQ.CTIME) THEN
    DO 999 I=1,4
      LPRINT(I)=.TRUE.
      CALL PRINT
      LPRINT(I)=.FALSE.
999 CONTINUE
    NTIME=1
    WRITE(6,*) 'START WRITING ON UNIT 9'
    WRITE(*,*) 'ONCE YAZDIM'
    REWIND (3)
    WRITE (3) NTIME,M1,L1
    WRITE (3) (YV(J),J=2,M1)
    WRITE (3) (XU(I),I=2,L1)
    WRITE (3) (Y(J),J=1,M1)
    WRITE (3) (X(I),I=1,L1)
    WRITE (3) CTIME
    DO 300 J=1,M1
300 WRITE (3) (V(I,J),I=1,L1)
    DO 301 J=1,M1
301 WRITE (3) (U(I,J),I=1,L1)
    DO 302 J=1,M1
302 WRITE (3) (E(I,J),I=1,L1)
    DO 303 J=1,M1
303 WRITE (3) (P(I,J),I=1,L1)
    DO 305 J=1,M1
305 WRITE (3) (STO(I,J),I=1,L1)
    DO 304 J=1,M1
304 WRITE (3) (F(I,J,3),I=1,L1)
    DO 306 J=1,M1
306 WRITE (3) (IBODY(I,J),I=1,L1)
    WRITE(6,*) 'CLOSE UNIT 3'
    CLOSE (3)
  ENDIF
C STORE OLD VALUES
DO 881 I=1,L1
DO 881 J=1,M1
  UOLD(I,J)=U(I,J)
  VOLD(I,J)=V(I,J)
  EOLD(I,J)=E(I,J)
881 CONTINUE
  LSTOP=.FALSE.
  LSWICH=.FALSE.
  ITER=0.0
  DTIME=DTIME+DELT
  RETURN
C
C ENTRY DENSE
RETURN
C
C ENTRY BOUND
RETURN
C
C ENTRY OUTPUT
IF(ITER.NE.0) GOTO 500
WRITE(*,501)
501 FORMAT(' ITER',6X,'SMAX',8X,' SSUM',7X,'VEL(FRONT)',
16X,'T(HEATER)',6X,'CURRENT TIME')
CONTINUE
500 WRITE(*,502) ITER,SMAX,SSUM,V(NBOFNX+1,NHTRY+6)
1,E(NHTRX+1,NHTRY+6),CTIME
502 FORMAT (I6,1P5E12.3)

```

```

      RETURN
C
      ENTRY GAMSOR
      IF (NF.EQ.3) RETURN
      IF (NF.EQ.1.OR.NF.EQ.2) THEN
        DO 400 J=1,M1
          DO 400 I=1,L1
            RHO(I,J)=RHOF
            GAM(I,J)=DYNVIS
            CON(I,J)=0.0
            IBODY(I,J)=1
400      CONTINUE
          DO 401 I=NBOSTX,NBOFNX
            DO 401 J=NBOSTY,NBOFNY
              GAM(I,J)=1.E+20
401      @CONTINUE
          ENDIF
          IF(NF.EQ.2) THEN
            DO 402 I=2,L2
              DO 402 J=3,M2
                TEM=(FY(J)*E(I,J)) + (FYM(J)*E(I,J-1))
                CON1=RHOF*G*BETA*(TEM-TSTART)
                CON(I,J)=ALFA*CON1+ALFAM*STO(I,J)
                STO(I,J)=CON1
402      CONTINUE
          ENDIF
          IF(NF.EQ.4) THEN
            DO 403 J=1,M1
              DO 403 I=1,L1
                RHO(I,J)=RHOF*CP
                GAM(I,J)=CONFLD
                CON(I,J)=0.0
403      CONTINUE
              DO 404 I=NBOSTX,NBOFNX
                DO 404 J=NBOSTY,NBOFNY
                  RHO(I,J)=RHOS*CPS
                  GAM(I,J)=CONPLX
404      CONTINUE
              DO 405 I=NHTRX,NHTRX1
                DO 405 J=NHTRY,NHTRY1
                  RHO(I,J)=RHOH*CPHTR
                  GAM(I,J)=CONHTR
                  CON(I,J)=ENGEN
405      CONTINUE
          ENDIF
          RETURN
        END

```

APPENDIX B. STEADY STATE AND TRANSIENT POWER PROGRAMS

FOR HP_85

```

10 | !!!!!!!!!!!!!!!!!!!!!!!
20 | POWER PROGRAM FOR
30 | HP-59501B PROGRAMMER !
40 | TO SUPPLY STEADY VOLT
50 | TO THE HEATER AT THE
60 | BOTTOM OF CENT. COL. !
70 | 29450 !!!!!!!!!!!!!!!!!!!!!!!
80 | DISP "INPUT MAX. AND AVE. VO
    | LTAGE"
90 | INPUT M1,V1
100 | R1=V1/M1*1000+2000
110 | OUTPUT 706 USING "#.40" ; R1
120 | END

```

```

10 | !!!!!!!!!!!!!!!!!!!!!!!
20 | TRANSIENT POWER PROGRAM !
30 | !!!!!!!!!!!!!!!!!!!!!!!
40 | !!
50 | DIM E(199),V1(199)
60 | DISP "INPUT MAX. VOL"
70 | DISP "AND MIN. VOL"
80 | INPUT R1,R2
90 | DISP "INPUT PERIOD"
100 | INPUT P
110 | D=.05
120 | Z=P/C
130 | N=INT(Z)
140 | K=N/2
150 | V1(K)=INT(R1/25*100)*10+2000
160 | V1(0)=INT(R2/25*100)*10+2000
170 | E(K)=R1
180 | E(0)=R2
190 | L=K-1
200 | FOR I=1 TO L
210 | E(I)=(R1-R2)/K+E(I-1)
220 | E(N-I)=E(I)
230 | V1(I)=INT(E(I)/25*100)*10+20
    | 00
240 | V1(N-I)=V1(I)
250 | NEXT I
260 | M=N-1
270 | BEEP
280 | FOR I=0 TO M
290 | OUTPUT 706 USING "#.40" ; V1
    | (I)
300 | WAIT 50
310 | NEXT I
320 | GOTO 270
330 | END

```

APPENDIX C. TEMPERATURE AND POWER ACQUISITION PROGRAM

FOR THE HEATER AT THE BOTTOM OF THE CENTRAL COLUMN

```

10  !!!!!!!!!!!!!!!!!!!!!!!!!!!!!!!!!!!!!!!!!!!!!!!!!!!!!!!!!!!!!!!!!!!!!
20  !!!                                TRANSIENT                                !!!
30  !!!  TEMPERATURE AND POWER ACQUISITION PROGRAM FOR THE HEATER  !!!
40  !!!                                AT THE BOTTOM OF CENTRAL COLUMN          !!!
50  !!!!!!!!!!!!!!!!!!!!!!!!!!!!!!!!!!!!!!!!!!!!!!!!!!!!!!!!!!!!!!!!!!!!!
60  OPTION BASE 1
70  REAL Tul(350),Yig(180),Cas(350),Tem(180),Vol(350),Bath(3),Bat(3)
80  CREATE BDAT "YIGIT:,700,1",180
90  ASSIGN @Path4 TO "YIGIT:,700,1"
100 CREATE BDAT "CANSU:,700,1",350
110 ASSIGN @Path5 TO "CANSU:,700,1"
120 Resist=1.885
130 R2=Resist*Resist
140 BEEP
150 FOR I=1 TO 350
160 OUTPUT 709;"CONFMEAS DCV ,508-509,USE 0"
170 ENTER 709;V,V1
180 Vol(I)=V
190 Tul(I)=V1
200 NEXT I
210 FOR I=1 TO 180
220 OUTPUT 709;"CONFMEAS DCV ,209,USE 0"
230 ENTER 709;T
240 WAIT .09
250 Tem(I)=T
260 NEXT I
270 FOR I=1 TO 350
280 IF I>180 THEN GOTO 300
290 Yig(I)=.0006797+(25825.1328*Tem(I))-(607789.2467*(Tem(I)*Tem(I)))-(2195203
4.3364*(Tem(I)^3))+(8370810996.1874*(Tem(I)^4))+.039
300 Cas(I)=(Vol(I)-Tul(I))/2.01*(Tul(I)-(Vol(I)-Tul(I))/2.01*(4700/147.))
310 NEXT I
320 OUTPUT 709;"CONFMEAS DCV ,317-319,USE 0"
330 FOR I=1 TO 3
340 ENTER 709;Bat(I)
350 NEXT I
360 FOR I=0 TO 3
370 Bath(I)=.0006797+(25825.1328*Bat(I))-(607789.2467*(Bat(I)*Bat(I)))-(219520
34.3364*(Bat(I)^3))+(8370810996.1874*(Bat(I)^4))+.036
380 NEXT I
390 A$="TOP(C)"
400 B$="MID(C)"
410 C$="BOT(C)"
420 PRINT USING "2X,AAAAAAAAAAAAAAAAAAAAAAAA,3X,DD.DD";A$,Bath(1)
430 PRINT USING "2X,AAAAAAAAAAAAAAAAAAAAAAAA,3X,DD.DD";B$,Bath(2)
440 PRINT USING "2X,AAAAAAAAAAAAAAAAAAAAAAAA,3X,DD.DD";C$,Bath(3)
450 PRINTER IS CRT
460 OUTPUT @Path5;Cas(*)
470 OUTPUT @Path4;Yig(*)
480 END

```

APPENDIX D. TEMPERATURE ACQUISITION PROGRAM

```

10  !!!!!!!!!!!!!!!!!!!!!!!!!!!!!!!!!!!!!!!!!!!!!!!!!!!!!!!!!!!!!!!!!!!!!!!!!!!!!
20  !!                                TEMPERATURE ACQUISITION PROGRAM                                !!
30  !!                                FOR 15 HEATERS IN (STEADY STATE)                                !!
40  !!!!!!!!!!!!!!!!!!!!!!!!!!!!!!!!!!!!!!!!!!!!!!!!!!!!!!!!!!!!!!!!!!!!!!!!!!!!!
50  OPTION BASE 1
60  REAL Volts(18)
70  REAL Temp(18)
80  PRINT DATES(TIME$)
90  PRINT "INPUT AVERAGE POWER"
100 INPUT Power
110 PRINTER IS 701
120 PRINT DATES(TIME$)
130 PRINT " "
140 PRINT Power,"WATT INPUT POWER"
150 PRINT " 15 HEATER ELEMENTS "
160 PRINT " 3 MM SHROUD SPACING "
170 PRINT " "
180 PRINT " "
190 PRINT " "
200 !!!!!!!!!!!!!!!!!!!!!!!!!!!!!!! SURFACE #1-5
210 OUTPUT 709;"CONFMEAS DCV, 115-119,USE 0"
220 FOR I=1 TO 5
230 ENTER 709;Volts(I)
240 Temp(I)=.0006797+(25825.1328*Volts(I))-(607789.2467*(Volts(I)*Volts(I)))-
21952034.3364*(Volts(I)^3)+(8370810996.1874*(Volts(I)^4))+.039
250 NEXT I
260 !!!!!!!!!!!!!!!!!!!!!!!!!!!!!!! SURFACE #21-30
270 OUTPUT 709;"CONFMEAS DCV,200-209,USE 0"
280 FOR I=6 TO 15
290 ENTER 709;Volts(I)
300 Temp(I)=.0006797+(25825.1328*Volts(I))-(607789.2467*(Volts(I)*Volts(I)))-
21952034.3364*(Volts(I)^3)+(8370810996.1874*(Volts(I)^4))+.039
310 NEXT I
320 !!! PRINT OUTPUT TEMPERATURES
330 PRINT " "
340 FOR I=1 TO 15
350 PRINT "HEATER #";I," TEMPERATURE IN DEG. C =";Temp(I)
360 NEXT I
370 PRINT " "
380 PRINT " "
390 PRINT " "
400 PRINT " "
410 PRINT " "
420 OUTPUT 709;"CONFMEAS DCV,317-319,USE 0"
430 FOR I=16 TO 18
440 ENTER 709;Volts(I)
450 Temp(I)=.0006797+(25825.1328*Volts(I))-(607789.2467*(Volts(I)*Volts(I)))-
21952034.3364*(Volts(I)^3)+(8370810996.1874*(Volts(I)^4))+.036
460 PRINT "TEMP. DEG. C ";Temp(I)
470 NEXT I
480 PRINTER IS CRT
490 END

```

APPENDIX E. POWER INPUT PROGRAM

```

40  OUTPUT 709;"RST"
50  OPTION BASE 1
60  REAL Volts(18)
70  REAL Pow(15)
80  REAL Ptot,Pavg,Perdif
90  OUTPUT 709;"CONFMEAS DCV,316,USE 0"
100 ENTER 709;Volts(16)
110 OUTPUT 709;"RST"
120 OUTPUT 709;"CONFMEAS DCV,410-417,USE 0"
130 FOR I=1 TO 8
140 ENTER 709;Volts(I)
150 NEXT I
160 OUTPUT 709;"RST"
170 OUTPUT 709;"CONFMEAS DCV,401,USE 0"
180 ENTER 709;Volts(18)
190 OUTPUT 709;"RST"
200 OUTPUT 709;"CONFMEAS DCV,503-509,USE 0"
210 FOR I=9 TO 15
220 ENTER 709;Volts(I)
230 NEXT I
240 OUTPUT 709;"RST"
250 OUTPUT 709;"CONFMEAS DCV,500,USE 0"
260 ENTER 709;Volts(17)
270 OUTPUT 709;"RST"
280 PRINT DATE$(TIMEDATE)
290 PRINT " "
300 PRINT " "
310 PRINT "INPUT VOLTAGE D.C. VOLTS PAN 1";Volts(18)
320 PRINT "INPUT VOLTAGE D.C. VOLTS PAN 2";Volts(17)
330 PRINT " "
340 PRINT " "
350 Resist=2.0
360 R2=Resist*Resist
370 Pow(3)=(Volts(18)-Volts(3))*(Volts(3)*(Resist+.55)-Volts(18)*.55)/R2
380 Pow(8)=(Volts(18)-Volts(8))*(Volts(8)*(Resist+.55)-Volts(18)*.55)/R2
390 Pow(10)=(Volts(17)-Volts(10))*(Volts(10)*(Resist+.3)-Volts(18)*.3)/R2
400 Resist=1.972
410 R2=Resist*Resist
420 Resist=1.886
430 R2=Resist*Resist
440 Pow(15)=(Volts(14)-Volts(15))/2.01*(Volts(15)-((Volts(14)-Volts(15))/2.01*
4700/147.))
450 Resist=1.862
460 R2=Resist*Resist
470 Pow(12)=(Volts(17)-Volts(12))*(Volts(12)*(Resist+.5)-Volts(17)*.5)/R2
480 Pow(13)=(Volts(17)-Volts(13))*(Volts(13)*(Resist+.0)-Volts(17)*.0)/R2
490 Resist=1.852
500 R2=Resist*Resist
510 Pow(9)=(Volts(17)-Volts(9))*(Volts(9)*(Resist+.1)-Volts(17)*.1)/R2
520 Resist=1.8182
530 R2=Resist*Resist
540 Pow(6)=(Volts(18)-Volts(6))*(Volts(6)*(Resist+.7)-Volts(17)*.7)/R2
550 Resist=1.8
560 R2=Resist*Resist
570 Pow(4)=(Volts(18)-Volts(4))*(Volts(4)*(Resist+.2)-Volts(18)*.2)/R2
580 Pow(5)=(Volts(18)-Volts(5))*(Volts(5)*(Resist+.7)-Volts(18)*.7)/R2
590 Pow(14)=(Pow(15)+Pow(13))/2.
600 Pow(7)=(Pow(6)+Pow(8))/2

```

```

610 Resist=1.6667
620 R2=Resist*Resist
630 Pow(1)=(Volts(18)-Volts(1))*(Volts(1)*(Resist+.4)-Volts(18)*.4)/R2
640 Pow(2)=(Volts(18)-Volts(2))*(Volts(2)*(Resist+.4)-Volts(18)*.4)/R2
650 Pow(11)=(Volts(17)-Volts(11))*(Volts(11)*(Resist+.2)-Volts(17)*.2)/R2
660 FOR I=1 TO 15
670 PRINT "BLOCK # ";I," POWER = ";Pow(I)," WATTS"
680 WAIT .5
690 NEXT I
700 Ptot=0
710 FOR I=1 TO 15
720 IF I=14 THEN 740
730 Ptot=Ptot+Pow(I)
740 NEXT I
750 Pavg=Ptot/14
760 PRINT " "
770 PRINT "AVERAGE POWER = ";Pavg," WATTS"
780 PRINT " "
790 FOR I=1 TO 15
800 Perdif=ABS((Pavg-Pow(I))/Pavg)*100
810 PRINT "HEATER #";I," PERCENT DEVIATION ";Perdif
820 WAIT .5
830 NEXT I
840 END

```

APPENDIX F. TEMPERATURE ACQUISITION AND REDUCTION

PROGRAM (STEADY STATE)

```

10  !!!!!!!!!!!!!!!!!!!!!!!!!!!!!!!!!!!!!!!!!!!!!!!!!!!!!!!!!!!!!!!!!!!!!!!!!!!!!!!
20  !!          TEMPERATURE ACQUISITION AND REDUCTION PROGRAM          !!
30  !!          STEADY STATE      (CENTER COL)          !!
40  !!  PROGRAM PERFORMS THE REQUIRED FUNCTIONS NEEDED TO OBTAIN DATA  !!
50  !!  FROM THE ACQUISITION SYSTEM AND CONVERT THE THERMOCOUPLE OUT-  !!
60  !!          PUT VOLTAGES INTO TEMPERATURE VALUES.          !!
70  !!!!!!!!!!!!!!!!!!!!!!!!!!!!!!!!!!!!!!!!!!!!!!!!!!!!!!!!!!!!!!!!!!!!!!!!!!!!!!!
80  OPTION BASE 1
90  REAL Volts(18)
100 REAL T(18),Xtol(15),Nu(15),Ra(15),Delt(15)
110 REAL Lnu(15),Lgr(15)
120 REAL Power,Tamb,G,Kpg,Delx,As,Per,Ta,Qconv,Lbar
130 REAL Qflux,Tfilm,Beta,Spvol,Dynvisc,Qcond
140 REAL Kinvisc,Kf,Pr,Theta,Hx,Grm,Hux
150 PRINTER IS CRT
160 PRINT
170 PRINT "ENTER AVERAGE POWER -WATTS"
180 INPUT Power
190 PRINT
200 PRINT "ENTER SHROUD SPACING IN mm"
210 INPUT Space$
220 !PRINT " "
230 !!!!!!!!!!!!!!!!!!!!!!!!!!!!!!!!!!!!! SURFACE #16-20
240 OUTPUT 709;"CONFMEAS DCV, 115-119,USE 0"
250 FOR I=1 TO 5
260 ENTER 709;Volts(I)
270 T(I)=.0006797+(25825.1328*Volts(I))-(607789.2467*(Volts(I)*Volts(I)))-(219
52034.3364*(Volts(I)^3))+(8370810996.1874*(Volts(I)^4))+.039
280 Xtol(I)=(31.75-6.985-(I-16)*1.27)/31.75
290 NEXT I
300 !!!!!!!!!!!!!!!!!!!!!!!!!!!!!!!!!!!!! SURFACE #21-#30
310 OUTPUT 709;"CONFMEAS DCV,200-207,USE 0"
320 FOR I=6 TO 13
330 IF I=14 THEN 370
340 ENTER 709;Volts(I)
350 T(I)=.0006797+(25825.1328*Volts(I))-(607789.2467*(Volts(I)*Volts(I)))-(219
52034.3364*(Volts(I)^3))+(8370810996.1874*(Volts(I)^4))+.039
360 Xtol(I)=(31.75-6.985-(I-16)*1.27)/31.75
370 NEXT I
380 OUTPUT 709;"CONFMEAS DCV,209,USE 0"
390 ENTER 709;Volts(15)
400 T(15)=.0006797+(25825.1328*Volts(15))-(607789.2467*(Volts(15)*Volts(15)))-
(21952034.3364*(Volts(15)^3))+(8370810996.1874*(Volts(15)^4))+.090
410 OUTPUT 709;"CONFMEAS DCV,317-319,USE 0"
420 FOR I=16 TO 18
430 ENTER 709;Volts(I)
440 T(I)=.0006797+(25825.1328*Volts(I))-(607789.2467*(Volts(I)*Volts(I)))-(219
52034.3364*(Volts(I)^3))+(8370810996.1874*(Volts(I)^4))+.036
450 PRINT "TEMP. DEG. C ";T(I)
460 NEXT I
470 PRINT "INPUT AMBIENT TEMPERATURE"
480 Tamb=(T(16)+T(17)+T(18))/3

```



```

490  PRINTER IS 701
500  PRINT " "
510  PRINT DATE$(TIMEDATE)
520  PRINT "DATA REDUCTION OUTPUT"
530  PRINT " "
540  PRINT "POWER LEVEL (WATTS)      :",Power
550  PRINT
560  PRINT "SHROUD POSITION (mm)      :",Space$
570  PRINT
580  PRINT "AMBIENT TEMPERATURE (C) :",Tamb
590  PRINT
600  PRINT
610  I
620  I
630  G=9.81
640  Kpg=.1421
650  Delx=.006731
660  As=.0239*.0078
670  Per=2*.0239+2*.0078
680  Lbar=As/Per
690  A$="Qcond"
700  B$="X/L"
710  D$="LOG(Nux)"
720  E$="LOG(Grx*)"
730  F$="DELT"
740  G$="Hx"
750  H$="Nux"
760  I$="Grx*"
770  J$="Temp"
780  PRINTER IS CRT
790  !!!!!!!!!!!!!!!!!!!!!!!!!!!!!!!!!!!!!!!
800  !          ENTER CONDUCTION LOSSES          !
810  !!!!!!!!!!!!!!!!!!!!!!!!!!!!!!!!!!!!!!!
820  PRINT "INPUT CONDUCTION LOSSES AS COMPUTED FROM ELLPACK"
830  INPUT Qcond
840  !!!!!!!!!!!!!!!!!!!!!!!!!!!!!!!!!!!!!!!
850  PRINTER IS 701
860  PRINT "                                CENTER COLUMN"
870  PRINT " "
880  FOR I=1 TO 15
890  PRINT " "
900  PRINT "                                SURFACE #",I
910  PRINT " "
920  PRINT USING "2X,AAAA,3X,AAA,3X,AAAAAAAA,2X,AAAAAAAA,3X,AAA,4X,AA,4X,AAA
,3X,AAAA,2X,AAAA";A$,B$,D$,E$,F$,G$,H$,I$,J$
930  Qconv=Power-Qcond
940  Qflux=Qconv/As
950  Delt(I)=T(I)-Tamb
960  Tfilm=273.15+(T(I)+Tamb)/2
970  Beta=(-7.944858E-8*(Tfilm^2))+(5.7356479E-5*Tfilm)-.0097810563
980  Spvol=(4.69699E-9*(Tfilm^2))+(-2.53745E-6*Tfilm)+.001341903
990  Dynvisc=(3.2348511E-7*(Tfilm^2))+(-.00021474487*Tfilm)+.036166792
1000  Kinvisc=Spvol*Dynvisc
1010  Kf=(1.418181818E-3*Tfilm)+.1866
1020  Pr=(4.65706E-3*(Tfilm^2))+(-2.922094*Tfilm)+463.3319
1030  Theta1=Power1/(.0220*Kf)
1040  Temp=T(I)
1050  Theta=Qflux*Lbar/Kf
1060  Hx=Qflux/Delt(I)
1070  Grm=(6*Beta*Qflux*(Lbar)^4)/(Kf*Kinvisc^2)
1080  Nux=Hx*Lbar/Kf
1090  Nu(I)=Nux
1100  Ra(I)=Pr*Grm

```

```

1110 Lgr(I)=LGT(Grm)
1120 Lnu(I)=LGT(Nux)
1130 Lg=Lgr(I)
1140 Lnn=Lnu(I)
1150 PRINT USING "1X,D.0000,2X,D.000,2X,D.000,5X,D.000,4X,00.000,2X,0000.D,1X,D
0.000,00000.D,1X,00.00";Qcond,Xtol(I),Lnn,Lg,Delt(I),Hx,Nux,Grm,Temp
1160 NEXT I
1170 CREATE BDAT "NU:,700,0,2",15
1180 ASSIGN @Path4 TO "NU:,700,0,2"
1190 OUTPUT @Path4;Nu(*)
1200 CREATE BDAT "RA:,700,0,2",15
1210 ASSIGN @Path5 TO "RA:,700,0,2"
1220 OUTPUT @Path5;Ra(*)
1230 PRINTER IS CRT
1240 CREATE BDAT "DTEMP2W3MM:,700,1",15
1250 ASSIGN @Path7 TO "DTEMP2W3MM:,700,1"
1260 OUTPUT @Path7;Delt(*)
1270 END

```

LIST OF REFERENCES

1. A. Bar-Cohen and A. D. Kraus "Advances in Thermal Modeling of Electronic Components and Systems" (1988)
2. E. Baker "Liquid Immersion Cooling of Small Electronic Devices", *Microelectronics and Reliability*, Vol. 12, pp. 163-173. (1973)
3. K. A. Park and A. E. Bergles "Natural Convection Heat Transfer Characteristics of Simulated Microelectronic Chips", *ASME Journal of Heat Transfer*, Vol. 109, pp. 90-96. (1987)
4. A. Bar-Cohen and H. Schweitzer "Convective Immersion Cooling of Parallel Vertical Plates" *IEEE Transactions on Components, Hybrids and Manufacturing Technology*, Vol. CHMT-8, pp. 343-351. (1985)
5. M. D. Kelleher, R. H. Knock and K. T. Yang "Laminar Natural Convection in A Rectangular Enclosure Due To A Heated Protrusion on A Vertical Wall- Part I: Experimental Investigation", *Proc. Second ASME/JSME Therm. Engr. Joint Conf.*, Honolulu, pp. 169-177. (1987)
6. K. V. Lee, M. D. Kelleher, R. H. Knock and K. T. Yang "Laminar Natural Convection in A Rectangular Enclosure Due To A Heated Protrusion on A Vertical Wall- Part II: Numerical Simulations", *Proc. second ASME/JSME Therm. Engr. Joint Conf.*- Honolulu. , pp. 179-185. (1987)

7. Y. Joshi, M. D. Kelleher and T. J. Benedict "Natural Convection Immersion Cooling of An Array of Simulated Chips in An Enclosure Filled With Dielectric Fluid", Presented at the XXth International Symposium of the International Center for Heat and Mass Transfer, Dubrovnic, Yugoslavia. (1988)
8. Y. Joshi, T. Willson and S. J. Hazard "An Experimental Study of Natural Convection From an Array of Heated Protrusions on A Vertical Test Surface in Water", *ASME J. Electronic Packaging*, Vol. 111, pp. 121-128. (1989)
9. Y. Joshi, T. Willson and S. J. Hazard "An Experimental Study of Natural Convection From an Array of Heated Protrusions on A Vertical Channel in Water", *ASME J. Electronic Packaging*, Vol. 111, pp. 33-40. (1989)
10. A. Gaiser "Natural Convection Liquid Immersion Cooling of High Density Columns of Discrete Heat Sources in A Vertical Channel", M.E. Thesis, Naval Postgraduate School. (1989)
11. S. Sathe and Y. Joshi "Natural Convection Arising from A Heat Generating Substrate Mounted Protrusion in A Liquid Filled Two-Dimensional Enclosure", *Int. J. Heat Mass Transfer*, To Appear (1991)
12. L. Haukenes "A Computational and Experimental Study of Flush Heat Sources in Liquids", M.E. Thesis, Naval Postgraduate School. (1990)

13. L. Knight "Natural Convection Liquid Immersion Cooling of High Density Columns of Discrete Heat Sources in A Vertical Channel", M.S.M.E Thesis, Navy Postgraduate School. (1988)
14. S. V. Patankar "Numerical Heat Transfer and Fluid Flow", Hemisphere/McGraw-Hill, New York. (1980)
15. Y. Touloukian "Thermophysical Properties of Matter", Vols 1 and 2. (1970)

INITIAL DISTRIBUTION LIST

		No	Copies
1.	Defense Technical Information Center Cameron Station Alexandria, VA 22304-6145	2	
2.	Library, Code 52 Naval Postgraduate School Monterey, CA 93943-5002	2	
3.	Superintendent Naval Postgraduate School Attn: Professor A. J. Healey, Code ME/HY Department of Mechanical Engineering Monterey, CA 93943-5004	1	
4.	Superintendent Naval Postgraduate School Attn: Professor M. D. Kelleher, Code ME/Kk Department of Mechanical Engineering Monterey, CA 93943-5004	1	
5.	Superintendent Naval Postgraduate School Attn: Professor Y. Joshi, Code ME/Ji Department of Mechanical Engineering Monterey, CA 93943-5004	2	
6.	Superintendent Naval Postgraduate School Attn: Professor A. D. Kraus, Code EC/Ks Department of Elec. and Comp. Engineering Monterey, CA 93943-5004	1	
7.	Deniz Harp Okulu K.ligi Kutuphanesi Tuzla, Istanbul / TURKEY	1	
8.	Mr. A. Bosler Naval Weapons Support Center Code 6042 Crane, IN 47522	1	
9.	Mr. Tony Buechler Naval Weapons Support Center Code 6042 Crane, IN 47522	1	

- | | | |
|-----|--|---|
| 10. | Istanbul Teknik Universitesi
Okul Kutuphanesi
Macka, Istanbul / TURKEY | 1 |
| 11. | Superintendent
Naval Postgraduate School
Attn:Curricular Officer, Code 34
Monterey, CA 93943-5004 | 1 |
| 12. | Erhan Murat Akdeniz
Arifiye Mah. Attila Sok. Kabadayi Apt. No:37/18
Eskischir / TURKEY | 1 |